CHARACTERISATION AND ANALYSIS OF GLUT4 VESICLES IN 3T3-L1 ADIPOCYTES, AND THE MUNC18-SYNTAXIN INTERACTION

Martin Norman Mackay

This thesis is submitted for the degree of Master of Science, to the Faculty of Biomedical & Life Sciences

Division of Biochemistry & Molecular Biology,

Institute of Biomedical & Life Sciences,

University of Glasgow

March 2006

Declaration

I declare that the work described in this thesis has been carried out by myself unless otherwise cited or acknowledged. It is entirely of my own composition and has not, in whole or in part, been submitted for any other degree

Martin N Mackay

March 2006

ACKNOWLEDGEMENTS

I would like first of all to thank my supervisor Gwyn Gould for his guidance, help and ideas throughout the period of my post-graduate study. I would also like to thank the BBSRC and Astra Zeneca for providing funding for this project.

The Circular Dichroism and Mass Spectroscopy analysis were carried out at the University of Glasgow by Sharon Kelly, and I would like to take this opportunity to thank her.

I would also like to thank all the various members of Lab 241 for their friendship and company. Luke Chamberlain is due many thanks for teaching me many of the methods here and helping me with different ideas. Thanks are also due here to Johanne Matheson (for help using the BIACORE system), and also Marie-Ann Ewart and Declan James in the Adenovirus work

Finally I would like to thank my family. My parents for all their support throughout my life, and also my brother and grandmother for being there for me.

ABSTRACT

The translocation of GLUT4 from intracellular stores to the plasma membrane in response to insulin results in the large insulin-mediated glucose uptake in fat and muscle tissue. Individuals with insulin resistance and type II diabetes are known to have a defect in this translocation mechanism. As such, a greater understanding of the molecular basis of GLUT4 translocation and recycling is essential in order to design therapies for these diseases.

In this study, we have used sucrose gradient analysis to examine the intracellular distribution of GLUT4. This method allowed for the intracellular GLUT4 to be separated into the two pools of GLUT4 containing vesicles. One of these is highly insulin responsive and corresponds to the specialised GLUT4 storage vesicles (GSVs), while the other corresponds to the less insulin responsive endosomal GLUT4 vesicles. It is these specialised GSVs which are believed to allow the large (up to 20-fold) increase in plasma membrane levels of GLUT4, compared to only ~2-fold increase in levels of recycling proteins (such as the transferrin receptor) in response to insulin. The GSVs are small vesicles (~50nm) and exclude the transferrin receptor (and other recycling proteins) found in endosomal vesicles.

Here we demonstrated that in response to insulin there is ~50% decrease in levels of GLUT4 in GSVs compared to only a 10-20% decrease in levels of GLUT4 in endosomes. We also demonstrate that these sucrose gradients can be used to determine whether other proteins co-localise with GSVs or the endosomal pool.

The Sec1/ Munc18 (SM) protein munc 18c is known to interact with syntaxin4 (a t-SNARE present in insulin responsive cells), which is an interaction that appears to inhibit glucose transport by preventing GLUT4 vesicles from undergoing fusion with the plasma membrane. Here we investigated whether a mutated form of the neuronal SM isoform (munc 18a) is capable of functioning in a similar manner to munc 18c (from a sequence alignment of munc 18a and munc 18c we identified specific amino acids to mutate based on the known 3D structure of the munc 18a-syntaxin1 interaction). If indeed the mutated protein is seen to exhibit binding characteristics similar to munc 18c, then it may be possible to establish the importance of the munc 18c-syntaxin4 interaction on GLUT4 integration into the plasma membrane by making recombinant Adenoviral constructs of the munc 18 proteins, and expressing these in mammalian cells.

Having made the initial mutations, we demonstrate here that *in vitro* the mutant munc 18 protein has inherited the syntaxin4 binding capabilities of the wild-type munc 18c. However, we were not able to then get expression of each of the recombinant Adenoviral constructs in mammalian cells, and as such we were unable to establish the effect that these mutations would have upon GLUT4 fusion with the plasma membrane, and ultimately glucose transport.

CONTENTS

LIST OF FIGURES

LIST OF TABLES

3.3 ABBREVIATIONS

ATB-BMPA	2-N-4-(1-azi-2,2,2-trifluoroethyl)benzoyl-1,3-bis(D-mannos-4 - yloxy)-2- propylamine
ATP	Adenosine triphosphate
CD	Circular Dichroism
CSP	Cysteine string protein
DAB	diaminobenzadine
DMEM	Dulbecco's modified Eagle's serum
DTT	Dithiothreitol
ECL	Enhanced chemiluminescence
EDTA	Diaminoethanetetra-acetic acid, Disodium salt
EM	Electron microscopy
FBS	Foetal bovine serum
GLUT	Glucose transporter
GSV	GLUT4 storage vesicle
h	Hours
HEPES	N-2-Hydroxyethylpiperazine-N'-2-ethanesulfonic Acid
HES	HEPES EDTA Sucrose
HDM	High density microsome/ membrane
HRP	Horseradish peroxidase
IBMX	Methyl isobutylxanthine
IgG	Immunoglobulin gamma
IRAP	Insulin responsive amino peptidase
IRS	Insulin receptor subunit
LDM	Low density microsome/ membrane

mA	Milliamps
min	Minutes
NCS	New born calf serum
NSF	N-ethylmaleimide sensitive factor
PAGE	Polyacrylamide gel electrophoresis
PBS	Phosphate buffered saline
PDK	Phosphoinositide dependent protein kinase
PH	Pleckstrin homology
PI3-kinase	Phosphatidylinositol 3-kinase
PIP_2	Phosphatidylinositol 3,4-bisphosphate
PIP_3	Phosphatidylinositol 3,4,5 –trisphosphate
PKB	Protein Kinase B
PM	Plasma membrane
PTB	Phosphotyrosine binding
s	Seconds
SDS	Sodium dodecyl sulphate
SH3	Src homology 3
SNAP23/25	Synaptosome-associated protein 23/25
SNAP	Soluble NSF attachment protein
SNARE	SNAP receptor
TEMED	N,N,N',N'-Tetramethylethylenediamine
TfR	Transferrin receptor
TGN	Trans-Golgi network
UV	Ultra violet
VAMP	Vesicle-associated membrane protein

v/v	volume/volume ratio
w/v	weight/ volume ratio

CHAPTER 1-INTRODUCTION

1.1 Glucose as an energy source

Glucose is a fundamental source of energy for all eukaryotic cells. In humans, the main consumer of glucose under basal conditions is the brain, which accounts for as much as 80% of whole body consumption. The energy is provided by the breakdown of endogenous glycogen stores that are mainly in the liver. These energy stores are then replenished by glucose in the diet that, after being digested and absorbed across the gut wall, is distributed among various tissues of the body (reviewed in Shepherd & Kahn 1999).

The distribution of glucose is carried out by a family of glucose transporters (called GLUTs), which function by moving sugar across the cell membrane. An important function of one specific glucose transporter is to respond to increased levels of glucose in the bloodstream by storing glucose in muscle and adipose tissue. This tightly controlled process prevents large fluctuations in blood glucose levels, which can be harmful (this will be discussed in further detail below).

1.2 Insulin action in fat and muscle

In 1980, it was established that, in rat adipocytes, insulin stimulates the movement of the specialised glucose transporter that is found in these cells from an intracellular store to the plasma membrane (Suzuki & Kono 1980; Cushman & Wardzala 1980).

The emergence of this glucose transporter at the cell surface meant that increased glucose transport (above the basal level) could then take place into these cells.

Insulin is secreted by the β-cells of the pancreas in response to high blood glucose levels. A specific glucose transporter (GLUT2) mediates entry of glucose into these β-cells, and as such allows them to respond to an increased level of glucose in the bloodstream. An increased level of glucose within β-cells initiates a chain of events ultimately leading to the release of insulin from these cells, and into nearby blood vessels.

The effects of insulin are dependent on the presence of an insulin receptor, to which insulin binds, and this leads to a cascade of events indicating to the cell the presence of elevated blood glucose levels. In both adipose and muscle cells this signal results in the uptake of glucose into those cells, and as such blood glucose levels are restored to normal. In these cells the glucose is metabolised and either converted into glycogen (in muscle), or fatty acids (in adipose tissue).

It has since been determined that this specialised glucose transporter is GLUT4. A defect in the translocation of GLUT4 will result in a reduced uptake of glucose in response to insulin, and is thought to be the underlying cause of diseases such as diabetes mellitus.

1.3 Diabetes

Diabetes mellitus can be divided into two different types: insulin-dependent diabetes mellitus (IDDM) and non insulin-dependent diabetes mellitus (NIDDM), now called type I and II respectively. Type I diabetes often occurs in childhood, and is thought to

be genetically determined leading to the destruction of β-cells in the pancreas and hence to insulin deficiency. Type I can often be treated successfully by the administration of insulin. On the other hand, type II diabetes is often called "late onset diabetes" and is greatly influenced by external factors such as diet and lifestyle. Both types of diabetes show a phenotype of hyperglycemia, but as mentioned before type I patients produce no insulin, whereas type II patients are often hyperinsulinaemic. Type II as well as obesity is characterised by insulin resistance. Studies on non-diabetic offspring of two diabetic patients determined that they have a 50% risk of becoming diabetic in later life, suggesting that type II is also genetically determined. This possibility increased greatly if the individuals were also obese, suggesting an environmental influence in the development of type II diabetes (reviewed in Kahn 1994).

Insulin resistance precedes the development of type II diabetes. Patients that are diabetic have probably been insulin resistant for several years prior to the disease being diagnosed, usually only as the consequence of the appearance of side effects of the disease. These side effects are caused by the increased blood glucose levels over an extended period of time, and include (in extreme cases) blindness, kidney failure and cardiovascular disease. Often the decreased insulin sensitivity seen in patients leads to an increase in insulin production, which again could further reduce insulin sensitivity. On the other hand, in other patients, insulin secretion is severely impaired before the onset of diabetes. In such patients, insulin treatment is only sometimes effective due to the fact that the patients are insulin resistant. There is therefore a great demand for drugs which can alleviate this by increasing insulin sensitivity.

The prevalence of type II diabetes is increasing at a large rate. In 1998, 143 million people worldwide suffered from the disease, and it is estimated that this could double in the next 20-30 years (Harris *et al.* 1998). Therefore, there has been a significant level of research looking into finding the molecular basis for insulin resistance. Any defect in the insulin-signalling cascade or in GLUT4 translocation could lead to the development of insulin resistance. Studies making use of human tissue and rodent models of diabetes have determined that there is probably not just one point in the cascade of events that is defective. There could be an accumulation of different defects, and there may be different reasons for the development of insulin resistance in different patients.

It is now known that a defective glucose transport is the main reason for insulin resistance in type II patients (Bonadonna *et al.* 1993; Bonadonna *et al.* 1996; Kelley *et al.* 1996). These results suggest a defect in the translocation of GLUT4 to the plasma membrane, leading to a reduced number of transporters in the plasma membrane. In support of this, impaired GLUT4 translocation has been found in muscle of obese, insulin resistant and type II diabetic patients (Kelley *et al.* 1996; Garvey *et al.* 1998).

Muscle tissue accounts for the majority of post-prandial glucose uptake at about 70-80% compared to 5-20% in adipose tissue (as reviewed in Hunter & Garvey 1998). Down regulation of GLUT4 in those tissues could explain the decreased glucose transport in diabetic patients, and indeed in adipocytes GLUT4 levels are down by about 80-90% (Garvey *et al.* 1991). However, GLUT4 levels in muscle are unchanged (Garvey *et al.* 1992) and therefore GLUT4 depletion cannot be the only reason for insulin resistance in type II diabetes. This defect in muscle tissue could be due to

either a defect in the translocation mechanism of GLUT4, or due to mis-targeting of GLUT4 to an insulin insensitive location.

1.4 Insulin signalling

1.4.1 The insulin receptor

The insulin receptor is expressed ubiquitously and is composed of two α and two β subunits (reviewed in Virkamäki *et al.* 1999; Elmendorf & Pessin 1999). These form a heteroteramer linked via disulphide bonds. The α subunits are extracellular and contain the insulin binding domain. The β subunits span the membrane but the majority of this polypeptide is located within the cytosol. This receptor belongs to the tyrosine kinase family of receptors, and the intracellular β subunits contain tyrosine kinase activity (reviewed in Kahn 1994; Virkamäki *et al.* 1999). Insulin binding to the α subunits results in a conformational change in the receptor that increases the intrinsic kinase activity and leads to the autophosphorylation of the receptor β subunits (reviewed in Kahn 1994). The tyrosine residues on the receptor that become phosphorylated in response to insulin binding, and are important for the activation of downstream signalling pathways, have been identified by mutagenesis (Holman & Kasuga 1997).

Recent studies have demonstrated the presence of two insulin signalling pathways leading to GLUT4 translocation. These will be summarised below.

1.4.2 The classic pathway of insulin signalling

The most important downstream targets for the insulin receptor in terms of glucose transport are the insulin receptor substrate (IRS) family of proteins. IRS proteins have a similar overall structure, containing a N-terminal pleckstrin homology (PH) domain and a phosphotyrosine binding (PTB) domain, both of which are required for efficient tyrosine phosphorylation of IRS by the insulin receptor (Virkamäki *et al.* 1999).

These phosphotyrosine residues on IRS proteins provide docking sites for proteins with Src homology 2 (SH2) domains. Many proteins contain such domains, and hence can bind IRS proteins. However, the most important for glucose transport is Phosphatidylinositol 3-kinase (PI3-kinase) (Zhou *et al.* 1997). PI3-kinases consist of two subunits, both of which have several isoforms. It is the regulatory subunit (p85) of PI3-kinase that recruits the catalytic subunit (p110) to the plasma membrane, where it catalyzes the phosphorylation of the 3' position in the inositol ring of phosphoinositide (PI) lipids. Specifically PI3-kinase catalyses the formation of $PI(3,4)P_2$ and $PI(3,4,5)P_3$ (Fruman *et al.* 1998).

The phosphorylation of the 3' position recruits and activates proteins containing PH domains, including 3' phosphoinositide-dependent kinase-1 (PDK-1) and AKT (protein kinase B) (Rameh & Cantley 1999). In turn, PDK-1 phosphorylates and activates downstream effectors including PKB and the atypical protein kinase C ζ/λ.

A variety of functional data has determined the importance of the PI3-kinase pathway in glucose transport. For example, experiments using the PI3-kinase inhibitors

wortmannin and LY294002 have shown that PI3-kinase is crucial for insulin-mediated glucose uptake (Okada *et al.* 1994; Cheatham *et al.* 1994; Clarke *et al.* 1994). The roles of PKB and the atypical protein kinase C, and their downstream targets are less well understood (see Figure1.1 Signal 1).

1.4.3 An alternative pathway of insulin signalling – Cbl/CAP complex

Cbl is the cellular homologue of the v-Cbl onco-protein. It is approximately 120kDa in size, predominantly cytosolic and contains many proline-rich motifs, with which it can bind SH3 domains on other proteins. It has been established that insulin can tyrosine phosphorylate Cbl in 3T3-L1 adipocytes (Ribon & Saltiel 1997) and this can allow the binding of Cbl with several other proteins. In β cells Cbl was shown to bind to p85, and consequently it is believed that it may be important in PI3-kinase recruitment and activation in these cells (Kim *et al.* 1995). However in 3T3-L1 adipocytes, this interaction between tyrosine phosphorylated Cbl and PI3-kinase was not seen (Ribon & Saltiel 1997).

It is now believed that Cbl can bind the insulin receptor via the Cbl associated protein (CAP). The interaction of CAP with Cbl is mediated by binding of the SH3 domains in CAP to the proline-rich motifs in Cbl, and is independent of insulin action. CAP also binds to the insulin receptor and insulin stimulation results in a time-dependent dissociation of the CAP-insulin receptor complex (Ribon *et al.* 1998). The tyrosine phosphorylation of Cbl is known to occur through the insulin receptor in collaboration with CAP and the adaptor protein APS. When Cbl is phosphorylated, the CAP–Cbl–APS protein complex is recruited to the lipid raft microdomain, through association with the raft protein flotillin (Baumann *et al.* 2000).

An interesting discovery is that the introduction of CAP lacking the SH3 domains (CAPΔSH3) into 3T3-L1 adipocytes had no effect on PI3-kinase activity, but was found to inhibit insulin-mediated GLUT4 translocation by ~50-60% (Baumann *et al.* 2000). This finding would suggest that insulin can generate a signal (through the CAP-Cbl complex) leading to glucose transport, but is independent of PI3-kinase. Phosphotyrosine on Cbl was found to recruit a complex containing the associate with the adaptor protein CrkII and the guanine nucleotide exchange factor C3G into the lipid raft domain. The recruited C3G then causes the GTP/GDP exchange and activation of the TC10 GTPase (Watson *et al.* 2001) (see Figure 1.1 Signal 2).

It has recently been suggested that a downstream target of this TC10 protein could be the exocyst complex, and that the TC10–exocyst complex is then responsible for targeting GLUT4-containing vesicles to appropriate plasma membrane fusion sites (Inoue *et al.* 2003; Kanzaki & Pessin 2003). The exocyst complex is responsible for tethering the exocytotic vesicles to the appropriate sites of the plasma membrane, and this will be discussed below.

A recent study has however provided evidence to counter the potential role of this alternate pathway in insulin stimulated glucose transport. By means of the administration of small interfering RNAs (siRNA) it has been possible to selectively deplete the intermediates of this pathway (notably CAP, Cbl and CrkII) and observe the resulting effects. Results from this study showed that these intermediates can each be depleted in cultured adipocytes without compromising GLUT4 translocation by insulin. These results would indicate that these proteins are not required components

of insulin signaling to GLUT4 transporters (Mitra *et al.* 2004), and as such would question whether there are indeed two separate signals leading to glucose transport.

Taken together, these results therefore suggest that insulin can potentially generate two independent signals leading to glucose transport, one dependent on and the other independent of PI3-kinase.

1.4.4 Insulin signalling in diabetes

Clearly defects in insulin signalling could lead to insulin resistance and diabetes (as reviewed in Virkamäki *et al.* 1999; Saltiel 2001). Although rodent models are valuable in studying insulin resistance, and have been used extensively, very few provide a real model of type II diabetes with the same phenotype as that found in human diabetes. Consequently, recent studies have focussed upon finding signalling defects in diabetic patients.

Signalling defects that cause insulin resistance are rare, but some will be mentioned here. It has however been established that there are several acquired defects in insulin resistance. A down regulation of insulin receptor as well as decreased tyrosine kinase activity has been found in type II diabetics, but this can be restored through weight loss (Friedenberg *et al.* 1988). Decreased IRS-1 expression has also been identified in adipocytes of insulin resistant patients, although interestingly IRS-2 was found to substitute for IRS-1 and the main insulin-stimulated PI3-kinase activity was now associated with IRS-2 (Rondinone *et al.* 1997). However, in skeletal muscle no difference in IRS-1 expression was observed, but decreases in its tyrosine phosphorylation in response to insulin have been reported, together with a defect in

insulin-stimulated PI3-kinase activity in type II diabetic patients (Bjornholm *et al.* 1997). PKB activity and levels had originally been shown to be unaltered in diabetic patients. However, a recent study screening genomic DNA from patients with severe insulin-resistance (for mutations in genes implicated in insulin signalling) has identified a mutation in PKB that promotes insulin resistance (George *et al.* 2004).

Genetic defects in insulin signalling proteins, such as the insulin receptor, are very uncommon and only found in some syndromes such as leprechaunism and type A insulin resistance (reviewed in Hunter & Garvey 1998). There are several polymorphisms occurring in IRS-1, which are increased in type II diabetic patients. These do not cause a large defect on IRS-1 function, but decreased PI3-kinase activity has been reported in some (Almind *et al.* 1996; Imai *et al.* 1997). To date the only mutation discovered in PI3-kinase is present at the same frequency in diabetic and normal individuals, and it is therefore unlikely to be important in the development of insulin resistance and type II diabetes (as reviewed in Sheperd *et al.* 1998; Virkamäki *et al.* 1999).

1.5 Glucose Transport

Glucose is the major energy source for most mammalian cells, and in order to be used in the cytosol, it has to be transported across the plasma membrane.

There are two major types of glucose transporters: The sodium-dependent transporters use a Na^+ gradient to drive accumulation of glucose (as reviewed in Bell *et al.* 1993),

and will not be discussed further here, and the facilitative glucose transporters that move glucose down its chemical gradient (and do not use energy for this transport).

1.5.1 The family of glucose transporters

There are several isoforms of the facilitative glucose transporters. At present the family comprises thirteen members, which are separated into three subclasses based on sequence homology and structural similarity. They are products of distinct genes, exhibit tissue-specific expression, and are independently controlled. These facilitative glucose transporters are integral membrane proteins, and their structures will be discussed below.

GLUT1 was the first to be isolated from red blood cells and is ubiquitously expressed. It is the major transporter at the blood-tissue barriers and provides cells with glucose even if extracellular levels are low. GLUT1 is sometimes referred to as the "house-keeping" glucose transporter as it provides tissues with a constant low level supply of glucose (as reviewed in Gould & Seatter 1997).

GLUT2 is a bi-functional glucose/fructose transporter and is mainly expressed in the liver, the β-cells of the pancreas and the small intestine. In the liver it is important for both the import and export of glucose (depending on blood glucose levels), thereby ensuring the important role of the liver in whole body glucose homeostasis (as reviewed in Gould & Holman 1993; Gould & Seatter 1997).

GLUT3 is the neuronal glucose transporter, and is crucial for supplying the brain with glucose. The brain has a high glucose demand, and cannot use any other energy source. Consequently GLUT3 has the lowest Km of all the transporters studied functionally to date (as reviewed by Bell *et al.* 1993).

GLUT4, the "insulin-sensitive glucose transporter" is the most intensively studied member of the family (as reviewed in Rea & James 1997). It is expressed in muscle, heart and fat tissue and undergoes insulin-mediated translocation from an intracellular store to the plasma membrane thereby ensuring the insulin responsiveness of those tissues. This results in glucose uptake into glucose storage tissues and subsequently glycogen is synthesised in muscle, and fatty acids and triglycerides are made in fat cells. This transporter is discussed in more detail below.

These four GLUT's comprise the class I glut transporters. GLUTs 5, 7, 9 and 11 comprise class II transporters, and transport fructose. GLUTs 6, 8, 10, 12 and HMIT1 comprise class III transporters, and at present these are poorly defined (as reviewed in Joost and Thorens 2001).

1.5.2 Structure

Analysis of the hydropathy plots of the predicted amino acid sequences of the different isoforms has shown that these proteins adopt similar structures (Figure 1.2). These studies predict an integral membrane protein with twelve amphipathic helices spanning the membrane, and with both the N- and C-terminus on the cytoplasmic side. There are large loops between helices 1 and 2 (extracellular) and 6 and 7 (intracellular) (as reviewed in Gould & Holman 1993). The major features of this

model have been experimentally confirmed (as reviewed in Gould & Seatter 1997) and it is believed that in order to allow glucose to traverse the membrane, five of the twelve helices form an aqueous pore through which transport may occur (as reviewed in Barrett *et al.* 1999). Conformational studies using chimeras of the different glucose transporter isoforms have allocated specific functions to certain structure, sequences or even amino acids within these transporters. The substrate-binding site is known to be composed from different regions of the transporter. Binding of substrate to the exofacial site causes a conformational change re-orientating the sugar-binding site to the endofacial conformation and subsequent release of the substrate into the cytoplasm (as reviewed in Gould *et al.* 1997; Barrett *et al.* 1999).

1.6 GLUT4

1.6.1 The translocation hypothesis

In contrast to the other glucose transporter isoforms, which are located principally at the plasma membrane, 95% of GLUT4 (the "insulin-sensitive glucose transporter") is located in intracellular vesicles and tubules (Slot *et al.* 1991a; Slot *et al.* 1991b). When present, insulin causes the translocation of these vesicles to the cell surface, resulting in up to 20-fold increased levels of GLUT4 at the plasma membrane and therefore increased glucose transport (as reviewed in Rea & James 1997). The intracellular location of GLUT4, and the mechanism of its translocation will be discussed in detail below.

1.6.2 Localisation by EM

Since it was discovered that GLUT4 is predominantly located intracellularly, much research has focussed into examining the nature of the GLUT4 containing compartment. Electron microscopy studies (using brown adipose tissue or rat cardiac muscle) determined GLUT4 to be localised to about 40% in tubulo-vesicular structures near the Golgi, some of this being TGN probably. A further 50% was found in tubulo-vesicular structures scattered throughout the cytoplasm (Slot *et al.* 1991a; Slot *et al.* 1991b). GLUT4 localisation in tubulo-vesicular structures both near the TGN as well as throughout the cytoplasm has also been confirmed in skeletal muscle (Ploug *et al.* 1998). In order to determine whether GLUT4 is actually located within the TGN, and not just near it, experiments using rat atrial cardiomyocytes (a secretory cell type) were used. In these cells, a large proportion of GLUT4 (50-60%) was found in the secretory granules, which proves that GLUT4 traffics through the TGN during recycling (Slot *et al.* 1997). However, GLUT4 vesicle purification studies argue against the TGN being the principal intracellular storage compartment in adipocytes (Martin *et al.* 1994).

In brown adipose tissue, GLUT4 levels at the plasma membrane were observed to be around 1% in the absence of insulin, confirming the theory that GLUT4 is excluded from the cell surface in the absence of insulin stimulation. The presence of insulin then resulted in a redistribution of GLUT4 from these intracellular structures to the plasma membrane by about 40 % (Slot *et al.* 1991a; Slot *et al.* 1991b). Another effect of insulin stimulation was an increased labelling of GLUT4 in clathrin lattices and early endosomes, implying that GLUT4 is endocytosed via clathrin- coated pits. This

is a well-described mechanism for other membrane proteins (reviewed by Robinson *et al.* 1996).

More recently, a method to isolate cytoplasmic sheets from rat adipocytes has allowed a 3-D resolution of the intracellular GLUT4 compartments using electron microscopy (Ramm *et al.* 2000). In this study the majority of GLUT4 was found associated with small vesicles (60%) whilst a smaller level of GLUT4 was associated with tubules (25%). Interestingly, insulin caused a recruitment of GLUT4 mainly from the small vesicles, and translocation of GLUT4 is thought to occur via fusion of these vesicles with the plasma membrane, rather than sorting of GLUT4 out of the vesicles (Ramm *et al.* 2000).

Studies using Brefeldin A in 3T3-L1 adipocytes have provided indirect evidence in favour of the concept that GLUT4 is targeted to an intracellular insulin-responsive compartment that is distinct from the TGN and/or endosomes (Martin *et al.* 2000). Here, through the co-localisation of GLUT4 with a TGN/endosomal marker protein, it was shown that a significant proportion of GLUT4 recycles between the TGN & endosomes. However, disruption of this recycling pathway by Brefeldin A had no significant effect on the basal distribution of GLUT4; the insulin-dependent movement of GLUT4 to the plasma membrane; and the reformation of the insulin-responsive GLUT4 compartment (Martin *et al.* 2000).

Taken together these results provide evidence of GLUT4 in different intracellular compartments, and this will be discussed in further detail below.

1.6.3 Multiple compartments

It is known that GLUT4 is endocytosed via clathrin-coated pits (Slot *et al.* 1991a; Robinson *et al.* 1992), and recycles constantly between the plasma membrane and intracellular sites both in the presence and absence of insulin (Robinson *et al.* 1992; Yang & Holman 1993). GLUT4 partially co-localises with a number of other proteins such as GLUT1 (Calderhead *et al.* 1990; Robinson & James 1992), the mannose-6-phosphate receptor (M6PR) (Kandror & Pilch 1996) and the transferrin receptor (TfR) (Tanner & Lienhard 1989) in endosomes. These proteins also undergo insulin responsive translocation to the cell surface in 3T3-L1 adipocytes (Tanner & Lienhard 1987; Tanner & Lienhard 1989; Calderhead *et al.* 1990; Kandror & Pilch 1996; Kandror & Pilch 1998; Subtil *et al.* 2000). This increase however is only about 2-fold compared to the ~ 20-fold increase of GLUT4 (Tanner & Lienhard 1987; Calderhead *et al.* 1990; Piper *et al.* 1991). This implies that although GLUT4 is partly present in the same compartments as these proteins, a significant fraction is localised to a compartment that is distinct from endosomes, and which is highly responsive to insulin (Yang & Holman 1993).

The idea that GLUT4 populates at least two different intracellular compartments (endosomes and GSVs) has been suggested from data using a variety of methods. From a kinetic viewpoint, the behaviour of GLUT4 recycling kinetics can only be explained by the presence of at least two intracellular GLUT4 pools (Holman *et al.* 1994). In this study, the membrane impermeant bismannose photolabel ATB-BMPA was used to tag GLUT4 at the plasma membrane after insulin treatment, and the subsequent re-distribution of this tagged GLUT4 was examined. The behaviour of

tracer-tagged GLUT4 was then fitted into different models for GLUT4 recycling (Figure 1.3). The 3-pool model with two intacellular pools, one early endosome pool (T_{ee}) and one tubulo-vesicular pool (T_{tv}), can account for the above mentioned differences in recycling between GLUT4 and other proteins. It also allows for a very rapid translocation of GLUT4 to the plasma membrane and fits into the observation that the main effect of insulin is to increase the rate of exocytosis of GLUT4, rather than decrease the endocytosis rate (Slot *et al.* 1991a; Yang & Holman 1993). This model however involves only one plasma membrane pool of glucose transporter, and hence does not account for the presence of GLUT4 in clathrin coats (Slot *et al.* 1991a; Robinson *et al.* 1992) or more significantly for the time differences observed between appearance of GLUT4 at the plasma membrane and increase in glucose transport (Holman *et al.* 1994). Therefore the two different 4-pool models using occluded pools were proposed, where T_{po} (Figure1.3 C) represents vesicles that have docked with the plasma membrane, but not yet fused and T_{pc} (Figure1.3 D) represents GLUT4 in clathrin-coated pits ready for endocytosis. It is important to note here that the ATB-BMPA can access GLUT4 in the occluded pool. The authors of the paper propose that the only possible way to explain all of the data about GLUT4 trafficking is through a 5-pool or multiple-pool model (Figure 1.3E), which contains the two intracellular pools as well as the occluded pools (Holman *et al.* 1994).

The visualisation of GLUT4 compartments in a 3-D way has helped to distinguish between the intracellular GLUT4 pools (Ramm *et al.* 2000). As mentioned above, the majority of GLUT4 was targeted to small vesicles (~50nm in diameter), and this vesicular compartment was shown to be distinct from early and late endosomes as well as TGN. Co-localisation studies implied that, on one hand, a subset of these

vesicles fuse with the plasma membrane in response to insulin, but that GLUT4 is also found in M6PR positive vesicles, and that insulin induced a sorting of GLUT4 out of these vesicles.

The presence of two intracellular pools of GLUT4 (the endosomal pool and highly insulin responsive pool) has also been confirmed biochemically, and some of the experiments will be discussed here.

Studies in rat adipocytes have suggested that GLUT4 containing vesicles are structurally (as well as functionally) different from other intracellular endosomes (Kandror *et al.* 1995). Many other studies have attempted to separate the insulin-sensitive GLUT4 storage vesicles (GSVs) from the endosomal pool. Sucrose density gradients (which exploit the different density properties of membranes) found two pools containing GLUT4 in rat skeletal muscle. Only one of these pools showed a 30% decrease in GLUT4 levels due to insulin, whilst the other pool contained TfR (Aledo *et al.* 1997). The use of hypotonic lysis instead of homogenisation (as a method to fractionate cells) has also permitted the seperation of strongly insulin-sensitive cells (GSVs) from the less insulin-sensitive endosomes (Lee *et al.* 1999).

More recently, an effective method used to separate the internal GLUT4 membranes in 3T3-L1 adipocytes is by the use of iodixanol as a gradient material (Hashiramoto & James 2000). Sucrose gradients have also been used to separate the internal membranes in 3T3-L1 adipocytes (Guilherme *et al.* 2000), and these two methods will be discussed in Chapter 3.

Another method, which has given similar results, is compartment ablation. Here cells are loaded with transferrin bound to horseradish peroxidase (Tf-HRP), which is taken into the cell via the transferrin receptor. Incubation of intact cells with diaminobenzadine (DAB) and hydrogen peroxide allows HRP to transfer electrons from DAB to peroxide. This produces a highly reactive cross-linker within the lumen of transferrin receptor positive vesicles/ tubules, and thus any protein in proximity to the transferrin receptor is ablated (Livingstone *et al.* 1996). Both GLUT1 and the transferrin receptor were ablated by about 70% after 2h incubation with Tf-HRP, whilst GLUT4 was ablated by only 40%. This would imply that the larger proportion of GLUT4 (60%) is localised to a TfR-negative compartment, which was also devoid of the endosomal markers rab5 and M6PR (Livingstone *et al.* 1996). This data supports the kinetic and gradient studies mentioned above, and confirms the idea that GLUT4 is localised in two intracellular compartments, one being the endosomes and the other being the GSVs.

1.6.4 The GSV model

The current model for the transport of GLUT4 is therefore that GLUT4 in the basal state is present in an insulin responsive compartment, now termed GLUT4 storage vesicles (GSVs) (Figure 1.4). Insulin then causes a rapid translocation of GLUT4 to the plasma membrane. This occurs both via fusion of GLUT4 containing vesicles with the plasma membrane as well as the sorting of GLUT4 from an endosomal compartment. GLUT4 undergoes endocytosis from the plasma membrane, via clathrin-coated pits, and enters the recycling endosomes. From these endosomes,

many proteins (such as TfR, GLUT1 and M6PR) enter a continous recyclying pathway with the plasma membrane (cycle 1 in Figure 1.4).

However, in contrast to this a large proportion of GLUT4 enters an intracellular transport loop between the TGN and endosomes (cycle 2 in Figure 1.4). Here GLUT4 is selectively targeted to a seemingly futile cycle that prevents it from entering the cell-surface recycling pathway of these other proteins. GLUT4 emerging from the TGN is contained within the specialised insulin sensitive GSVs. These either undergo trafficking to the plasma membrane (in the presence of insulin), or fuse with the recycling endosomes and undergo recycling through the TGN. If this recycling in cycle 2 (from Figure 1.4) did not occur, then the endosomal and TGN pools of GLUT4 would become depleted, and all of the GLUT4 would be found in GSVs in the absence of insulin.

1.6.5 GLUT4 defects in diabetes

As mentioned in section 1.3, a defective glucose transport is the main reason for insulin resistance in type 2 patients (Bonadonna *et al.* 1993; Bonadonna *et al.* 1996; Kelley *et al.* 1996). Decreased GLUT4 levels at the plasma membrane after insulin treatment could be due to defects in any stage of GLUT4 recycling, and this can therefore lead to the development of type 2 diabetes.

Garvey and co-workers have studied GLUT4 levels and trafficking in both adipocytes and muscle cells from type 2 diabetic patients. Although in adipocytes GLUT4 down regulation can explain most of the decrease in insulin-stimulated glucose uptake (Garvey *et al.* 1991), there is a discrepancy between the amount of transporters found

at the plasma membrane and glucose transport (Garvey *et al.* 1988). This could be because these patients have a defect in their GLUT4 activity, meaning that although GLUT4 is present at the plasma membrane it is not functional. It could also mean that GLUT4 is not inserted correctly into the plasma membrane, and therefore not transporting glucose (the transporter may be docked to the plasma membrane, but not yet fused).

A study from the same laboratory in muscle from insulin-resistant patients also suggested that GLUT4 was mis-targeted and that this could be the reason why insulin was unable to recruit GLUT4 to the plasma membrane (Garvey *et al.* 1998). Interestingly, in these insulin-resistant patients, GLUT4 was mis-targeted to a fraction that also contained plasma membrane and this is therefore similar to the study in adipocytes described above.

1.6.6 GLUT4 knock out mice

The generation of GLUT4 knock out mice led to the surprising discovery that GLUT4 is not actually required for maintaining nearly normal blood glucose levels (Katz *et al.* 1995). These mice are growth-retarted and have decreased longevity, but are not diabetic. It was demonstrated that GLUT1, the only other glucose transporter present in fat and muscle cells, was not upregulated. However, GLUT2 was upregulated in liver, and this is believed to demonstrate an increased uptake of glucose into this organ (reviewed in Mueckler & Holman 1995).

Significantly, heterozygous knockout mice for GLUT4 (in contrast to the homozygous knockout mentioned above) develop a diabetic phenotype (Stenbit *et al.* 1997). It is believed that the reason for this is that these mice produce normal levels of GLUT4 until they are 8 weeks old, but then GLUT4 content declines. As a result of this, the heterozygous mice do not develop the compensating mechanism seen in GLUT4 null mice, and therefore can not deal with the decreased glucose uptake into peripheral tissue.

1.7 IRAP

IRAP (vp165) is an aminopeptidase, which was first cloned from rat adipocytes (Keller *et al.* 1995), and has been found to colocalise with GLUT4 in rat adipocytes (Malide *et al.* 1997c), 3T3-L1 adipocytes (Ross *et al.* 1996) and rat skeletal muscle (Aledo *et al.* 1997). It has been shown through immunoadsorption experiments of both GLUT4 vesicles and IRAP vesicles that these two proteins colocalise perfectly in the basal state in 3T3-L1 adipocytes (Ross *et al.* 1996). Through subcellular fractionation it has been discovered that IRAP translocates to the plasma membrane to a similar extent as GLUT 4 in both 3T3-L1 adipocytes (Ross *et al.* 1996) and rat adipocytes (Malide *et al.* 1997c). Biotinylation experiments showed that the increase at the plasma membrane due to insulin to be about 8-fold (Ross *et al.* 1996). Confocal microscopy of rat adipocytes using double labelling with GLUT4 and IRAP indicated an overlap of about 85% between the two proteins (Malide *et al.* 1997c). This was also seen using electron microscopy on GLUT4 or IRAP vesicles, which revealed a 70-90% overlap depending on cell type (Martin *et al.* 1997). Ablation experiments

determined that IRAP was ablated to a similar extent as GLUT4, indicating that it (like GLUT4) is localised within two or more intracellular compartments (Martin *et al.* 1997). IRAP, in parallel with GLUT4, recycles constantly between the plasma membrane and intracellular membranes, and is endocytosed via clathrin coated pits (Garza & Birnbaum 2000). A number of studies have endorsed the idea that GLUT4 and IRAP recycle through the endocytic pathway in a very similar way (Malide *et al.* 1997c; Ross *et al.* 1997; Garza & Birnbaum 2000).

The exact function of IRAP, and specifically the role that it may play in the regulation of GLUT4 translocation, is however unknown at present. The injection of IRAP (and particularly a 28 amino acid sequence of the cytoplasmic tail of the protein) into 3T3-L1 adipocytes causes GLUT4 translocation in the absence of insulin (The N-terminus of IRAP contains a di-leucine motif and several acidic regions similar to those that occur in Glut4. The similarity between the C-terminus of Glut4 and the N-terminus of IRAP suggests that these two molecules are sorted within the cell by a common mechanism). This movement to the plasma membrane could not be inhibited by wortmannin, the PI3-kinase inhibitor. These results indicate that the action of IRAP on GLUT4 is downstream of PI3-kinase activity (Waters *et al.* 1997). One theory from these results is that retention/ sorting proteins may interact with the C-terminus of GLUT4 and/or the N-terminus of IRAP. Injecting IRAP peptides into cells causes competition between these peptides and the intracellular IRAP for the retention/ sorting proteins and thereby translocation of the GLUT4 vesicles to the plasma membrane occurs (Waters *et al.* 1997). This data was supported by the generation of a chimeric reporter molecule vpTR, which contains the N-terminal cytoplasmic domain of IRAP and the transmembrane and extracellular domains of the transferrin receptor,

and behaves much like IRAP. A mutation in the di-leucine motif in the cytoplamsic domain of vpTR established that this motif interacts with the machinery responsible for insulin-regulated intracellular retention (Johnson *et al.* 1998; Subtil *et al.* 2000).

Recently it has been proposed that IRAP may have a role to play in the association of the putative rabGAP AS160 (Akt substrate of 160 kDa) with GLUT4 vesicles (Larance *et al.* 2005). It has been shown (both *in vivo* and *in vitro*) that AS160 interacts with the cytosolic tail of IRAP, which could account for this association. However, this association is seen only in the basal state, and is lost in response to insulin when AS160 is phosphorylated by PKB. It has therefore been postulated that this interaction allows the GAP activity of AS160 to maintain a key rab protein in the inactive GDP-bound form. It is proposed that once AS160 is phosphorylated, it dissociates from the GLUT4 vesicles, and this then allows for GTP loading of one (or more) rab protein leading ultimately to docking and fusing of GLUT4 vesicles with the plasma membrane (Larance *et al.* 2005). Thus a role for IRAP could be insuring the intracellular localisation of GLUT4 in the basal state by interacting with AS160.

A physiological function of IRAP has been hypothesized to be hormonal modulation of circulating vasoactive peptides such as vasopressin (Herbst *et al.* 1997). The aminopeptidases homologous to IRAP are constitutively expressed at the cell surface and as such, have continued access to their extracellular substrates (Kenny 1986). IRAP however, in the basal state, is sequestered intracellularly and as such has limited access to its extracellular substrates. Therefore, it is expected to process its extracellular substrates only after translocation to the cell surface, upon insulin stimulation. In support of this, it has been shown that insulin, in parallel with the

translocation of IRAP to the plasma membrane, increases aminopeptidase activity toward extracellular vasopressin in isolated adipocytes (Herbst *et al.* 1997). Thus, insulin, by bringing IRAP to the cell surface, could increase the processing of extracellular peptide hormones and thereby change their activities.

In individuals with type II diabetes, the insulin-stimulated translocation of IRAP to the cell surface of muscle and fat cells is impaired. This defect may lead to decreased cleavage and consequently increased action of peptide hormones that are substrates for IRAP. Impaired IRAP action may thus play a role in the development of complications in type II diabetes. This theory is supported by the finding that in mice where IRAP was deleted, decreased expression of GLUT4 and the enlargement of the heart (both common findings in patients with type II diabetes) are seen. This suggests that impaired IRAP function at the plasma membrane may lead to complications in insulin resistant individuals (Keller 2004).

1.8 Other molecules in GLUT4 vesicles

VAMP/ Cellubrevin

Both vesicle-associated membrane protein 2 (VAMP2) and cellubrevin/ VAMP3 have been found on GLUT4 vesicles (Cain *et al.*1992; Volchuk *et al.* 1995; Tamori *et al.* 1996; Martin *et al.* 1996; Malide *et al.* 1997a). These proteins are important for the SNARE-type mechanism of GLUT4 translocation to the plasma membrane, and will be discussed in detail below. Both VAMP2 and cellubrevin display insulin-simulated translocation to the plasma membrane (Cain *et al.*1992; Volchuk *et al.* 1995; Tamori

et al. 1996; Martin *et al.* 1996). A number of studies have determined that VAMP2 is important in the translocation of the GSVs to the plasma membrane, whilst cellubrevin plays a role in the endosomal translocation of GLUT4 and other proteins. The use of an IgA protease, which cleaves VAMP2 but not cellubrevin, blocked the majority of insulin-stimulated GLUT4 translocation (Cheatham *et al.*1996). Also, the introduction of GST-VAMP2 into permeabilised adipocytes caused an inhibition of insulin-stimulated GLUT4 translocation (Cheatham *et al.*1996; Martin *et al.* 1998; Millar *et al.* 1999), while in contrast GST-cellubrevin had no effect on insulin-stimulated GLUT4 translocation (Martin *et al.* 1998). GLUT4 translocation in 3T3-L1 adipocytes was also inhibited by 40-50% when they were treated with an N-terminal peptide of VAMP2 (Macaulay *et al.*1997; Olsen *et al.* 1997; Martin *et al.* 1998) and this same peptide was without effect on insulin-stimulated GLUT1 translocation (Martin *et al.* 1998). Conversely GST-cellubrevin inhibits insulin-stimulated GLUT1 translocation partially (Millar *et al.* 1999). From all of this evidence it was proposed that cellubrevin is important in the translocation of endosomal proteins (such as GLUT1) to the plasma membrane, whilst VAMP2 acts to specifically regulate the docking of GSVs in response to insulin.

Sortilin

Sortilin is a 110kDa protein that was originally found by its presence in GLUT4 vesicles of adipocytes (Morris *et al.* 1998). Insulin causes only a very small redistribution of sortilin from the LDM to the plasma membrane in 3T3-L1 adipocytes, which is surprising due to its presence in GLUT4 vesicles. This however could be because most of the sortilin may be in GLUT4 vesicles arising from

endosomes, rather than from the GSVs (Morris *et al.* 1998). Thus far a role for sortilin in GLUT4 trafficking has not been identified.

1.9 The SNARE hypothesis

The SNARE hypothesis provides a conceptual framework to explain how synaptic vesicles dock and fuse to the plasma membrane. This model states that the vesicle that is intended to fuse with the membrane contains a protein called a vesicle-SNARE (v-SNARE) and that the target membrane contains a target-SNARE (t-SNARE). Complementary v-SNARE and t-SNARE pairs are able to engage, and this could start the fusion event (Söllner *et al.* 1993a). It has been determined that all SNARE proteins share a homologous domain of ~60 amino acids that is referred to as the SNARE motif (Terrian & White 1997; Weimbs *et al* 1997; Weimbs *et al* 1998), which combine to form the SNARE complex (this will be discussed below). Several other proteins are also believed to be involved in the process, and will be discussed below.

One of these proteins is NSF (N-ethylmaleimide-sensitive factor (Block et al 1988). NSF is an ATPase that can bind several other proteins in the ATP bound state (Wilson *et al.* 1992) and NSF activity is required for membrane fusion to occur (Whiteheart *et al.* 1994). In the original experiments, which led to the formation of the SNARE hypothesis, Rothman and colleagues assembled a so-called 20S particle using NSF in the ATP bound state as bait. Five proteins were discovered to be part of the 20S complex: NSF, α-SNAP, syntaxin, SNAP25 and synaptobrevin/VAMP2 (Söllner *et*

al. 1993a and b). VAMP, syntaxin and SNAP25 are called SNAREs (soluble NSF attachment protein receptors) and it was determined that they can form a complex even in the absence of NSF and α-SNAP (Söllner *et al.* 1993b). When ATP was added to the 20S complex, it was hydrolysed by NSF and the complex was disassembled.

Many different isoforms of the SNAREs have since been identified, leading to the belief that the formation of a SNARE complex is an obligatory step in all membrane fusion (Bock *et al.* 1996; Advani *et al.* 1998; Prekeris *et al.* 1998). VAMPS are located on the cytoplasmic surface of vesicles (therefore named v-SNAREs) and are anchored in the membrane via their hydrophobic C-terminus, which contains a membrane- spanning domain (Trimble *et al.* 1988). Syntaxin and SNAP 25 are located in the target or plasma membrane (Söllner *et al.* 1993b) and are hence called t-SNAREs.

The original SNARE hypothesis proposed that pairing of the v-SNARE with the t-SNAREs results in vesicle docking at the plasma membrane, and that this complex must be broken up in order for fusion to occur. As a consequence of the fact that these three SNARE proteins can form a stable complex, an energy input is needed for this to happen. This was believed to be the reason why ATP hydrolysis by NSF, with the help of α-SNAP, is required. Consequent studies have indicated that this is an over-simplified view, and only accurate in parts. A modified model for SNARE complex function will be discussed below.

1.9.1 Evidence for the role of SNARE proteins and their specificity

Experiments using eight different botulinum and tetanus toxins provided evidence in favour of a role for these proteins in membrane fusion. These toxins act to inhibit synaptic vesicle exocytosis, and hence block nerve function. The toxins are proteases, five of which can cleave VAMP, two cleave SNAP25 and one cleaves syntaxin (as reviewed in Südhof 1995). However, these proteins can only be cleaved before assembly of the SNARE complex, and not when the complex has been formed (Hayashi *et al.* 1994). This indicates that the cleaving sites are not available to the toxins once the complex has formed. The cleavage of VAMP using these toxins resulted in inhibition of neurotransmitter release in the squid giant synapse, but increased the amount of docked synaptic vesicles. Taken together this evidence suggests that VAMP is not important in the docking of the vesicles, but that it has a later, post-docking function (Hunt *et al.* 1994).

Analysis of SNARE function in an *in vitro* assay demonstrated that the interaction of SNAREs on distinct vesicle populations promoted vesicle-vesicle fusion (Weber *et al.* 1998). This report gave rise to the so-called SNAREpin model of fusion, in which the SNARE proteins represent the minimal machinery necessary for membrane fusion. Although current models support the view that SNAREs mediate membrane fusion (or function just upstream from fusion), it is clear that SNAREs alone are not sufficient for membrane fusion *in vivo*, and that a large number of other accessory proteins are required for effective exocytosis.

1.9.2 The structure of the SNARE complex

The crystal structure of the SNARE complex of syntaxin1A, synaptobrevin 2 (VAMP2) and SNAP25 has been solved (Sutton *et al.* 1998) (Figure 1.5). Prior to this discovery, it was already known that the SNARE proteins form coiled coils (Chapman *et al.* 1994) and that syntaxin and synaptobrevin lie parallel to each other when in the complex (Hanson *et al.* 1997). This is relatively suprising, because both syntaxin and synaptobrevin/ VAMP are anchored in their respective membranes via their C-terminus. However, this position of the SNARE proteins brings the two opposite membranes in close proximity and this may help to drive the fusion of the membranes. The crystal structure revealed that the synaptic fusion complex is arranged as a cylinder consisting of one helix from both syntaxin and synaptobrevin, and of two helices from SNAP25 (Figure 1.5). The helices are positioned such that the N-termini are at one end of the bundle, and the C-termini at the other end. SNAP25 is not an integral membrane protein (it is bound to the membrane by palmitylation of cysteine residues present near the middle of the sequence (Chapman *et al.* 1994)), and thus has a linker region between the two helices. This linker region traverses the length of the cylinder. It is also of note that inside the coiled-coil, there is a highly conserved hydrophilic layer made of an arginine (R) residue from synaptobrevin, and three glutamine (Q) residues, one from syntaxin and two from SNAP25 (one from each helix). These residues are thought to stabilise each other and are sealed away from the surrounding solvent by a hydrophilic layer. For this reason, synaptobrevin/VAMP is sometimes called an R-SNARE and syntaxin and SNAP25 are called Q-SNAREs. Initially it was not clear why these polar residues are in the middle of the complex, but it has been demonstrated that they are required in order to

get efficient disassembly of the SNARE complex by α-SNAP and NSF (Scales *et al.* 2001). The SNARE complex is exceptionally stable and resistant to treatment with SDS which would usually be sufficient to dissociate other macromolecular complexes.

1.9.3 Syntaxin

Syntaxin was originally discovered as a consequence of its ability to bind to synaptogamin/p65 (Bennet *et al.* 1992), a synaptic vesicle protein important in calcium sensing (as reviewed in Südhof 1995). Syntaxin was cloned from rat brain and two isoforms were found, p35A and p35B (syntaxin 1A and 1B) both of which were found to be present largely at the plasma membrane at the site of neurotransmitter release (Bennet *et al.* 1992). Syntaxin is an integral membrane protein, with a short transmembrane region at the C-terminus of the protein (Bennet *et al.* 1992; Kee *et al.* 1995). The cytoplasmic region of syntaxin contains 4 coiled coil domains of which the one closest to the transmembrane region (H3) is the most important for binding VAMP, α-SNAP and SNAP25 (Calakos *et al.* 1994; Chapman *et al.* 1994; Kee *et al.* 1995; Hanson *et al.* 1995). Mutational studies of syntaxin have shown that the VAMP-syntaxin interaction is very specific and sensitive to mutations, whereas the interaction of SNAP25 with syntaxin is much less specific (Kee *et al.* 1995). Both the H3 region (Wu *et al.* 1999) and the N-terminal H_{abc} helical region of syntaxin1A can bind synaptogamin in a Ca^{2-} manner, and this is part of the calcium trigger in neurotransmitter release (Fernandez *et al.* 1998).

One protein thought to be important in SNARE complex regulation that can bind syntaxin is nsec1/munc 18. This protein requires both the H3 region and the N-

terminal H_{abc} helical region of syntaxin1A for binding, and thus prevents the binding of syntaxin to the other SNARE proteins (Pevsner *et al.* 1994, Kee *et al.* 1995; Fernandez *et al.* 1998). Recently the crystal structure of the munc18a-syntaxin1A structure has been identified (Figure 1.6) (Misura *et al.* 2000). The crystal structure showed that when syntaxin1A is in complex with munc 18a, that the H_{abc} helical region of syntaxin1A is brought into close proximity with the H3 helix involved in interacting with VAMP and SNAP25, and consequently prevents SNARE complex formation. It is therefore believed that syntaxin can form three different conformations, one in isolation, one in the SNARE complex, and a third when bound to munc 18a (Misura *et al.* 2000).

There are many non-neuronal forms of syntaxin, and syntaxin is involved not only with fusion of vesicles with the plasma membrane, but also in trafficking between various membrane compartments, such as ER to Golgi, and Golgi to endosomes (Bock *et al.* 1996; Advani *et al.* 1998; Prekeris *et al.* 1998; Tang *et al.* 1998). The non neuronal isofrom syntaxin4 is important in the translocation of GLUT4 and will be discussed in detail below.

1.9.4 VAMP

VAMP1 was originally cloned from the brain of a cartilaginous fish and found to be predominantly present on the synaptic vesicles (Trimble *et al.* 1988). This protein has a molecular mass of 13KDa,and can be divided into three structural domains. The C-terminus is hydrophobic and spans the vesicle membrane, and the N-terminal domain, which contains a proline-rich sequence, and a long hydrophilic stretch, is exposed to the cytoplasm (Trimble *et al.* 1988). Many homologues of VAMP have been

identified, varying in length, and not all of them have this proline-rich N-terminus (Advani *et al.* 1988). As detailed above, VAMP can bind both syntaxin and SNAP25 (Söllner *et al.* 1993b) via coiled-coil regions, but the individual interactions between both proteins are relatively weak, and it was shown that SNAP25-syntaxin heterodimers form a high affinity binding site for VAMP (Chapman *et al.* 1994; Hayashi *et al.* 1994). Unlike syntaxin, VAMP does not bind α-SNAP directly (McMahon & Südhof 1995; Hanson *et al.* 1995) and this suggests a post-docking role for α-SNAP (McMahon & Südhof 1995).

1.9.5 The regulation of the SNARE complex and Munc 18/nsec1

Undoubtedly the regulation of the formation of the SNARE complex is crucial to permit the fusion of the correct vesicles with the target membrane. Rab proteins are believed to play a role in regulating the specificity of vesicle trafficking events, and the large number of rab proteins present would make them suitable candidates for SNARE complex regulation (as reviewed in Lin & Scheller 2000). Although rab proteins are not part of the SNARE complex (Söllner *et al.* 1993b), they are believed to play a role in the assembly of the SNARE complex, and were suggested to act as a catalyst (Søgaard *et al.* 1994).

Another important regulatory protein of SNARE complex formation is Munc 18. This protein is part of the Sec1/Munc18 protein family (SM proteins). These proteins are ~60kDa in size and show homology throughout their sequence, indicating no particular domain is associated with their primary function. The first SM protein to be identified was UNC-18 in a genetic screen for uncoordinated phenotypes in *C.*

elegans (Brenner 1974). Sec1 was later identified in screens for genes involved in the yeast secretory family. The mammalian homologue, munc 18a, was identified by virtue of its ability to bind syntaxin1 (Hata *et al.* 1993). It has since been discovered that all types of intracellular membrane traffic require an SM protein (for a review see Jahn *et al.* 1999; Jahn & Südhof 1999).

Munc 18a/nSec1 is the neuronal homologue of the yeast protein sec1p, and it is known to be important in neurotransmitter release (as reviewed in Lin & Scheller 2000). Munc 18 has been shown to bind to syntaxin alone, but not to syntaxin in the SNARE complex, and the binding of Munc 18 to syntaxin inhibits the formation of the syntaxin-VAMP-SNAP25 complex (Pevsner *et al.* 1994). An interesting discovery is that phosphorylation of Munc 18 by PKC inhibits the Munc 18-syntaxin interaction, and this may facilitate the formation of the SNARE complex (Fujita *et al.* 1996).

A recent elucidation was the three dimensional structure of the complex of syntaxin1A with nSec1/ munc 18a (Misura *et al.* 2000). Interaction between the two proteins is complex, involving both the N- and C- terminal cytoplasmic domain of syntaxin, and the whole of Munc 18. The munc 18a was seen to be an arch-shaped molecule, divided into three domains, with a central cavity. This central cavity provides the binding surface for syntaxin1A. Syntaxin1A binds to this surface making extensive contacts through the H_{abc} domain and the SNARE motif. This interaction therefore prevents the syntaxin1A protein from forming a SNARE complex, and suggests that a mechanism must exist in order to dissociate or alter the conformation of the Munc 18a so as to permit SNARE complex formation (Misura *et al.* 2000).

A structure-based sequence alignment (of four SM proteins with Munc 18a, and four syntaxin proteins with syntaxin1A) identified that most of the interactions between syntaxin1A and Munc 18a are largely conserved throughout the Sec1 and syntaxin like proteins. A smaller number of interactions are not conserved among Sec1 family members, and this may contribute to the binding specificity between a particular Sec1-like protein and its partner syntaxin (Misura *et al.* 2000). One such pair is munc 18c and syntaxin4, and the importance of munc 18c in translocation of GLUT4 will be discussed below.

Dissociation of the syntaxin-munc 18 complex is believed to be brought about by a conformational change in munc 18, and is probably mediated by other protein(s) such as rab or a rab effector. Two proteins that have been implicated in mediating the transition between the syntaxin1-Munc 18a complex and the SNARE complex are UNC-13/ Munc 13 and Rab3 interacting molecule (RIM). Munc 13 was shown to interact with an amino-terminal region of syntaxin1 (Betz *et al.* 1997), and in *C.Elegans*, UNC-13 displaces syntaxin from UNC-18 (Sassa *et al.* 1999). RIM and Munc 13 have been shown to interact functionally, suggesting a role for RIM in regulating the primary activity of Munc 13 (Betz *et al.* 2001).

It was thought originally that all SM proteins functioned by binding to closed conformations of syntaxins. However recent discoveries have shown this not to be the case. Sec1 binds to core complexes containing the plasma membrane syntaxin Sso1, rather than to isolated Sso1 (Carr *et al.* 1999). Furthermore, the yeast and mammalian syntaxins that function at the TGN and in early endosomes (Tlg2/syntaxin16), and in

the endoplasmic reticulum (Ufe1/syntaxin18) and the Golgi (Sed5/syntaxin5) bind tightly to their corresponding SM proteins (Vps45 and Sly1) through a short amino-terminal motif (Yamaguchi *et al.* 2002; Dulubova *et al.* 2002). The crystal structure of the SM protein Sly1 showed considerable conservation, and had the same arch-shape, to that of Munc 18a. However, here the Sed5 does not bind to the central cavity of the SM protein (unlike syntaxin1A), but instead to the outer surface of one of the domains (Bracher & Weissenhorn 2002). This binding pattern is very different from the syntaxin1-Munc 18a interaction, and is compatible with core complex formation and may recruit SM proteins to the sites of fusion, permitting SM proteins and SNAREs to carry out active functions simultaneously.

1.9.6 The docking and fusion of vesicles with the membrane

The release of neurotransmitter into the presynaptic cleft, and indeed many other processes involving the fusion of vesicles with target membranes, initiates with the translocation of those vesicles to the membrane (Figure 1.7). Attachment of these vesicles to the membrane can be divided into two stages: tethering and docking (as reviewed in Foster & Klip 2000).

Tethering of the vesicles on the membrane occurs by a process of which there is limited knowledge, probably involving rab proteins and their effectors. The exocyst complex has also been implicated in either the tethering or docking of exocytotic vesicles (Lipschutz & Mostov 2002). The yeast exocyst complex consists of eight proteins: Sec3, Sec5, Sec6, Sec8, Sec10, Sec15, Exo70 and Exo84. Recent evidence has suggested a role for this complex in the fusion of GLUT4 vesicles with the plasma

membrane (Inoue *et al.* 2003). A number of studies have however established that neither SNARE proteins nor NSF and α-SNAP are required for this tethering step (Hunt *et al.* 1994; DeBello *et al.*1995; McMahon & Südhof 1995; Nichols *et al.* 1997)

The formation of the SNARE complex then docks the vesicles to the plasma membrane and leads ultimately to membrane fusion. Syntaxin is initially in the closed conformation, bound to Munc 18 as described above. A conformational change in Munc 18, mediated by other proteins, allows syntaxin to now form a SNARE complex with VAMP and SNAP25. This brings the two membranes into close proximity and leads to fusion by a mechanism not clearly understood.

Disassembly of the SNARE complex is known to involve NSF and α-SNAP (Hayashi *et al.* 1995; Nagiec *et al.* 1995; Barnard *et al.* 1997; Rice & Brunger 1999), but in contrast to the original SNARE hypothesis, NSF and α-SNAP are not required for the fusion itself (Nichols *et al.* 1997). Instead NSF and α-SNAP are required to disassemble the *cis* SNARE complexes, using the ATPase activity of NSF, which recycles the SNARE proteins for a further round of exocytosis.

Evidence from yeast vacuolar fusion has shown that NSF and α-SNAP are involved in a pre-docking stage (Mayer *et al.* 1996). This is unexpected, but could be explained by the suggestion that NSF and α-SNAP are necessary for the disassembly of *cis* SNARE complexes that occur after membrane fusion. In order for a new cycle of vesicle fusion to occur, the complex of SNARE proteins has to be disassembled and the proteins recycled to their correct location (as reviewed in Lin & Scheller 2000). However, NSF has also been identified in a complex with rab5 and EEA1, and it was suggested that NSF could prime SNARE proteins before fusion (McBride *et al.* 1999).

Evidently more research is needed in order to further determine the full function of the proteins involved in the translocation and fusion of vesicles with their target membrane.

1.10 SNARE proteins in GLUT4 translocation

Despite GLUT4 exocytosis being a much slower process than neurotransmitter release, it resembles this process in a number of ways. In both processes, vesicles containing cargo are stored intracellularly until a signal triggers their translocation to the plasma membrane. For neurotransmitter release this signal is entry of calcium into the cell, whilst in GLUT4 exocytosis the signal is the binding of insulin to its receptor, and the consequent signalling cascade. Docking of vesicles at the plasma membrane then leads to fusion and release of cargo either into the synaptic cleft (in neurotransmitter release) or by insertion of GLUT4 into the plasma membrane. The similarity of the two mechanisms led to the search for a SNARE type mechanism in insulin sensitive tissue, and resulted in a more detailed knowledge of GLUT4 translocation in these cells.

Homologues of many SNARE proteins have been identified in fat and muscle cells. VAMP2 and cellubrevin (a VAMP homologue) have been found in rat adipocytes (Cain *et al.* 1992; Martin *et al.* 1996), 3T3-L1 adipocytes (Tamori *et al.* 1996; Martin *et al.* 1996) and muscle cells (Volchuk *et al.* 1994; Kristiansen *et al.*1996). The use of *Clostridial botulinum* neurotoxins has demonstrated that cleavage of cellubrevin and VAMP2 will inhibit insulin-mediated GLUT4 translocation (Cheatham *et al.*1996;

Macaulay *et al.*1997). The use of an IgA protease, which cleaves VAMP2 but not cellubrevin, also blocked the majority of insulin-stimulated GLUT4 translocation (Cheatham *et al.*1996). Also, the introduction of GST-VAMP2 into permeabilised adipocytes caused an inhibition of insulin-stimulated GLUT4 translocation (Cheatham *et al.*1996; Martin *et al.* 1998; Millar *et al.* 1999), while in contrast GST-cellubrevin had no effect on insulin-stimulated GLUT4 translocation (Martin *et al.* 1998). GLUT4 translocation in 3T3-L1 adipocytes was also inhibited by 40-50% when they were treated with an N-terminal peptide of VAMP2 (Macaulay *et al.*1997; Olsen *et al.* 1997; Martin *et al.* 1998) and this same peptide was without effect on insulin-stimulated GLUT1 translocation (Martin *et al.* 1998). Conversely GST-cellubrevin inhibits insulin-stimulated GLUT1 translocation partially (Millar *et al.* 1999). From this evidence it was proposed that cellubrevin is important in the translocation of endosomal proteins (such as GLUT1) to the plasma membrane, whilst VAMP2 acts to specifically regulate the docking of GSVs in response to insulin.

There has been much research directed on identifying the exact intracellular location of both VAMP2 and cellubrevin. Both proteins translocate from intracellular stores to the plasma membrane in response to insulin and are found in GLUT4 vesicles (Cain *et al.* 1992; Martin *et al.* 1996; Tamori *et al.* 1996; Timmers *et al.* 1996). Endosome ablation determined that cellubrevin was ablated to a similar degree as TfR, whilst VAMP2 was only ablated by around 10%. This data and vesicle adsorption together with ablation indicate that cellubrevin is enriched in the endosomal GLUT4 vesicles, whilst VAMP2 is present in the GSVs (Martin *et al.* 1996).

Syntaxin4 is expressed in a number of tissues, and high levels of the protein were found at the plasma membrane in adipocytes (Timmers *et al.* 1996; Tellam *et al.* 1997) and muscle (Volchuk *et al.* 1996). Lower levels of syntaxin4 were also found in intracellular membranes (Timmers *et al.* 1996; Tellam *et al.* 1997) and from there it apparently undergoes translocation to the plasma membrane in response to insulin in a similar manner to GLUT4 (Tellam *et al.* 1997).

Insulin stimulated glucose transport was shown to be inhibited by injection of either antibodies to syntaxin4 (Tellam *et al.* 1997) or of a syntaxin4 peptide into adipocytes (Macaulay *et al.* 1997; Olson *et al.* 1997). Likewise the treatment of permeabilised 3T3-L1 adipocytes with GST-syntaxin4 caused the inhibition of insulin stimulated GLUT4 translocation (Cheatham *et al.* 1996). However the introduction of a cytoplasmic syntaxin4 peptide into cells did not inhibit insulin mediated GLUT1 translocation (Olson *et al.* 1997). Taken together, this supports a specific role for syntaxin4 in GLUT4 vesicle fusion at the plasma membrane.

Evidence for the presence of SNAP25 in adipocytes is uncertain, but two SNAP25 homologues called SNAP23 and syndet have been identified, and shown to be expressed in fat and muscle tissue (Ravichandran *et al.* 1996; Wong *et al.* 1997; Araki *et al.* 1997; Rea *et al.* 1998). Both proteins are predominantly located within the plasma membrane fraction, as expected (Wong *et al.* 1997; Araki *et al.* 1997; Rea *et al.* 1998).

An antibody to syndet as well as a C-terminal peptide have been shown to inhibit insulin stimulated GLUT4 translocation by 40%, but did not inhibit GLUT1 translocation (Rea *et al.* 1998). The use of yeast two hybrid studies revealed that

SNAP23 can bind strongly to syntaxin1 and 4 (Araki *et al.* 1997) as well as VAMP1 and 2 (Ravichandran *et al.* 1996). Similarly, surface plasmon resonance experiments have shown that syndet can bind syntaxin4 and VAMP2 individually and that this is disrupted by 0.5% SDS, while incubation of all three proteins together resulted in a 0.5% SDS resistant complex formation (Rea *et al.* 1998).

Screening of rat adipocytes for α-SNAP and NSF determined that both proteins are intracellularly located, and to a substantial extent are present on GLUT4 vesicles (Mastick *et al.* 1997).

It is believed that in insulin-sensitive tissues, GLUT4 translocation occurs via a SNARE type mechanism, similar to neuronal cells, involving the formation of a complex made of syntaxin4, VAMP2, syndet/SNAP23 as well as α-SNAP and NSF. Furthermore the formation of a 20S SNARE complex in vitro has been confirmed and shown to be independent of insulin treatment (St-Denis *et al.* 1999).

Regulation of SNARE mechanism in GLUT4 translocation

The importance of a SNARE mechanism for GLUT4 translocation presents a question of how it is regulated and how insulin affects the mechanism. As mentioned previously, there are a number of proteins important for the regulation of the SNARE complex. One such protein is Munc 18, of which several isoforms exist (Tellam *et al.* 1995). Munc 18c is ubiquitously expressed, and its subcellular location in adipocytes is almost identical to that of syntaxin4 with highest levels found in the plasma

membrane fraction, and lower levels in the LDM fraction (Tellam *et al.* 1997). In vitro binding studies demonstrated that Munc 18c bound strongly to syntaxin4 (Tellam *et al.* 1997; Tamori *et al.* 1998) and that it was able to reduce the association of syntaxin4 and VAMP2 by 75%. Munc 18c was also able to reduce the binding of cellubrevin to syntaxin4 by 60% (Tellam *et al.* 1997). Co-immunoprecipitation experiments demonstrated that syntaxin4 can bind both SNAP23 and Munc 18c *in vivo*, but that Munc 18c decreases the affinity of syntaxin4 for SNAP23 (Araki *et al.* 1997).

Overexpression of Munc 18c in 3T3-L1 adipocytes inhibits insulin-stimulated GLUT4 translocation, but not that of GLUT1 (Tamori *et al.* 1998), suggesting an inhibitory role for munc 18c. Similarly, microinjection of antibodies to Munc18c into 3T3-L1 cells stimulated GLUT4 translocation (Macaulay *et al.* 2002).

These munc18c-syntaxin4 interactions have been demonstrated to be lost upon insulin stimulation (Thurmond *et al.* 1998), which again suggests that munc 18c has an inhibitory role, preventing SNARE complex formation until the correct signal (the presence of insulin) is received.

In contrast, the introduction into adipocytes of a peptide fragment of Munc18c (18c/pep3) that inhibits the binding of Munc18c to syntaxin4 resulted in inhibition of insulin-stimulated integration of GLUT4 vesicles into the plasma membrane (Thurmond *et al.* 2000), which suggests that the interaction between Munc18c and syntaxin4 is required for this process. In these cells, GLUT4 vesicles were found just below the membrane, though unable to undergo fusion. It is however thought that this peptide may be derived from a region that does not directly contact syntaxin but instead represents Rab or Rab effector binding sites whose conformations are critical

to syntaxin binding (Misura *et al.* 2000; Bracher & Weissenhorn 2002). Thus, this peptide may induce some other effects on Rab or Rab effectors in addition to disrupting the association between synatxin4 and Munc18c. Thus the exact function of munc 18c in GLUT4 translocation is not certain.

Another SNARE complex regulator is synip (Min *et al.* 1999). Synip is a syntaxin4 binding protein, and its expression is restricted to adipocyte and muscle cells. Synip binding to syntaxin4 prevents VAMP2 from interacting with syntaxin4, but not SNAP23/syntaxin4 binding (Min *et al.* 1999). Interestingly in the presence of insulin the affinity of synip for syntaxin4 is reduced, implying that this protein is an insulin-sensitive regulator for GLUT4 translocation. This theory is supported by the fact that a C-terminal peptide of synip can inhibit insulin-mediated GLUT4 but not GLUT1 translocation. It is believed that the N-terminus of synip may contain a regulatory domain, which causes the insulin-mediated decrease of syntaxin-synip interaction, thereby allowing SNARE complex formation and subsequent fusion of the GSVs with the plasma membrane (reviewed in Bennet 1999).

A further protein identified in insulin-sensitive cells is the cysteine-string protein Csp1 (Chamberlain *et al.*2001). This protein interacts with syntaxin4 in 3T3-L1 adipocytes, and it has been proposed that it may be a chaperone of syntaxin4, regulating the conformational status of the protein.

Two proteins have been identified that interact with VAMP2, and proposed to prevent the entry of the v-SNARE into the SNARE complex in the absence of insulin. These proteins are pantophysin (Brooks *et al.* 2000) and VAP33 (vesicle-associated protein

33) (Foster *et al.* 2000), although the mechanism by which this regulation occurs is unknown.

From these studies it is therefore evident that the SNARE mechanism is absolutely vital for GLUT4 entry into the plasma membrane and subsequent glucose transport. Decreased insulin-stimulated glucose uptake due to a defect in GLUT4 translocation could therefore be explained by a fault in the SNARE mechanism.

Aims of this Study

The first objective of this study was to initially repeat the experiment, using sucrose gradients, in order to isolate GSVs from 3T3-L1 adipocytes. It was intended then to further characterise these GSVs by determining whether a number of proteins co-localise with GLUT4, and whether any co-localisation was seen to be with the GSVs or the endosomal GLUT4 vesicles. It was also an aim to identify any proteins found to be exclusive to GSVs via a number of gel-staining techniques. If these methods proved successful using 3T3-L1 adipocytes, it was then an objective to carry out similar analysis in other cell-types, in order to identify any proteins native to GSVs from different cell-types. Any such proteins are likely to be of significance.

In Chapter 4, we aimed to produce a mutated form of the neuronal munc 18a, in order to alter its syntaxin-binding properties to become more like munc 18c, which has an inhibitory role to play in GLUT4 translocation to the plasma membrane. If the mutations were successful in allowing interaction with syntaxin4 to occur, it was then proposed to produce a recombinant Adenovirus construct (of the mutated protein) to

drive expression in mammalian cells. If this step was successful, it was then an objective to overexpress the munc 18 in insulin sensitive cells in order to determine whether the mutated munc 18 protein, with its altered syntaxin-binding properties, had any effect upon glucose transport. This could make it possible to establish the importance of the munc 18c-syntaxin4 interaction on GLUT4 integration into the plasma membrane.

Figure 1.1 Insulin signalling pathways in insulin mediated glucose uptake (from Kanzaki & Pessin 2003)

Shown opposite are the two insulin signalling pathways involved in the translocation of GLUT4 containing vesicles to the plasma membrane. 'Signal 1' represents the classical PI3-kinase pathway, where the insulin receptor uses IRS proteins to activate PI3-kinase, leading ultimately to the activation of PKB and atypical PKC.

'Signal 2' represents the PI3-kinase independent pathway. Here upon insulin binding its receptor, ultimately the TC10 GTPase is activated. It is believed that a downstream target for TC10 could be the exocyst complex, and that the TC10–exocyst complex is then responsible for targeting GLUT4-containing vesicles to appropriate plasma membrane fusion sites.

Figure 1.1

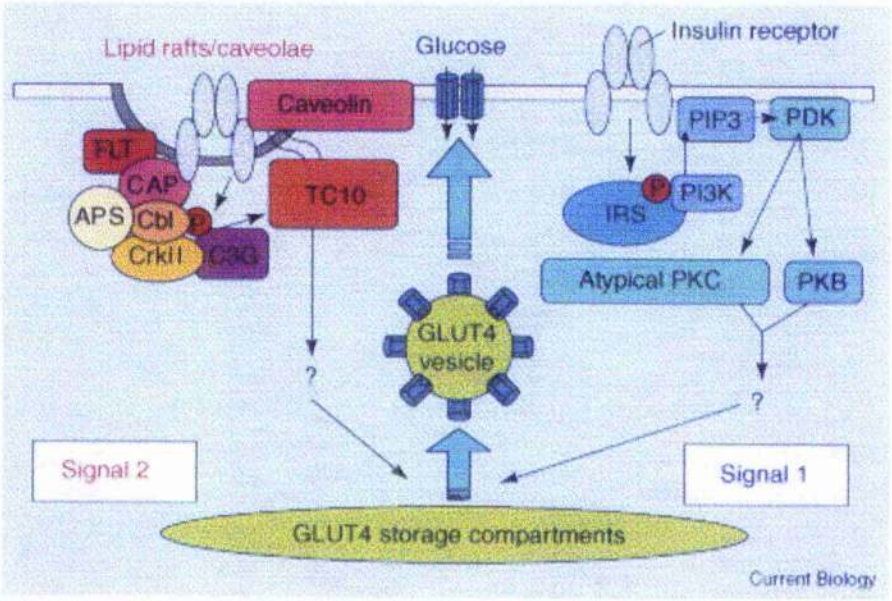
Lipid rafts/caveolae
Glucose
Insulin receptor
Caveolin
FLT
CAP
APS
Cbl
CrkII
C3G
TC10
PIP3
PDK
P
PI3K
IRS
Atypical PKC
PKB
GLUT4
vesicle
?
?
Signal 2
Signal 1
GLUT4 storage compartments
Current Biology

Figure 1.2 Glucose transporter structure

A schematic model for the transmembrane organisation of a GLUT is shown opposite. Shown are the twelve membrane-spanning helices, and the loops between helices 1 and 2, and 6 and 7. Note that both the N- and C-terminus are intracellular.

Figure 1.2

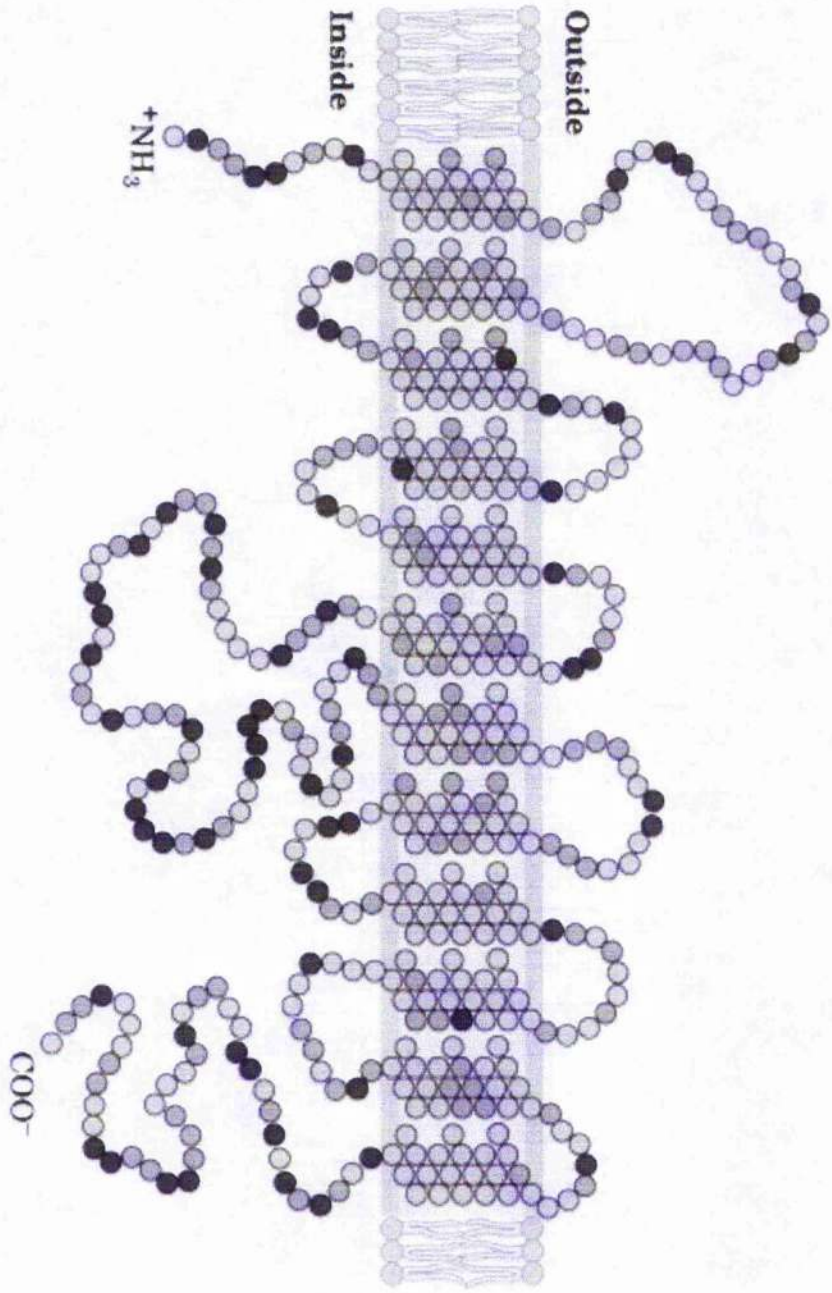

Figure 1.3 Membrane-protein recycling models (Holman *et al.* 1994)

A In the 2-pool model, the fully functional plasma membrane protein (T_p) is in equilibrium with only one intracellular pool (T_{ee}). **B** In the 3-pool model, two distinct intracellular pools are designated. These are the early endosomal pool (T_{ec}), and the tubulo-vesicular compartment (T_{tv}). **C** and **D** In the 4-pool models, occluded forms are added to the plasma membrane occurring either before (T_{po}, **C**) or after (T_{pc}, **D**) the fully functional plasma membrane pool. **E** In the 5-pool model, two occluded plasma membrane pools are included, in addition to the two intracellular pools.

Figure 1.3

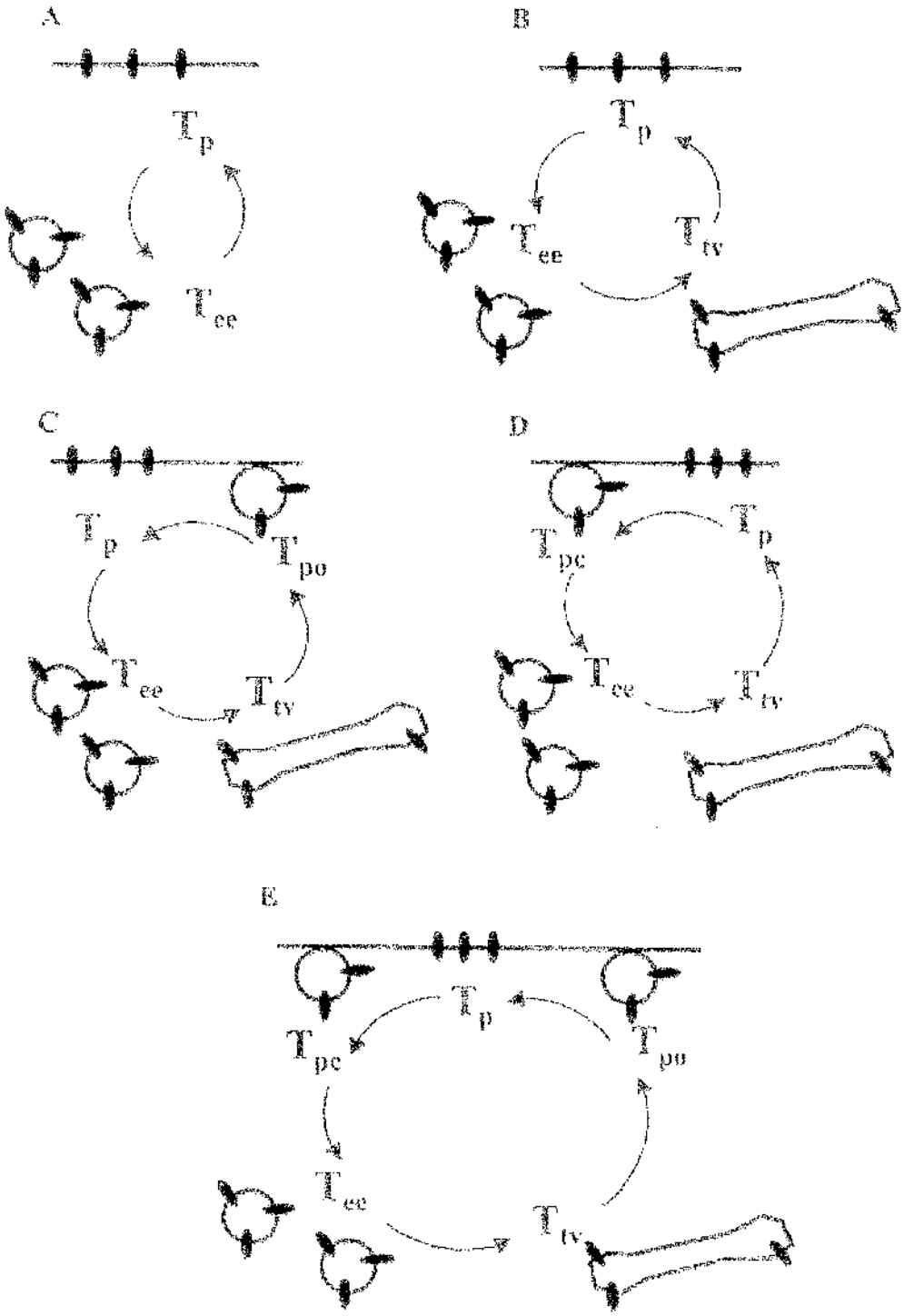
A
T_p
T_{ee}
B
T_p
T_{ee}
T_{tv}
C
T_p
T_{po}
T_{ee}
T_{tv}
D
T_{pc}
T_p
T_{ee}
T_{tv}
E
T_p
T_{pc}
T_{po}
T_{ee}
T_{tv}

Figure 1.4 GLUT4 trafficking in cells (from Bryant *et al.* 2002)

Shown is a schematic representation of GLUT4 trafficking. GLUT4 (and other proteins such as transferrin receptor) are internalised from the plasma membrane (PM) into endosomes, from where they are packaged into recycling endosomes. Most of the transferrin receptor, but only a low percentage of GLUT4 then recycles back to the plasma membrane (cycle 1).

GLUT4 is packed into specialised GLUT4 storage vesicles (GSVs) from the TGN. In the absence of insulin the GSVs may fuse with endosomes, accounting for the appearance of a small pool of GLUT4 in endosomes, even in the absence of insulin (cycle 2). In the presence of insulin however, these GSVs fuse with the PM, and therefore insertion of GLUT4 into the PM occurs.

Figure 1.4

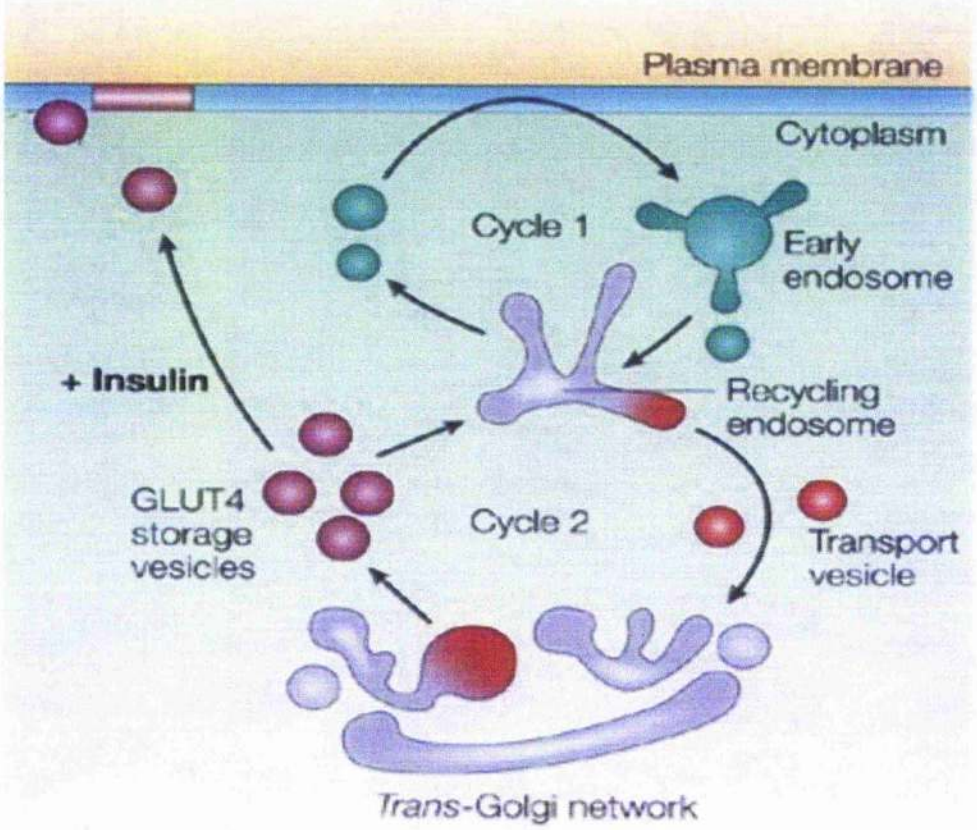
Plasma membrane
Cytoplasm
Cycle 1
Early endosome
+ Insulin
Recycling endosome
GLUT4 storage vesicles
Cycle 2
Transport vesicle
Trans-Golgi network

Figure 1.5 Crystal structure of the synaptic fusion complex (Sutton *et al.* 1998)

The SNARE complex is formed from four helices, one from syntaxin (red), one from VAMP/synaptobrevin (blue) and two from SNAP25 (green) form a coiled-coil structure. The 4 helices are arranged in a parallel manner. The transmembrane domains of VAMP/synaptobrevin and syntaxin are included (yellow) as well as the linker region of SNAP25 (brown). Note here that the illustrated helices form only a part of each protein.

Figure 1.5

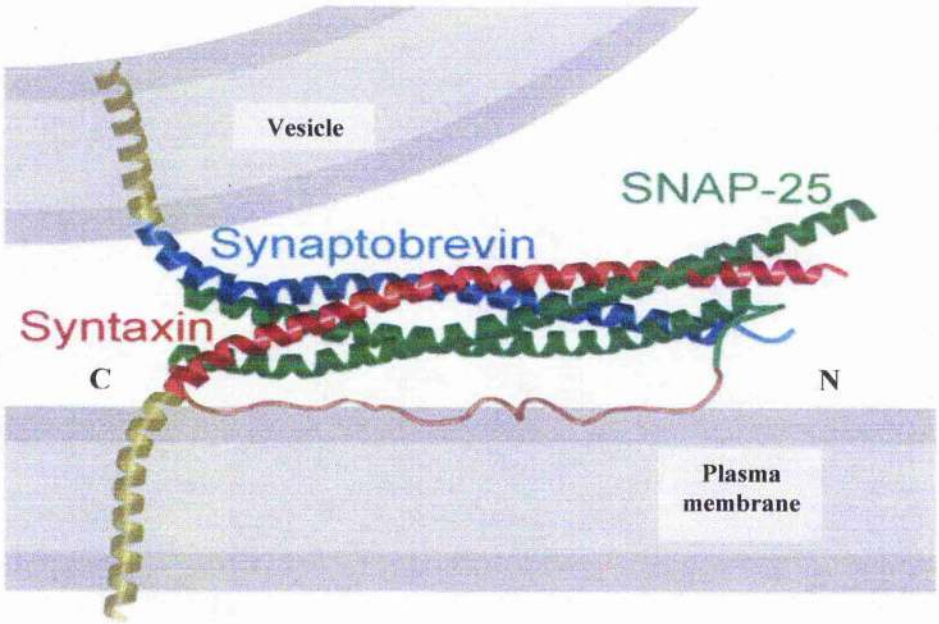
Vesicle
SNAP-25
Synaptobrevin
Syntaxin
C
N
Plasma membrane

Figure 1.6 The munc 18a-syntaxin1a complex crystal structure (from Misura *et al.* 2000).

The figures opposite show the crystal structure of the interaction between the SM protein munc 18a and syntaxin1A (**a** and **b** show the same structure, but with a 90° rotation about the vertical axis). Domain 1 (of munc 18a) is shown in blue, domain 2 in green and domain 3 in yellow. The three domains form an arch-shaped structure.

The H_{abc} domain of syntaxin1A is shown in red, the H3 domain (which can form part of the SNARE complex) is shown in purple and the linker region between these two is shown in orange.

Note here that syntaxin1A binds in the groove formed by the arch-shape of the three munc 18a domains, and that when the complex is formed the H_{abc} and H3 domains of syntaxin1A are in close proximity. This is thought to represent the "closed" conformation of synatxin1 that prevents SNARE complex formation.

Figure 1.6

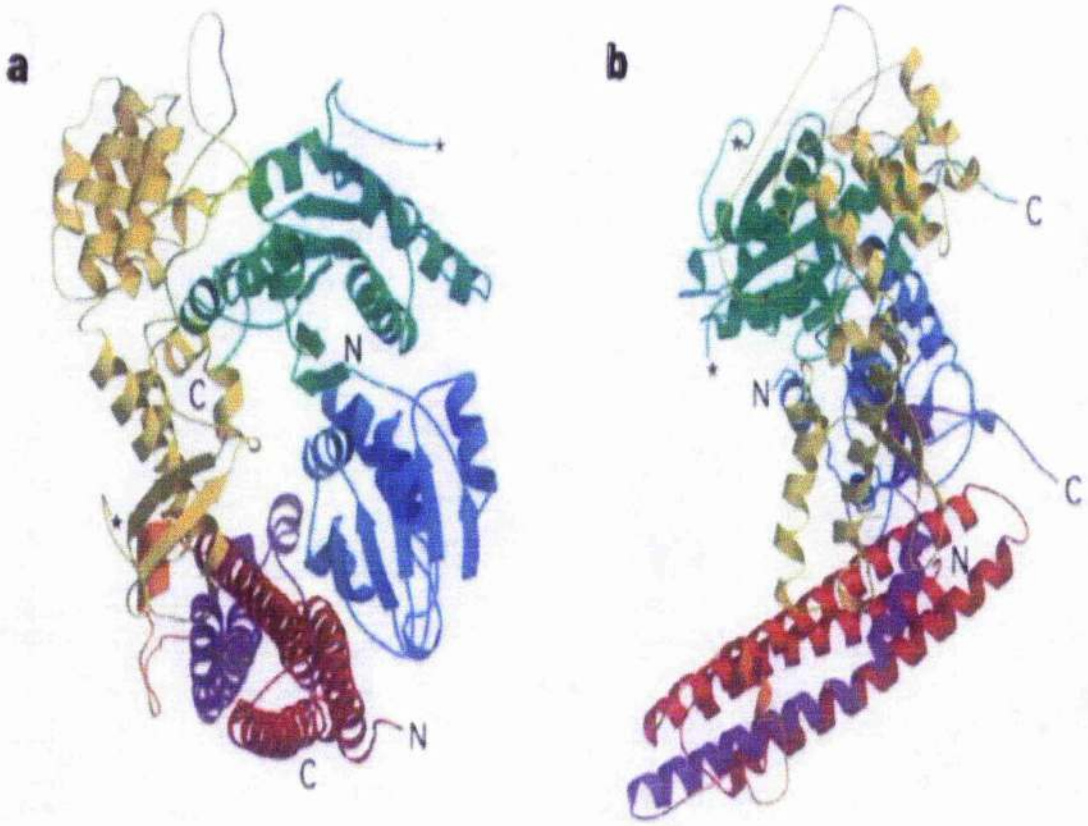

Figure 1.7 Model for the docking and fusion of vesicles with the plasma membrane

Syntaxin is initially in the 'closed' conformation, bound to the nsec1/munc 18. This interaction prevents SNARE complex formation. Action of a Rab/ Rab effector then causes a conformational change in nsec1, and a loss of interaction with syntaxin. As a result, the v-SNARE and t-SNARE proteins can form A SNARE complex, and membrane fusion occurs.

After fusion occurs, NSF and α-SNAP are required to disassemble the *cis*-SNARE complexes that remain on the same mebrane. This requires the ATP-ase activity of NSF, and allows the SNARE proteins to be recycled for a further round of fusion.

Figure 1.7

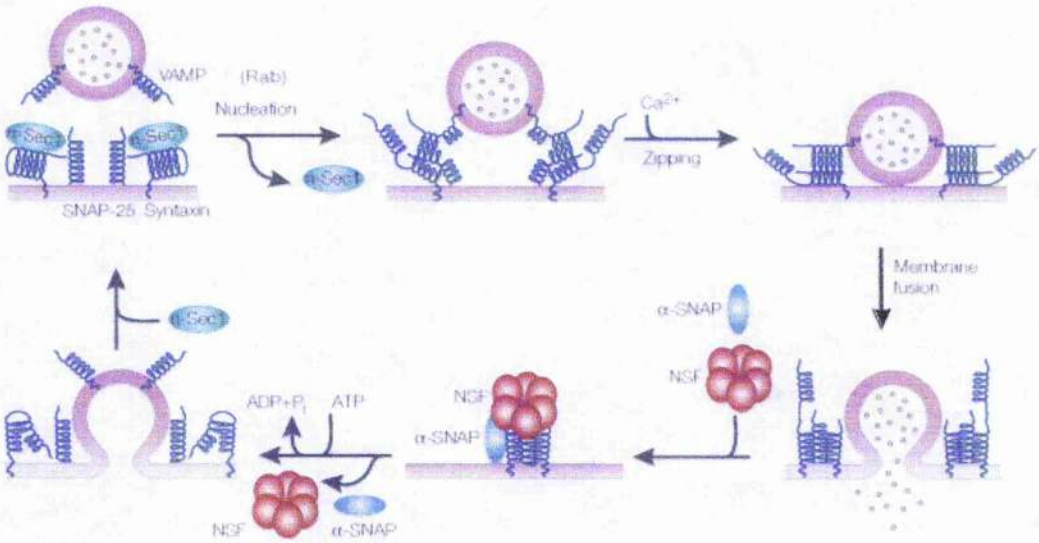
VAMP
(Rab)
Nucleation
Sec1
Sec1
Sec1
SNAP-25 Syntaxin
Ca2+
Zipping
Membrane fusion
α-SNAP
NSF
NSF
α-SNAP
ADP+Pi
ATP
Sec1
NSF
α-SNAP

CHAPTER 2 – MATERIALS AND METHODS

2.1 Materials

All reagents used in the course of the project were of a high quality and were obtained from the following suppliers:

2.1.1 General Reagents

Amersham International Plc, Aylesbury, Buckinghamshire, UK

Horseradish peroxidase (HRP)-conjugated donkey anti-rabbit IgG antibody

Horseradish peroxidase (HRP)-conjugated sheep anti-mouse IgG antibody

ECL Western blotting detecting reagents

ECL plus Western blotting detecting reagents

Glutathione Sepharose 4B

Anachem Ltd, Luton, Bedfordshire, UK

30% acrylamide/bisacrylamide

Bio-Rad Laboratories Ltd, Hemel Hempsted, Hertfordshire, UK

N, N, N', N'-tetramethylethylenediamine (TEMED)

Boehringer Mannheim, Germany

Tris

Protease Inhibitor cocktail tablets

Fisher Ltd, Loughborough, Leicestershire, UK

Ammonium persulfate

Diaminoethanetetra-acetic acid, Disodium salt (EDTA)

Disodium hydrogen orthophosfate (Na_2HPO_4)

Glycerol

Glycine

N-2-hydroxyethylpiperazine-N'-2-ethanesulphonic acid (HEPES)

Hydrochloric Acid (HCl)

Methanol

Potassium Chloride (KCl)

Potassium Dihydrogen orthophosfate (KH_2PO_4)

Sodium dodecyl sulfate (SDS)

Sodium Chloride (NaCl)

Sucrose

Kodak Ltd, Hemel Hempsted, Hertfordshire, UK

X-Omat S film

Merck Ltd (BDH), Lutterworth, Leicestershire, UK

Magnesium Chloride ($MgCl_2$)

Tween 20

New England Biolabs (UK) Ltd, Hitchin, Hertfordshire, UK

Prestained protein marker, broad range (6-175kDa)

Novo Nordisk, Denmark

Insulin

Nycomed, Norway

OptiPrep™ (Iodixanol)

Quiagen, Crawley, West Sussex, UK

Ni-NTA Agarose

Schleicher & Schuell, Dassel, Germany

Nitrocellulose membrane (pore size: 0.45μM)

2.1.2 Cell Culture Materials

American Type Culture Collection, Rockville, USA

3T3-L1 fibroblasts

Gibco BRL, Paisley, UK

Foetal bovine serum (FBS)

New born calf serum (NCS)

Dulbecco's modified Eagle's medium (without sodium pyruvate, with 4500mg/L glucose) (DMEM)

Opti-MEM

10000 U/ml penicillin, 10000U/ml streptomycin

Trypsin/EDTA solution

Costar

75cm^2 cell culture flasks

Falcon

10cm cell culture plates

Bibby Sterlin Ltd, Stone, Staffordshire, UK

Sterile pipettes

Unless inidicated all other reagents were obtained from Sigma Chemical Company, Dorset, UK

2.2 General Buffers

Phosphate Buffered Saline (PBS)

137mM NaCl, 2.6mM KCl, 10mM Na_2HPO_4, 1.7mM KH_2PO_4 (pH 7.4)

Homogenisation Buffer (HES)

255mM sucrose, 20mM HEPES, 1mM EDTA (pH 7.4)

Sucrose Gradient Buffer

20 mM HEPES, 100 mM NaCl, 1 mM EDTA (pH 7.4)

SDS-PAGE Buffers

Electrode Buffer

25mM Tris base, 192mM glycine, 0.1%(w/v) SDS

Sample Buffer

93mM Tris.HCl; pH 6.8, 1mM EDTA, 10% (v/v) glycerol, 2% (w/v) SDS, 0.002% (w/v) bromophenol blue and (20mM dithiothreitol added immediately prior to use).

Western Blotting Buffers

PBS-T

PBS (pH7.4), 0.1% (v/v) Tween-20

Transfer Buffer

25mM Tris base, 192mM glycine, 20% (v/v) methanol

Protein Purification & Binding Buffers

His_6-tag Purification Buffer

50mM imidazole, 20mM Hepes, 200mM KCl, 2mM β-mercaptoethanol, 2mM $MgCl_2$,10% glycerol (pH 7.0)

Breaking Buffer

100mM HEPES, 5mM $MgCl_2$, 2mM β-mercaptoethanol, 500mM KCl (pH 7.0)

GST Binding Buffer

20mM HEPES, 100mM NaCl, 1mM DTT (pH 7.4)

Ni^{2+}-NTA Binding Buffer

150mM potassium acetate, 1mM $MgCl_2$, 0.05% (v/v) Tween-20, 20mM HEPES (pH 7.4)

2.3 Cell Culture

2.3.1 3T3-L1 Murine Fibroblasts

3T3-L1 fibroblasts were cultured in $75cm^2$ flasks containing DMEM/10% (v/v) newborn calf serum and 1% (v/v) penicillin and streptomycin. Cells were cultured at 37°C in a humidified atmosphere of 10% CO_2, and the media was replaced every 48 h. When subconfluent (70-95% confluency) the cells were passaged into 10cm culture plates and a $75cm^2$ carry over flask. Cells were cultured to 4 days post confluency, and then differentiated into adipocytes.

2.3.2 Trypsination and Passage of 3T3-L1 Fibroblasts

Following aspiration of media from a $75cm^2$ flask, 1ml of trypsin/EDTA solution was added to wash the remaining media from the monolayer of cells. This was then removed and 3ml of fresh trypsin/EDTA solution were added and the flask was incubated at 37°C in a humidified atmosphere of 10% CO_2 for 5 min. Careful agitation of the flask resulted in the cells being lifted from the surface of the flask.

This cell suspension was the added to a maximum volume of 230ml DMEM/10% (v/v) newborn calf serum and 1% (v/v) penicillin and streptomycin. With occasional agitation, the cells were then split between 10cm culture plates and 75cm^2 flasks.

2.3.3 Differentiation of 3T3-L1 Fibroblasts

Differentiation media of DMEM/ 10% (v/v) foetal bovine serum, 1% (v/v) penicillin and streptomycin, 0.25μM dexamethasone, 0.5mM methyl isobutylxanthine and 1μg/ml insulin was prepared as described below.

A stock of 2.5mM dexamethasone (in ethanol) was diluted 1:20 with DMEM/ 10% (v/v) foetal bovine serum, 1% (v/v) penicillin and streptomycin immediately prior to use yielding a 500X stock solution. A 500X sterile solution of methyl isobutylxanthine (IBMX) was prepared by dissolving 55.6mg IBMX in 1ml of 2M KOH and passing the solution through a 0.22 micron filter. Insulin (1mg/ml) was prepared in 0.01 M HCl and filter sterilised using a 0.22 micron filter as before. Differentiation media was prepared by adding both the dexamethasone & IBMX solutions to a 1X concentration in DMEM/ 10% (v/v) foetal bovine serum, 1% (v/v) penicillin and streptomycin and then adding insulin to a final concentration of 1μg/ml.

3T3-L1 fibroblasts were cultured on 10cm plates until 4 days post confluency. Then the growth media was aspirated and replaced with differentiation media. After 48 h, this media was replaced with DMEM/ 10% (v/v) foetal bovine serum, 1% (v/v) penicillin and streptomycin and insulin at 1μg/ml. The cells were incubated in this media for a further 48 h. Following differentiation, the media was replaced with

DMEM/ 10% (v/v) foetal bovine serum, 1% (v/v) penicillin and streptomycin. The media was changed every 48 h and the cells were used 10-14 days post differentiation.

2.3.4 Freezing and Storage of Cells

Fibroblasts were cultured to 70-95% confluency, the media was aspirated and 1ml of trypsin/EDTA solution was added to wash the remaining media from the monolayer of cells. This was then aspirated, and 3ml of fresh trypsin/EDTA solution were added and the flask was incubated at 37°C in a humidified atmosphere of 10% CO_2 for 5 min. Careful agitation permitted the cells to be lifted from the surface of the flask. 3ml of DMEM/10% (v/v) newborn calf serum and 1% (v/v) penicillin and streptomycin were added to the cell suspension, and this was then transferred to a sterile tube and centrifuged at 2000 x g for 4 min. Following aspiration of the supernatant, the pellet was 'flicked' gently and then resuspended in 1ml of DMEM/10% (v/v) newborn calf serum, 1% (v/v) penicillin and streptomycin and 10% (v/v) DMSO. The suspension was then transferred to a 1.8ml polypropylene cryo-vial and place at –80°C overnight (wrapped in blue roll), before being stored in a liquid nitrogen vat.

2.3.5 Resurrection of Frozen Cell Stocks from Liquid Nitrogen

A vial of cells was removed from liquid nitrogen, transferred to a 37°C water bath and thawed. The cell suspension was then pipetted into a 75cm^2 flask containing DMEM/10% (v/v) newborn calf serum and 1% (v/v) penicillin and streptomycin

which had previously been equilibrated at 37°C in a humified atmosphere of 10% CO_2. The media was replaced after 24 h and the cells were cultured as described before.

2.4 SDS/Polyacrylamide Gel Electrophoresis

SDS/polyacryalamide gel elecrtrophoresis was carried out using Bio_rad mini-PROTEAN II gel apparatus. The percentage of acrylamide in each gel ranged between 7.5% - 15%, depending on the molecular weight of the protein(s) of interest. All reagents were of electrophoresis grade.

Upon assembly of the gel apparatus, the separating gel was prepared using 30% acrylamide/bisacrylamide, 1.5M Tris-HCl (pH 8.8) (to a final concentration of 375mM), 10% (w/v) SDS (to a final concentration of 0.1%), polymerised with 10% (w/v) ammonium persulphate (to a final concentration of 0.1%) and TEMED (to a final concentration of 0.01%). The stacking gel was prepared using 30% acrylamide/bisacrylamide, 1M Tris-HCl (pH 6.8) (to a final concentration of 125mM), 10% (w/v) SDS (to a final concentration of 0.1%), polymerised with 10% (w/v) ammonium persulphate (to a final concentration of 0.1%) and TEMED (to a final concentration of 0.05%).

Protein samples were resuspended in sample buffer, and loaded into wells in the stacking gel. 10µl of broad range pre-stained molecular weight markers were loaded into at least one well. Gels were immersed in electrode buffer and electrophoresed until the dye front had reached the desired position or until adequate separation of pre-

stained molecular weight markers. A constant voltage of 70 volts was applied through the stacking gel, which was increased to 120 volts through the resolving gel.

2.5 SDS/Polyacrylamide Gel Staining

2.5.1 Coomassie blue staining of protein gel

Following SDS/Polyacrylamide Gel Electrophoresis, a 0.25% Coomassie blue stain solution was prepared. For this, 10ml of glacial acetic acid was mixed with 90ml of a methanol:H_20 (1:1 v/v) mixture and 0.25g of Brilliant Blue R were added. This stain was then filtered through Whatman filter paper. The gel was submerged in the stain for about 1h and destained with the same acetic acid, methanol: H_20 mixture (without the dye) as above. Gels were destained for at least 3h or overnight, depending on resolution wanted. The destained gel was then scanned to record the results.

2.5.2 Silver Staining

Following SDS/Polyacrylamide Gel Electrophoresis, the gel was submerged in 50% methanol/ 10% acetic acid for 30min. The gel was then placed in 5% methanol/ 7% acetic acid for a further 30min, before being washed several times with H_20 over a 30min period. The gel was submerged in 0.02% sodium thiosulfate for 1min, and then subsequently washed twice with H_20 for 1min each. Following this, the gel was submerged for 30min in 0.2%$AgNO_3$, with 1mM formaldehyde, and gently rocked. The gel was then washed with H_20 for 1min. In order to develop the stain a mixture of 6% Na_2CO_3 and 6mM formaldehyde were added and again gently rocked. When

desired staining has occurred, this solution is discarded and replaced with 5% acetic acid. The gel can then be scanned & stored in 20% ethanol at 4°C.

2.5.3 Stains All Staining

Following SDS/Polyacrylamide Gel Electrophoresis, the gel was submerged in 50% methanol/ 7% acetic acid overnight. The gel was then washed extensively in 25% propan-2-ol for 24hr. The propan-2-ol was then replaced with the stains all solution (30mM Tris, 25% (v/v) propan-2-ol, 7.5% (v/v) formamide, adjusted to pH 8.8, followed by the addition of 0.025% (w/v) stains all) and incubated in a light-tight container for 24-48hr. In order to destain the gel, it was removed from this solution and exposed to light.

2.6 Western Blotting of Proteins

After separation of the proteins as described earlier, gels were removed from the plates and equilibrated in Transfer buffer for 10 minutes. A sandwiched arrangement of components, individually soaked in Transfer buffer, were made as follows from bottom to top: brillo pad, two pieces of Whatman 3MM filter paper, nitrocellulose paper, equilibrated polyacrylamide gel, two pieces of Whatman 3MM filter paper, brillo pad. The sandwich was placed in a cassette and slotted, bottom nearest to cathode, into a Bio-Rad mini trans-blot tank filled with Transfer buffer. Transfer of proteins was performed at room temperature for 3 hours at a constant current of 250mA, or overnight at 40mA. Efficiency of transfer was determined by staining the nitrocellulose membrane with Ponceau S solution.

Following transfer, the nitrocellulose membrane was incubated with 5% (w/v) dried skimmed milk made up in PBS-T for 1 hour to block non-specific binding sites. The membrane was then transferred to a plastic pocket containing primary antibody in 1% (w/v) dried skimmed milk in PBS-T at the appropriate dilution and shaken for at least 2h at room temperature. Following five washes with PBS-T over a period of 30 minutes, the membrane was incubated in 1% (w/v) dried skimmed milk in PBS-T with the appropriate secondary antibody, (HRP-linked IgG) for 1h at room temperature. The blot was then washed for 15 minutes with PBS-T supplemented with 0.5M NaCl, followed by 3 changes over 15 minutes with PBS-T.

Following incubation with the appropriate HRP-linked IgG and subsequent washing, the membrane was washed in distilled H_20. The signal was then detected using ECL. Equal volumes of Amersham "detection reagent 1" and "detection reagent 2" were mixed and the membrane was immersed and shaken in this mixture for 60 s. The membrane was then 'blotted' dry, placed in a plastic pocket in a light tight cassette and exposed to Kodak film. The film was then developed using an X-OMAT processor.

2.7 Subcellular Fractionation of 3T3-L1 Adipocytes

Subcellular fractions (PM, HDM and LDM) were obtained as described for the fractionation of rat adipocytes by Piper *et* al. 1991, modified by Martin *et* al. 1994.

Cells cultured on 10cm plates were either insulin treated (1μM insulin) or incubated at 37°C in serum-free DMEM for 2h. Following the transfer of plates onto ice, the cells

were washed 3 times with ice-cold HES buffer. On addition of 500µl/ plate of HES buffer containing protease inhibitors (protease inhibitor cocktail tablet from Boehringer Mannheim: 1 tablet used in 50ml) the cells were scraped and then homogenised with 20 strokes in a Dounce homogeniser. Homogenates were transferred to pre-chilled Oakridge Beckman centrifuge tubes and centrifuged at 16,000 x g for 20 min at 4°C.

The resulting pellet was resuspended in 1ml ice-cold HES buffer and layered onto 1ml of 1.12M sucrose in HES buffer in a Beckman tube and centrifuged at 100,000 x g for 60 min at 4°C in a swing out rotor. The upper layer was carefully removed to leave a brown band at the interface (plasma membrane). This fraction was then diluted in HES buffer containing protease inhibitors and pelleted at 180,000 x g for 60 min at 4°C.

Meanwhile, the supernatant from the initial spin was centrifuged at 46,000 x g for 20 min at 4°C, yielding a pellet designated as the high density microsomal fraction (HDM). The resulting supernatant was centrifuged at 180,000 x g for 60 min at 4°C yielding a pellet designated the low density microsomal fraction (LDM). All membrane fractions were resuspended in HES buffer and snap frozen in liquid nitrogen and stored at -80°C prior to analysis.

(A simplified flow-chart of this protocol is shown in Figure 2.1)

2.8. Iodixanol Gradients

OptiPrep is a sterile solution of Iodixanol (5,'[(2-hydroxy-1-1propanediyl)-bis(acetlamino)bis[N,N'-bis(2,3dihydroxypropyl-2,4,6-triiodo-1,3-benzenecarbox-amide].

Gradients were prepared as described by Hashiramoto *et al.* 2000 with slight changes.

LDM membranes were prepared as described before and mixed with iodixanol to a final concentration of 14% (w/v). Volumes were made up to 3.9ml using HES Buffer and the mixture was sealed in quick-seal Beckman polyallomer tubes. Tubes were inverted several times to ensure sufficient mixing, and then spun at 295,000 x g in a near vertical rotor (Beckman, TLN100) for 1 h at 4°C. Acceleration from 0 – 886 x g was set to be 5 min and deceleration was without breaks in order not to disturb the forming gradient. The tube was then pierced at the top (to allow air in) and then 300µl fractions were piercing the bottom of the tube.

All fractions were snap frozen in liquid nitrogen and stored at -80°C prior to analysis.

2.9 Sucrose Gradients

Gradients were prepared as described by Guilherme *et al.* 2000.

LDM samples were prepared as described before and 1.5-2 mg of LDM fractions were loaded onto a 10-35% (w/v) continuous sucrose velocity gradient (in Sucrose Gradient Buffer) and centrifuged for 3.5 h at 105,000 x g at 4°C in a SW40 rotor (Beckman).

Fractions containing GLUT4-membranes (fractions 4-10 typically) were pooled, pelleted by ultracentrifugation at 180,000 x g for 60 min at 4°C, and then resuspended in Sucrose Gradient Buffer. This was then loaded onto a 10-65% (w/v) continuous sucrose equilibrium density gradient (in Sucrose Gradient Buffer) and centrifuged at 218,000 x g for 18 h at 4°C in a SW40 rotor (Beckman). After centrifugation, fractions were collected starting from the top of the gradient.

2.10 Protein expression and purification

2.10.1 Munc 18 and syntaxin plasmids

The his_6-tagged munc 18a and 18c (in plasmid pQE-30), and GST-syntaxin 4 (in plasmid pGEX-5X1) were provided by Dr Luke Chamberlain (University of Glasgow). The GST-syntaxins 1,2 and 3 (in plasmid pGEX-KG) were obtained from Richard H. Scheller, Ph.D (Genentech).

The mutated form of his_6-tagged munc 18a/c was made through three rounds of site-directed mutagenesis, using the primers indicated in the table below. These amino acids were selected by examining the 3D structure of the munc18a- syntaxin 1 interaction. Amino acids on the munc 18a believed to interact with syntaxin 1 (based on their close proximity) were noted, and then mutated to the corresponding amino acid of munc 18c when their sequences were aligned [The mutations were carried out in order IGEARV· ›KE, then T(52)E and finally Q(338)R]. The sequence of this new munc 18a/c was confirmed by automated sequencing before continuing with protein expression.

Mutated amino acids	**Base Changes (Munc18a→Munc18a/c)**	**Primer Sequence (5'→3') (mutated bases in bold & underlined)**
T(52)E	ACC→GAA	CAG ACA TCA TG**G AA**G AGG GGA TCA
IGEARV→KE	ATT GGA GAG GCG AGG GTG→ AAG GAG	CAA GTA TGA GAC CAG CGG C**AA GGA G**AA GGA GGT GCT CCT GGA TG
Q(338)R	CCA→CCG	GCC CCA GTA **CCG** GAA GGA GCT CAG

2.10.2 Protein expression

Competent *E.coli* JM109 cells [Genotype: *e14-(McrA-) recA1 endA1 gyrA96 thi-1 hsdR17*(rK- mK+) *supE44 relA1 Δ(lac-proAB)* [F' *traD36 proAB lacI^{q}ZΔM15]*] were transformed with the above constructs, and protein expression induced by growing the cells in 0.5mM IPTG for 4hr at 37°C. Cells were pelleted by centrifugation at 2,500 x g, then washed and resuspended in breaking buffer (containing 1mM PMSF and a

protease inhibitor tablet [protease inhibitor cocktail tablet from Boehringer Mannheim: 1 tablet used in 50ml]) and this was stored overnight at -80°C. The cells were then thawed in cold water, and then lysozyme added (to a concentration of 1mg/ml) and left on ice for 30min. Following this the solution was ultrasonicated a total of three times. Cell debris was then pelleted by centrifugation at 43,000 x g for 40min at 4°C, and the supernatants (containing the protein) were recovered.

2.10.3 Protein purification

His_6-tagged munc 18 proteins were purified by Ni^{2+} affinity chromatography at 4°C. A 3ml Ni^{2+}-NTA agarose column was first washed with 5ml dH_2O, followed by 5ml His_6-tag Purification Buffer. The bacterial cell lysates were then loaded onto the Ni^{2+}-NTA agarose column and passed through twice. The column was then washed with 30ml His_6-tag Purification Buffer. Following this, the proteins were eluted from the column (12 x 1ml fractions collected) by applying a step gradient of increasing concentrations of imidazole in this buffer (ranging from 95mM-275mM). Peak fractions containing munc 18 proteins were identified by SDS-PAGE.

The GST-syntaxin proteins were purified using a Glutathione-Sepharose column at 4°C. Initially the 3ml Glutathione-Sepharose column was washed with 10ml dH_2O, followed by 20ml cold PBS. The cell lysate was then loaded onto the column and incubated for 1h at 4°C. Following this the column was washed four times with 20ml cold PBS to remove non-bound protein. The GST-syntaxin proteins were then eluted from the column with 10mM reduced glutathione in 50mM Tris, pH 8.0. 5 x 1.5ml fractions were collected.

2.11 Circular dichroism (CD) analysis

The work using CD analysis (in order to investigate protein structure and folding) was carried out by Dr Sharon Kelly and Professor Nick Price (from the Univeristy of Glasgow). Approximately 1mg/ml of each protein was required for Near UV analysis, and 0.3 mg/ml for Far UV analysis.

2.12 Munc 18-syntaxin binding studies

GST-pull down assay

Glutathione beads were washed three times in GST Binding Buffer, and incubated with a protein extract from *E.coli* (approximately 0.2μg/μl of bead slurry) for 1h at 4°C with end-over-end rotation. After washing the beads three times with the GST Binding Buffer, either 2μM of GST or GST-synatxin protein were added, and incubated at 4°C with end-over-end rotation.

An equivalent volume of his_6-tagged munc 18 protein was then added to make a final concentration of 1μM for munc 18 in a final reaction volume of 200μl, and the mixture was incubated for 2h at 4°C with end-over-end rotation. The beads were then washed twice with GST Binding Buffer containing 1mg/ml gelatin, and three times with GST Binding Buffer containing 5% glycerol.

Any bound proteins were then eluted by boiling the beads in Sample Buffer. Eluted proteins were then separated by SDS-PAGE and transferred onto nitrocellulose for immunoblotting analysis.

Ni^{2+}-NTA agarose binding studies

Ni^{2+}-NTA agarose beads were washed three times in Ni^{2+}-NTA Binding Buffer, and incubated with a protein extract from *E.coli* (approximately 0.2μg/μl of bead slurry) for 1h at 4°C with end-over-end rotation. After washing the beads three times with the Ni^{2+}-NTA Binding Buffer, 2μM of His_6-tag munc 18 protien was added, and incubated at 4°C with end-over-end rotation (there was also a control, with no His_6-tag munc 18 protien).

An equivalent volume of GST-synatxin protein was then added to make a final concentration of 1μM for syntaxin4 in a final reaction volume of 200μl, and the mixture was incubated for 2h at 4°C with end-over-end rotation. The beads were then washed twice with Ni^{2+}-NTA Binding Buffer containing 1mg/ml gelatin, and three times with Ni^{2+}-NTA Binding Buffer containing 5% glycerol.

Any bound proteins were then eluted by boiling the beads in Sample Buffer. Eluted proteins were then separated by SDS-PAGE and transferred onto nitrocellulose for immunoblotting analysis.

2.13 Adenovirus Production

2.13.1 Preparation for cloning into pShuttle-CMV

In order to successfully clone each munc 18 into the pShuttle-CMV vector it was first necessary to design primers (supplied by TAGN, Newcastle UK) to introduce suitable restriction sites at either end of the sequence, and a FLAG-tag sequence at the C terminus. The table below gives details of the primers used in order to introduce the

required restriction sites (to allow cloning into the multiple cloning site of pCR2.1 to occur) and the FLAG-tag. Following PCR, the product was TA cloned into vector pCR 2.1. The pCR2.1/munc 18 plasmid and the pShuttle-CMV were then digested with the relevant restriction enzymes and gel purified to permit ligation.

Primer Name	**Significance of base changes**	**Primer Sequence (5'→3') (additional bases in bold)**
Munc18a + a/c forward	Addition of *Bgl II* restriction site [AGA TCT] at N-terminus	**AGA TCT** ATG GCC CCC ATT GGC CTC
Munc18a + a/c reverse	Addition of FLAG-tag sequence and *Hind III* restriction site [AAG CTT] at C-terminus	**AAG CTT** TTA **CTT GTC GTC GTC GTC CTT GTA GTC** ACT GCT TAT TTC TTC GTC TGT
Munc18c forward	Addition of *Bam HI* restriction site [GGA TCC] at N-terminus	**GGA TCC** ATG GCG CCG CCG GTA TCG
Munc18c reverse	Addition of FLAG-tag sequence and *Xho I* restriction site [CTC CAG] at C-terminus	**CTC CAG** TTA **CTT GTC GTC GTC GTC CTT GTA GTC** CTC ATC CTT AAA GGA AAC TTT ATC

2.13.2 Ligation of munc 18 and pShuttle-CMV

5µl of each insert (munc 18), 2.5µl of plasmid (pShuttle-CMV), 1µl of Ligase Buffer and 1.5µl of T4 DNA Ligase were incubated on half water/ half ice for 16hr to allow ligation to occur. 3µl of the resulting mixture was then transformed into TOP 10 cells, and restriction digests of (DNA obtained from) selected colonies confirmed successful ligation.

2.13.3 BJ5183 co-transformation

Each recombinant pShuttle-CMV/munc 18 vector is first linearised using *Pme* I, which is then heat inactivated, and the DNA gel purified. Following this, the DNA is mixed with pAd-Easy and then added to a 40µl aliquot of electroporation competent BJ5183 cells [Genotype: *end*A *sbc*BC *rec*BC *gal*K *met thi*-1 *bio*T *hsd*R (*Str*^{r})] and electroporation carried out under the following conditions: 200 Ohms, 25µF, 2.5kV. This is immediately resuspended in SOC media and plated out on LB + kanamycin plates. Colonies are selected and the DNA digested with *Pac* I to identify successful incorporation of the munc 18 into the pAd-Easy.

2.13.4 DH5α transformation

The BJ5183 cells are not stable, and are prone to deletions, so it is necessary to transform the pAd-Easy/munc 18 into DH5α cells [Genotype: F- *deo*R *rec*A1 *end*A1 *hsd*R17(*rk*$^-$, mk$^+$] *sup*E44 λ^- *thi*-1 *gyr*A96 *rel*A1). 5µl of the recombinant DNA is added to 40µl of DH5α electrocompetent cells, and electroporated under the following conditions: 200 Ohms, 25µF, 2.5kV. This is immediately resuspended in SOC media and serial dilutions are plated out on LB + kanamycin plates. Colonies are selected and the DNA digested with *Pac* I to identify successful transformation into the DH5α cells.

2.13.5 Transfection of HEK 293 cells

20μg of each recombinant pAd-Easy/Munc 18 plasmid is then digested with *Pac* I, and extracted once with phenol/ chloroform and ethanol precipitated. The DNA is then resuspended in 50μl of TE 0.1X.

When the HEK 293 cells are ready to be transfected, the DNA is diluted into 1ml of OPTI-MEM (serum free) and mixed gently. 40μl of Lipofectamine 2000 is then diluted into 1ml of OPTI-MEM (serum free) and incubated at room temperature for 5 min. At this point the diluted DNA and diluted Lipofectamine 2000 are mixed gently and incubated for 20 min. A further 8ml of OPTI-MEM is then added to the mixture, which is added to the HEK 293 cells.

The next day this is aspirated off, and replaced with DMEM/5% (v/v) foetal bovine serum and 1% (v/v) Glutamine. Subsequent feeds are of DMEM/5% (v/v) foetal calf serum, 1% (v/v) Glutamine and 1% (v/v) penicillin and streptomycin.

After 10 days, the cells are spun down, resuspended in sterile PBS and subjected to freeze-thaw conditions in order to obtain the cell lysate. Aliquots of the lysate, media and membrane fraction are first removed (to analyse for expression of the Adenoviral protein) and the remainder is snap frozen and stored at -80°C.

Figure 2.1 Flow chart of the protocol for the subcellular fractionation of 3T3-L1 adipocytes

The flow chart opposite demonstrates the various centrifugation steps involved in obtaining each of the subcellular fractions from a crude cell homogenate.

Figure 2.1

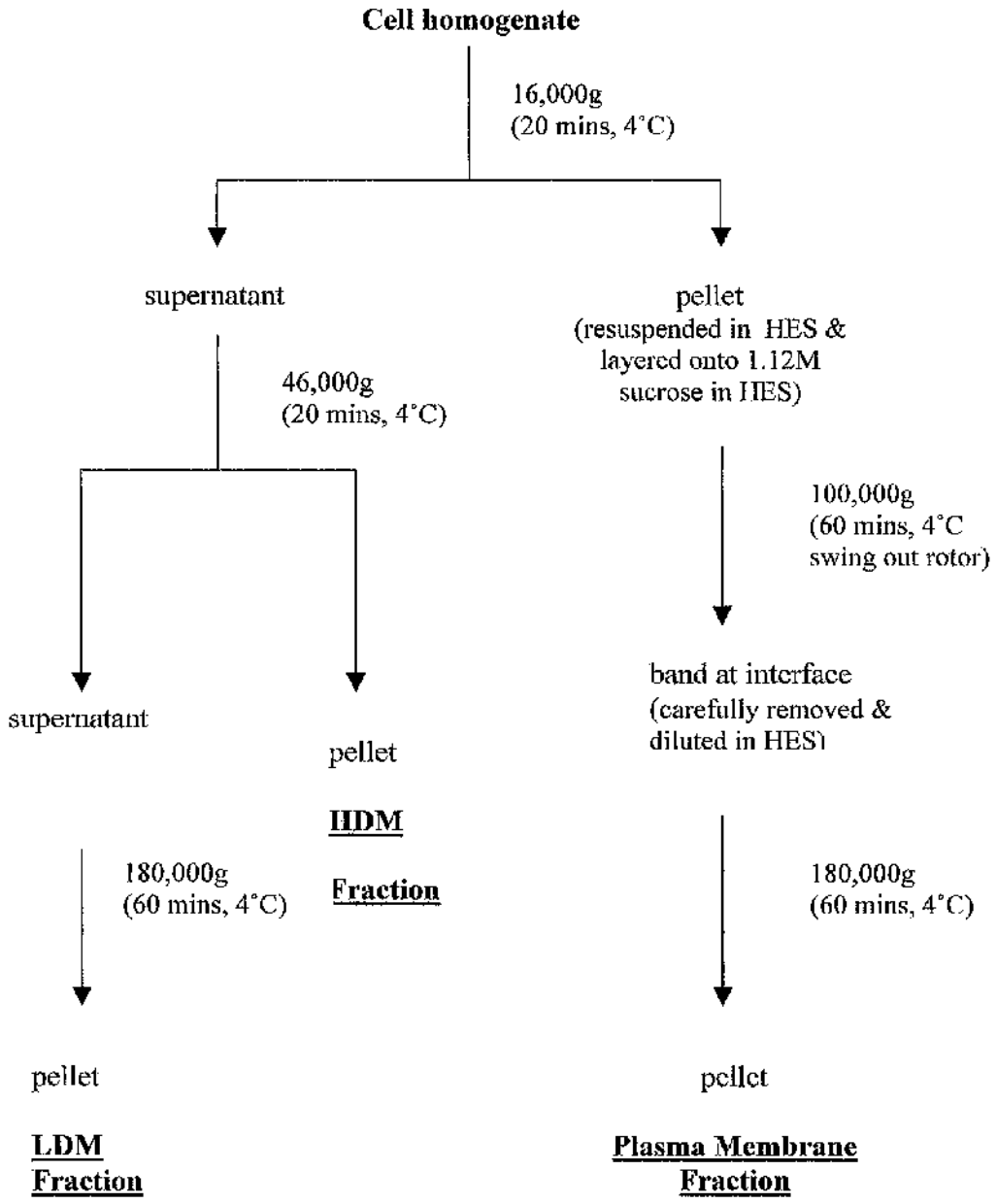
Cell homogenate
16,000g
(20 mins, 4°C)
supernatant
pellet
(resuspended in HES &
layered onto 1.12M
sucrose in HES)
46,000g
(20 mins, 4°C)
100,000g
(60 mins, 4°C
swing out rotor)
supernatant
pellet
band at interface
(carefully removed &
diluted in HES)
HDM
Fraction
180,000g
(60 mins, 4°C)
180,000g
(60 mins, 4°C)
pellet
pellet
LDM
Fraction
Plasma Membrane
Fraction

CHAPTER 3-SUCROSE GRADIENT ANALYSIS OF INTRACELLULAR GLUT4 STORES

3.1 Aims

1. To demonstrate the use of sucrose gradient centrifugation for resolving GLUT4 compartments in 3T3-L1 adipocytes

2. To characterise the GLUT4 storage vesicles

3.2 Introduction

Insulin stimulates the uptake of glucose into muscle and fat cells primarily due to the translocation of GLUT4 from intracellular membranes to the cell surface in the presence of insulin. In the absence of insulin, GLUT4 is found in both endosomes (~40%) and in specialised GLUT4 storage vesicles (GSV) (~60%) (Martin *et al.* 1997; Livingstone *et al.* 1996). These GSVs are highly insulin sensitive and explain why GLUT4 shows a greater level of translocation to the cell surface (around 15-fold) than other endosomal proteins such as the transferrin receptor (TfR) and GLUT1 (about 2-fold) (Tanner & Lienhard 1987; Piper *et al.* 1991).

Although it was understood that GLUT4 is found in both endosomes and GSVs, it has been difficult to separate the two. The relative amounts of GLUT4 present in the

endosomes and GSVs can be determined using endosomal ablation techniques (Livingstone *et al.* 1996) but does not resolve the compartments for purification purposes. One recent study has used iodixanol gradient centrifugation in order to separate the two vesicle populations (Hashiramoto & James 2000). Another study has made use of sucrose gradients (Guilherme *et al.* 2000), which although more time consuming may prove to be a more effective method of selective isolating GSVs. In 3T3-L1 adipocytes, sucrose gradient centrifugation has been used to separate intracellular GLUT4-containing membranes into two distinct peaks, one containing the GSVs (peak 1) and the other being enriched in endosomal/TGN markers (peak 2).

In these studies we have characterised sucrose gradients in 3T3-L1 adipocytes with respect to GLUT4 and other proteins that partly co-localise with GLUT4. We have demonstrated that is an effective way in which to resolve distinct intracellular GLUT4 pools.

We have also used different gel staining techniques in order to characterise the GSV compartment. These techniques proved problematic though did identify one potential protein of interest.

3.3 Results

3.3.1 Subcellular Fractionation

In order to obtain the LDMs needed for the sucrose gradients, it was first necessary to carry out a subcellular fractionation of 3T3-L1 adipocytes in both the basal and insulin stimulated state.

As can be seen from Figure 3.1, upon addition of insulin there is a marked reduction in the levels of both GLUT4 and IRAP in the LDM fraction, and a subsequent increase in levels of both at the plasma membrane as expected. Using this technique there is ~2-fold change in levels of both GLUT4 and IRAP (a decrease in the LDM fraction, and increase in the plasma membrane fraction). These values for the fold increase at the plasma membrane are however significantly smaller than the 15-20 fold changes observed using other experimental techniques (Tanner and Lienhard 1987; Calderhead *et al.* 1990). This discrepancy is primarily due to difficulties in preventing contamination of the fractions during the various centrifugation steps.

However, these results do show the reduction in the levels of both GLUT4 and IRAP in the LDM fraction, and the subsequent increase at the plasma membrane of both proteins. Having demonstrated this effect we could then use these LDM fractions in order to segregate the GLUT4 compartments.

3.3.2 Iodixanol Gradients

In order to visualise the two pools of GLUT4 (endosomal and GSV) it was originally intended to use the method of Hashiramoto and James, using iodixanol sedimentation analysis. Using this method, it had been possible to successfully isolate GSVs from the endosomal pool, and as such our aim was to repeat this in order to further characterise the GSVs.

However, when repeating this experiment, the expected results could not be obtained. It had been expected to see two distinct peaks of GLUT4 containing fractions, with peak 1 being highly insulin responsive (and hence contain the GSVs). Instead our results showed GLUT4 to be present in fractions throughout the gradient. The experiment was repeated a number of times, with similar results. As such it was decided that an alternative method of isolating the GSVs should be attempted.

In addition, there has also been some uncertainty as to the effectiveness of iodixanol gradients using rat tissues, and as such it may not be an efficient method of selectivetly isolating GSVs from different tissues.

3.3.3 Sucrose Gradients

Having abandoned the iodixanol gradient method, in order to resolve the two pools of GLUT4 we have used the method described by Guilherme *et al.* using two sucrose gradients (Guilherme *et al.* 2000).

The first sucrose gradient (a velocity gradient) uses a continuous density gradient, with an increasing density towards the bottom of the tube. This is a relatively short gradient (compared to the equilibrium gradient) and separates molecules by their molecular weight. This centrifugation step is able to isolate GLUT4 containing membranes form the majority of other protein membranes in the crude LDM sample. During the second sucrose gradient (the equilibrium gradient), the sucrose forms a gradient and molecules move to the position where their density is the same as the gradient material, and hence separation is due to density. This gradient takes significantly longer to run than the velocity gradient, and allows for a clearer resolution of the sample.

Using the sucrose velocity gradient centrifugation (1st sucrose gradient) it was possible to exclude the vast majority of the total membrane protein (fractions 1-3 typically) from the GLUT4 enriched membranes (fractions 4-10 typically), as shown in Figure 3.2 and Table 3.1. Here it is seen that whereas ~70% of total membrane protein is found in fractions 1-3 (Table 3.1), the GLUT4 containing vesicles are predominantly in fractions 4-10 (Figure 3.2). At this stage there was no significant difference in the protein content between those fractions containing GLUT4 and IRAP in the presence or absence of insulin.

These GLUT4 containing fractions were pooled, and subjected to sucrose equilibrium gradient centrifugation (2^{nd} sucrose gradient) in order to further resolve the membrane species present. Figure 3.3 shows the distribution of GLUT4 and IRAP after this equilibrium gradient, showing that both are found mainly in fractions 5-9.

These immunoblots however do not establish whether the two GLUT4 containing compartments have been isolated. In order to establish whether this has occurred, each of the GLUT4 and IRAP containing fraction must be compared both in the presence and absence of insulin stimulation.

In agreement with Guilherme *et al.*, we discovered that insulin induced a greater loss of GLUT4 and IRAP from peak 1 than from peak 2 (Figure 3.4), which is consistent with the thinking that peak 1 contains the GLUT4 storage vesicles. Peak 2 is believed to contain the recycling endosomes, and in the presence of insulin GLUT4 and IRAP levels in this peak are seen to decrease by less than in peak 1. From the results here it was determined that, upon the addition of insulin, levels of GLUT4 and IRAP are seen to be reduced by ~50% from the fractions in peak1. This is in contrast to a drop in levels of only 10-20% from the fractions in peak2. These findings are consistent with the idea that the endosomal GLUT4 vesicles are less insulin responsive than GSVs.

It is also important to note that the decrease in GLUT4 levels in fractions 5-7 upon insulin stimulation is mirrored by a similar decrease in the total protein concentration in these fractions (Table 3.2). At the same time, a much smaller decrease in total protein concentration is observed in fractions 8-9 upon insulin stimulation.

Taken together, these results would indicate that after the sucrose equilibrium gradient centrifugation, we have successfully isolated GSVs from recycling endosomes. We have also excluded the vast majority of other membrane proteins, meaning that these fractions contain relatively pure GLUT4 vesicles (demonstrated by the fact that the large decrease in GLUT4 and IRAP levels in peak 1 is matched by a significant reduction in protein concentration, whereas there is less of a protein concentration decrease in the less insulin-sensitive peak2 fractions).

3.3.4 Localisation of other proteins of interest

Having repeated the sucrose gradient experiments successfully, it was now possible to ascertain whether other proteins of interest co-localise with GSVs by carrying out immunoblot analysis (Figure 3.5)

In order to further characterise the nature of the two separate GLUT4 peaks, we examined the distribution of the v-SNARE VAMP2. VAMP2 was found to co-segregate with the GSV peak (the majority found in fraction 6). It is also notable that upon insulin stimulation there is a large decrease in VAMP2 found in these LDM fractions. Taken together, this supports the data that VAMP2 is the v-SNARE for GSVs (Martin *et al.* 1996).

Unlike GSVs, the transferrin receptor is known to undergo continual recycling between the plasma membrane and endosomes with only a small increase in plasma membrane levels upon insulin stimulation. This was supported by the data from Figure 3.5 that shows the transferrin receptor is localised in fractions 8-9 with only a

slight decrease seen in response to insulin. This is therefore a good indication that the GLUT4 containing vesicles in fractions 8-9 represent the recycling endosomal pool.

It is known that upon insulin stimulation of 3T3-L1 adipocytes, the secretion of a protein hormone ACRP30 (adipocyte complement related protein of 30 kD) is markedly enhanced. Like GLUT4, regulated exocytosis of ACRP30 appears to require PI3-kinase activity, since insulin-stimulated ACRP30 secretion is blocked by pharmacologic inhibitors of this enzyme (Bogan & Lodish 1999). We therefore sought to determine whether there was any co-localisation between ACRP30 and GLUT4. Although previous data would indicate that the secretion of ACRP30 is by a different pathway than GLUT4 translocation, and these proteins do not co-localise (Bogan & Lodish 1999), the results in Figure 3.5 show that ACRP30 may indeed co-localise with GLUT4, as they are present in the same fractions (fractions 8-9 predominantly). These results do not confirm a direct correlation between ACRP30 and GLUT4 trafficking, as it could be that both proteins (by chance) happen to be present in vesicles of a similar buoyant density. In order to confirm whether these proteins do indeed co-localise a further experiment could be to carry out immunoprecipitation of GLUT4 containing vesicles, and then check the resulting sample for presence of ACRP30 using SDS-PAGE and western blotting analysis. This was not attempted in the present study.

Sec6 and Sec8 are two proteins that are part of the exocyst complex. The exocyst complex is an eight protein complex that has recently been implicated in GLUT exocytosis as a downstream target for TC10 (Kanzaki & Pessin 2003). The data from Figure 3.5 indicates the presence of both of these proteins in fractions 8-9, although it

is difficult to establish whether insulin stimulation causes any significant change in the level of either protein. Although this co-localisation does not demonstrate a definite role for these exocyst proteins in GLUT4 exocytosis, it does provide evidence that they are at least partly co-localised with some GLUT4 containing membranes.

3.3.5 Identification of a potential calcium-dependent kinase in GLUT4 containing vesicles

In order to identify potential proteins of interest, GLUT4 containing fractions from the 2nd gradient SDS-PAGE gels were stained using both silver stain (to identify proteins in general) and Stains All (to possibly identify calcium-binding proteins). Ca^{2+} has been shown to be involved in the insulin-stimulated transport of glucose in 3T3-L1 adipocytes (Whitehead *et al.* 2001). It was implicated that Ca^{2+} could have a role to play in both GLUT4 translocation to the plasma membrane, and also in the fusion of GLUT4 vesicles with the plasma membrane. Consequently any calcium-binding proteins located within GLUT4 vesicles would be of potential interest.

In the initial silver stain of the 2nd gradient fraction, the gels were stained with the aim to identify any proteins in the GLUT4 containing fractions whose protein levels were reduced in the presence of insulin, and thus could be of interest. Several SDS-PAGE gels were stained from a number of fractions, without identifying any such protein. As a result, another method of gel staining was used.

Stains-All, which stains calcium-binding proteins a blue/purple colour, identified one potential protein of interest. This protein produced a very feint band (mainly in peak

2), and due to the light sensitivity of the dye an image could not be captured (even when a larger volume of these fractions was loaded on SDS-PAGE gels). The intensity of the band was the same in the presence and absence of insulin, implying that it's abundance was unaltered after insulin treatment. The protein was ~50kDa in size, and was carefully cut out from the gel and identified by Mass Spectroscopy. The resultant data identified a protein of mass 57,354Da, identified as a possible Serine/Threonine Kinase protein, first identified by Schaar *et al.* 1996. As such it was hoped that cDNA and an antibody could be obtained in order to further analyse its localisation with GLUT4. However, we were unable to obtain this, and as such further analysis of this protein was not carried out.

It is important to note that this protein was primarily seen to be present in the fractions containing the endosomal/ TGN GLUT4 vesicles rather than those containing GSVs. This study had aimed to identify proteins located exclusively in the GSVs, which could decrease the relevance of this finding. However, on the other hand, the fact that this protein was present (although in reduced levels) in the GSV containing fractions means that unless further analysis was carried out to establish its exact sub-cellular localisation, we are currently unable to exclude the possibility that this could be a potential protein of importance.

3.4 Discussion

It is known that insulin stimulates the uptake of glucose into muscle and fat cells due to an increase in the translocation of GLUT4 from intracellular membranes to the cell surface. Under basal conditions, GLUT4 is located in both endosomes (~40%) and specialised GLUT4 storage vesicles (GSVs) (~60%) (Martin *et al.* 1997; Livingstone *et al.* 1996). These GSVs are highly insulin sensitive and explain why GLUT4 shows a greater level of translocation to the cell surface (~15-fold) than other endosomal proteins such as TfR and GLUT1 (~2-fold) (Tanner & Lienhard 1987; Piper *et al.* 1991).

Although the presence of GLUT4 in both endosomes and GSVs is known, it has proved to be difficult to separate the two for analysis. Endosomal ablation techniques allow the relative amounts of GLUT4 present in each vesicle-type to be determined (Livingstone *et al.* 1996), but are unable to resolve the compartments for purification purposes. Two recent techniques developed in order to separate the two vesicle populations have been to use iodixanol gradient centrifugation (Hashiramoto & James 2000), and also to use sucrose gradients (Guilherme *et al.* 2000).

A number of differences between GSVs and GLUT4 vesicles from recycling endosomes are already known. For example it is known that GSVs are smaller (~50nm in diameter), and have VAMP2, rather than cellubrevin found in recycling endosomes, acting as a v-SNARE on them. The current study aimed to add to our knowledge of the composition of GSVs, and to identify proteins which could be significant.

Initially we sought to use the iodixanol gradient technique in order to isolate GSVs from the endosomal GLUT4 containing vesicles and then to characterise the GSVs. Having first repeated this experiment in 3T3-L1 adipocytes, it was then proposed to do likewise for other cell-types in order to identify proteins of interest that may be common to GSVs from different cell-types. However, as discussed in Section 3.3.2, the results obtained from the iodixanol gradient in this study did not match the expected results. As such, it was decided to attempt the sucrose gradient technique (as described by Guilherme *et al*) as an alernative. It is important to note that there has been some uncertainty as the effectiveness of the iodixanol gradient technique when using rat tissues, and as such it may not be an efficient method of selectively isolating GSVs from different tissues.

In the present study, we have confirmed the use of these two sucrose gradients as an efficient method to separate the endosomal GLUT4 compartments and GSVs. We have confirmed that 3T3-L1 adipocyte LDM samples can be separated into two peaks, as seen in Figure 3.4, with one being highly insulin responsive (mirrored by a similar decrease in protein concentration) and the other being less insulin responsive (with a smaller decrease in protein concentration identified).

In response to insulin, the loss of GLUT4 and IRAP is seen to be much greater from peak1 than from peak2. Levels of both of these proteins are seen to be reduced by ~50% from peak 1 (upon addition of insulin), compared to a reduction of only 10-20% in levels from fractions in peak 2 (Figure 3.4). This supports the argument that peak1 contains the GSVs, while peak 2 contains the recycling endomes (Guilherme *et al.* 2000).

In agreement with this, VAMP2 (the v-SNARE present in GSVs) is found in the fractions of peak1 only. Levels of VAMP2 are, like GLUT4 and IRAP, reduced in response to insulin. Also, the presence of TfR in peak2 fractions only is a good indication that vesicles from these fractions contain recycling endosomes (Figure 3.5). Both of these findings support peak1 as containing GSVs, and peak2 the recycling endosomes.

Our studies have also demonstrated that two proteins that form the exocyst complex (Sec6 and Sec8) are found to co-localise with GLUT4 (Figure 3.5). This protein complex has recently been implicated as having a role to play in GLUT4 translocation and tethering to the plasma membrane (Inoue *et al.* 2003) as a downstream target of TC10 from the PI3-kinase independent insulin-signalling pathway. While not confirming a role for the exocyst complex in GLUT4 trafficking, the data here suggests at least the complex is located to a similar intracellular location as some of the GLUT4 containing vesicles.

Results in the present study have also suggested that there may be some co-localisation between GLUT4 and ACRP30. This finding was in conflict with previous findings (Bogan & Lodish 1999), which indicated secretion of ACRP30 was via a different pathway than GLUT4 translocation and as such there would be no co-localisation. Further analysis (such as a co-immunoprecipitation) would have to be carried out in order to confirm whether GLUT4 and ACRP30 do indeed co-localise, or if they are only, by chance, found in vesicles of similar buoyancy.

Using a technique to stain for potential calcium binding proteins, we have identified a potential calcium-binding protein kinase in GLUT4 containing vesicles. This was of interest due to the fact it is known that Ca^{2+} is required for membrane fusion in neurotransmitters, and more recently it has been identified as having a possible role in the fusion of GLUT4 with the plasma membrane (Whitehead *et al.* 2001). Unfortunately, as we were unable to obtain cDNA or an antibody for this protein we were unable to investigate this protein, and whether it does indeed co-localise with GLUT4, in further detail.

In conclusion we have confirmed the use of sucrose gradients as being an effective tool to study GLUT4 trafficking. We have demonstrated that by using this method it is possible to isolate GSVs from the recycling endosomal pool of GLUT4. This finding has permitted initial experiments to take place to establish that there does seem to be co-localiastion of exocyst complex with GLUT4, and also a potential co-localisation of ACRP30 with GLUT4. Further analysis would have to be carried out in order to confirm whether this is indeed the case.

We have also been able to identify the presence of a potential calcium binding Serine/Threonine kinase within GLUT4 containing vesicles, although we have been unable to investigate the protein any further.

Figure 3.1 GLUT4 and IRAP are translocated from the LDM to PM upon insulin stimulation.

3T3-L1 adipocytes are either treated with (+) or without (-) 1μM insulin for 30min. Subcellular fraction was carried out as described in the Methods section. 10μg of each fraction were separated by SDS-PAGE. This experiment was repeated 3 times, and shown are typical immunoblots for the proteins indicated.

[For IRAP, the secondary antibody was HRP-conjugated donkey anti-mouse IgG, and for GLUT4, it was HRP-conjugated donkey anti-rabbit IgG antibody]

Figure 3.1

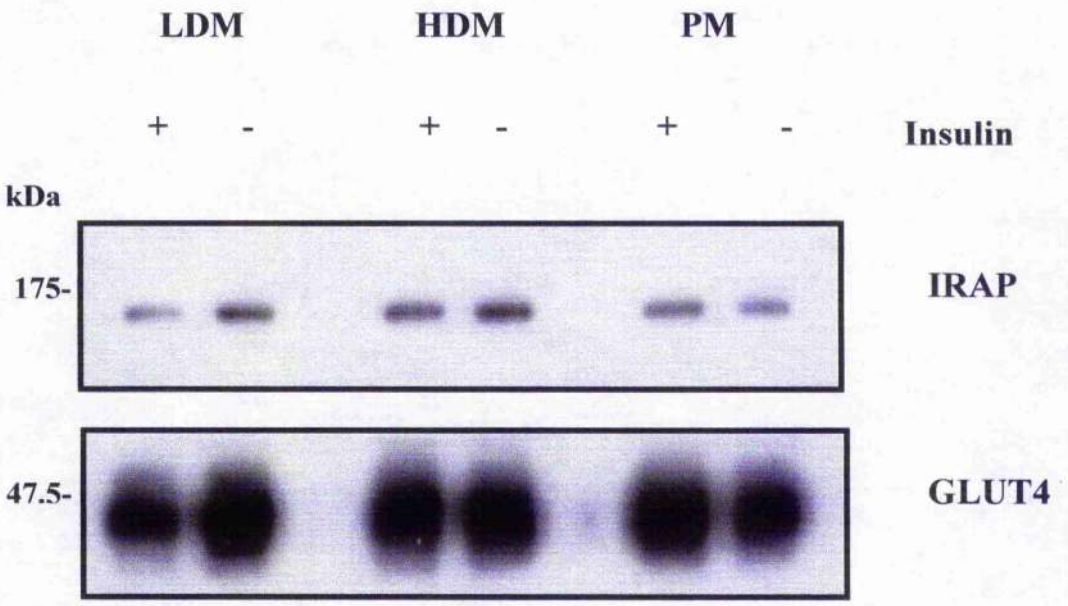

Figure 3.2 Sucrose velocity gradient analysis of GLUT4 and IRAP in 3T3-L1 adipocytes.

3T3-L1 adipocytes are either treated with or without 1μM insulin for 30min. LDM fractions were prepared and subjected to sucrose velocity gradient analysis as described in the Methods section. 1ml fractions were collected from the top of the gradient and 15μl of each fraction were separated by SDS-PAGE. The results shown are from a single gradient analysis, and are representative of three experiments. Typically fractions 4-10 were the GLUT4 peak fractions.

Figure 3.2

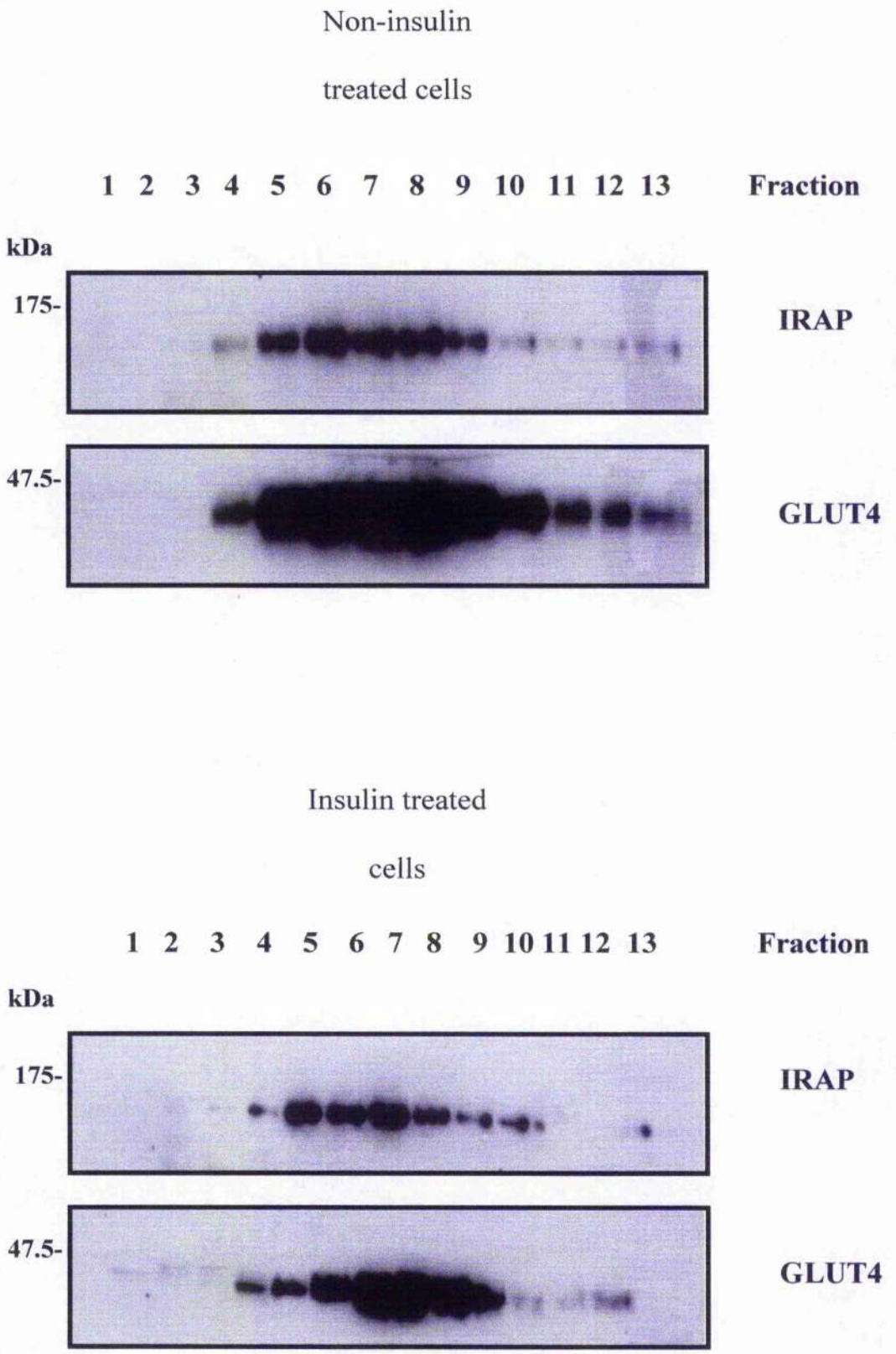
Non-insulin
treated cells
1 2 3 4 5 6 7 8 9 10 11 12 13
Fraction
kDa
175-
IRAP
47.5-
GLUT4
Insulin treated
cells
1 2 3 4 5 6 7 8 9 10 11 12 13
Fraction
kDa
175-
IRAP
47.5-
GLUT4

Table 3.1 Protein profile of sucrose velocity gradient fractions

3T3-L1 adipocytes are either treated with or without 1μM insulin for 30min. LDM fractions were prepared and subjected to sucrose velocity gradient analysis as described in the Methods section. 1ml fractions were collected from the top of the gradient, and then each fraction assayed for its protein concentration. The results shown (on the table opposite) are from a single gradient analysis, and are representative of three experiments.

Note that although fractions 4-10 (in bold) were found to be the GLUT4 containing fractions (see Figure 3.2), most of the membrane proteins (~70%) are found in fractions 1-3 and hence not pooled for the 2nd gradient. Note also that there are no significant differences between the protein concentration levels of the peak fractions whether or not the cells are stimulated with insulin.

Table 3.1

Fraction No.	Non-insulin stimulated cells (protein concentration mg/ml)	Insulin stimulated cells (protein concentration mg/ml)
1	0.78	0.71
2	0.42	0.39
3	0.21	0.24
4	**0.18**	**0.20**
5	**0.09**	**0.11**
6	**0.09**	**0.09**
7	**0.08**	**0.07**
8	**0.10**	**0.07**
9	**0.06**	**0.06**
10	**0.04**	**0.06**
11	0.03	0.04
12	0.03	0.04
13	0.04	0.09

Figure 3.3 Sucrose equilibrium gradient analysis of GLUT4 and IRAP in 3T3-L1 adipocytes.

The peak GLUT4 containing fractions from the sucrose velocity gradient were pooled and subjected to sucrose equilibrium gradient analysis as described in the Methods section. 1ml fractions were collected from the top of the gradient and 15µl of each fraction were separated by SDS-PAGE. The results shown are from a single gradient analysis, and are representative of three experiments. Typically fractions 5-10 were the GLUT4 containing fractions and were analysed further.

Figure 3.3

Non-insulin

treated cells

Insulin treated

cells

Table 3.2 Protein profile of sucrose equilibrium gradient fractions

The peak GLUT4 containing fractions from the sucrose velocity gradient were pooled and subjected to sucrose equilibrium gradient analysis as described in the Methods section. 1ml fractions were collected from the top of the gradient, and then each fraction assayed for its protein concentration. The results shown (on the table opposite) are from a single gradient analysis, and are representative of three experiments.

Note that unlike for the sucrose velocity gradient, here there is a significant difference between the protein concentration levels of the GLUT4 containing fractions. Fractions 5-7 are seen to correspond to the insulin responsive GSV (see Figure 3.4), and here there is a significant reduction in protein concentration upon stimulation by insulin. Fractions 8-9 correspond to the recycling endosomal GLUT4, and here it is demonstrated that there is far smaller reduction in protein concentration upon stimulation by insulin.

Table 3.2

Fraction No.	Non-insulin stimulated cells (protein concentration mg/ml)	Insulin stimulated cells (protein concentration mg/ml)
1	0.01	0.01
2	0.01	0.01
3	0.02	0.02
4	0.02	0.03
5	**0.12**	**0.05**
6	**0.18**	**0.12**
7	**0.15**	**0.12**
8	**0.11**	**0.08**
9	**0.03**	**0.04**
10	0.03	0.03
11	0.02	0.02
12	0.01	0.02
13	0.03	0.04

Figure 3.4 Analysis of peak GLUT4 containing fractions from the sucrose equilibrium gradient receptor.

The peak GLUT4 containing fractions from the sucrose equilibrium gradient were identified (fractions 5-10), and 15µl of each fraction was then separated by SDS-PAGE in order to identify the resolution of the two intracellular GLUT4 compartments. In order to do this, the basal and insulin-stimualated samples of each fraction were ran side-by side. Shown are typical immunoblots for the proteins indicated. Fractions 5-7 correspond to GLUT4 storage vesicles (GSVs) and 8-9 to the endosomal/TGN GLUT4 vesicles.

Figure 3.4

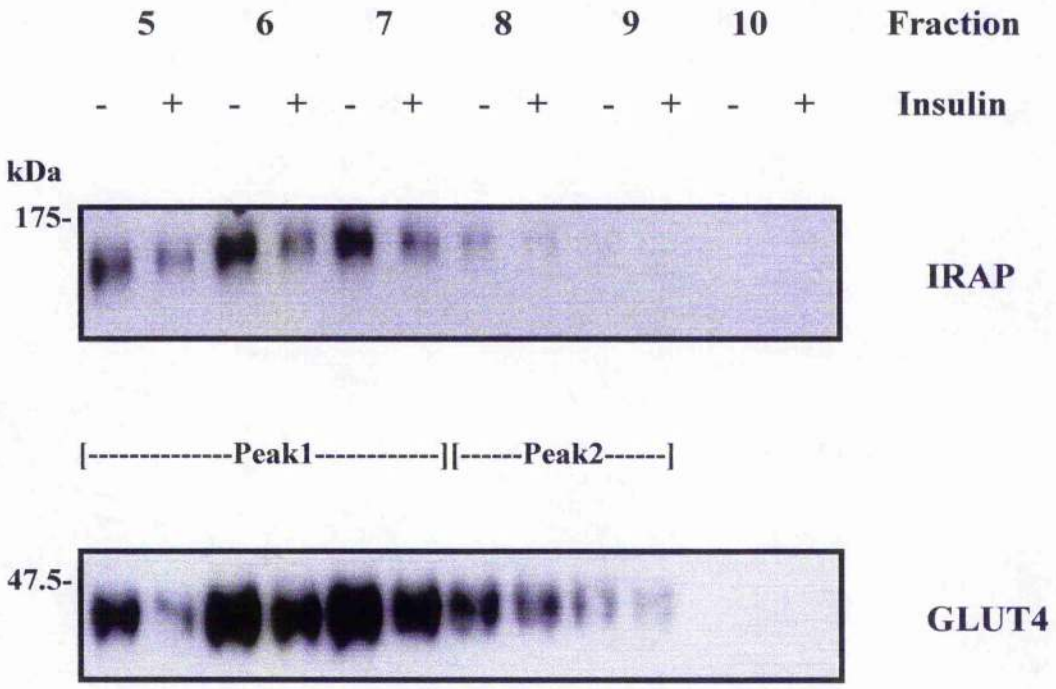
5 6 7 8 9 10 Fraction
- + - + - + - + - + - + Insulin
kDa
175-
IRAP
[----------Peak1----------][------Peak2------]
47.5-
GLUT4

Figure 3.5 Sucrose equilibrium gradient analysis of GLUT4, IRAP, VAMP2, TfR, ACRP30, Sec6 and Sec8 in 3T3-L1 adipocytes.

The peak GLUT4 containing fractions from the sucrose equilibrium gradient were identified (fractions 5-10), and 15μl of each fraction was then separated by SDS-PAGE. Having established which fractions correspond to GSVs and to endosomal GLUT4 it was possible to determine to what extent other trafficking proteins co-localise with the different GLUT4 pools. Shown are typical immunoblots for the proteins indicated, taken from 4 separate sucrose gradients.

[For IRAP, VAMP2, Sec6, Sec8 & TfR, the secondary antibody was HRP-conjugated donkey anti-mouse IgG, and for ACRP30 and GLUT4 the secondary antibody was HRP-conjugated donkey anti-rabbit IgG antibody]

Figure 3.5

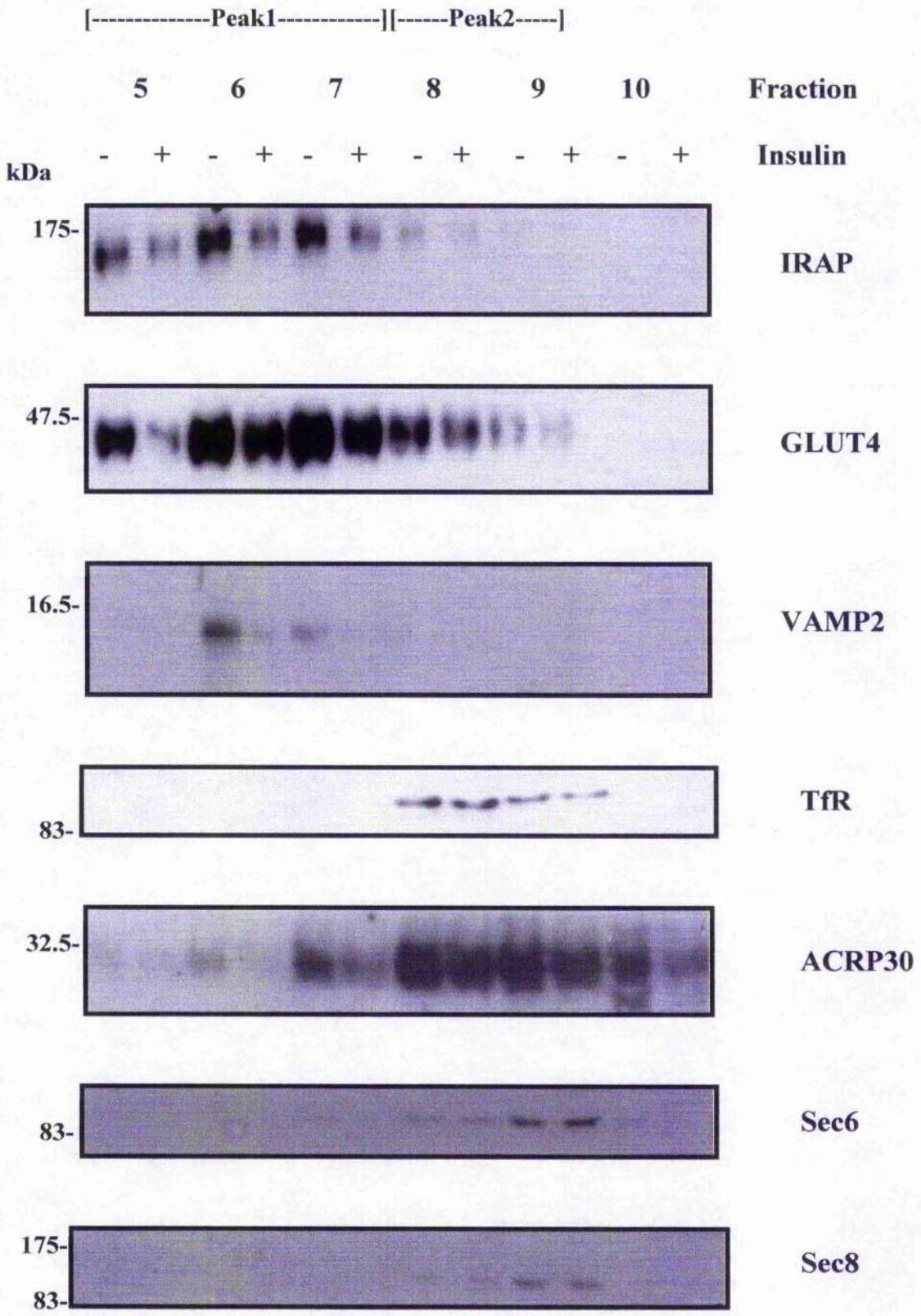
[----------Peak1----------][------Peak2-----]
5
6
7
8
9
10
Fraction
- + - + - + - + - + - +
Insulin
kDa
175-
IRAP
47.5-
GLUT4
16.5-
VAMP2
83-
TfR
32.5-
ACRP30
83-
Sec6
175-
83-
Sec8

CHAPTER 4 - PRODUCTION OF A MUTATED VERSION OF MUNC18A AND THE MUNC18-SYNTAXIN INTERACTION

4.1 Aims

1. To identify potential mutagenesis sites on munc 18a in order that its syntaxin-binding properties are altered to become more like munc18c.

2. To express and purify this mutated protein and characterise its syntaxin-binding properties compared to wild-type munc 18a and munc 18c.

3 To make a recombinant Adenovirus, of this mutated munc 18a, to drive expression in mammalian cells.

4.2 Introduction

GLUT4 has been shown to translocate to the plasma membrane via a SNARE type mechanism (Cheatham *et al.* 1996). VAMP2 has been identified as the v-SNARE responsible for GLUT4 translocation from GSVs, while cellubrevin is believed to be the v-SNARE involved in translocation of GLUT4 and (other proteins) from the endosomes to the plasma membrane (Martin *et al.* 1996; Martin *et al.* 1998; Miller *et al.* 1999). The corresponding t-SNAREs are syntaxin4 and SNAP23 (Rea *et al.* 1998) and these are found mostly on the plasma membrane.

The sec1/munc 18 (SM) proteins are believed to modulate the interaction between vesicle and target membrane SNAREs, and thus regulate intracellular vesicular transport. The first SM protein to be identified was UNC-18 in genetic screen for uncoordinated phenotypes in *C. elegans* (Brenner 1974). The mammalian homologue, munc 18a, was identified by virtue of its ability to bind syntaxin1 (Hata *et al.* 1993). It has since been discovered that all types of intracellular membrane traffic require an SM protein (for a review see Jahn *et al.* 1999).

Munc 18c is known to bind strongly to syntaxin4 (Tellam *et al.* 1997), an interaction that dramatically reduces the association of syntaxin4 and VAMP2 by 75%. Similarly munc 18c was also able to reduce the binding of cellubrevin to syntaxin4 by 60% (Tellam *et al.* 1997). Co-immunoprecipation studies determined that syntaxin4 can bind both SNAP23 and munc 18c *in vivo*, but that munc 18c decreases the affinity of syntaxin4 for SNAP23 (Araki *et al.* 1997). In the presence of insulin, it has been demonstrated that the munc18c-syntaxin4 interaction has been lost (Thurmond *et al.* 1998). Taken together, the above would suggest an inhibitory role for munc18c, preventing SNARE complex formation until the correct signal (the presence of insulin) is received.

In this chapter, we sought to mutate the neuronal munc 18a in such a manner to alter its syntaxin-binding characteristics to become more like those of munc 18c. Having shown this to have been achieved it was then possible to make a recombinant Adenovirus of the mutated munc 18a (in addition to wild-type munc 18a and munc 18c) in order to drive expression in mammalian cells.

4.3 Results

4.3.1 Production of munc18a/c

Potential sites of interaction between munc18a and syntaxin1

The recent elucidation of the 3D structure of the munc 18a-syntaxin1 interaction (Misura *et al.* 2000) allowed for potential points of contact to be identified between these proteins, based on close proximity of specific amino acids. From this, three particular sites on munc 18a were identified as being potential points of contact. These were a Threonine at postion 52 (T52); a sequence of Isoleucine, Glycine, Glutamic Acid, Alanine, Arginine and Valine (IGEARV) starting at position 271; and a Glutamine at position 338 (Q).

A sequence alignment of munc 18a and munc 18c allowed identification of the corresponding amino acids on the munc 18c sequence (Figure 4.1). From the alignments, the three mutations we planned to introduce into munc 18a were the T52 to Glutamic Acid (T(52)E); the IGEARV to Lysine and Glutamic Acid (IGEARV>KE); and Q338 to Arginine (Q(338)R) as highlighted.

Production of munc18 a/c

Primers were designed for these three mutations (described above) in order to make a modified munc 18a, called munc 18a/c. The mutagenesis was carried out as described in the Methods section, and the sequence confirmed by automated sequencing before continuing with protein expression [Briefly the mutations were introduced by three

sequential rounds of mutagenesis: in order IGEARV→KE, then T(52)E and finally Q(338)R] . Having confirmed the sequence, the mutated protein was expressed and purified (as in Methods) and this was confirmed by SDS-PAGE of the purified fractions. Figure 4.2 confirms the expression and purification of a munc 18a/c.

4.3.2 The munc18 a/c mutations do not alter protein structure

In order to discover whether the three mutations carried out on munc 18a had any significant effect on the folding and overall structure of the protein, Circular Dichroism Analyis (CD Analysis) was carried out.

Figure 4.3 shows the Far UV spectra for each of the three munc 18 proteins, which gives an indication of the secondary structure environment of a protein. As can be seen the spectra for all three are broadly the same (particularly for munc 18a and a/c). This provides evidence that the secondary structure features present are very similar after the mutations have been made.

Having shown no significant change caused to the secondary structure by the mutations, the Near UV spectra (Figure 4.4) allowed a comparison to be made between the tertiary structures of the three munc 18 proteins. As can be seen the spectra of munc 18a and a/c are again very similar, indicating that no significant alterations in the overall folding of the protein have been caused by the mutations. The spectrum seen for munc 18c is quite different, particularly in the 260-280nm wavelength range. Readings in this range of the spectrum attribute to phenylalanine

(and possibly tyrosine) residues and as such it would suggest that the overall folding of munc 18c is different from both munc 18 and munc 18a/c.

However, the most important result to notice here is that we have confirmed that the three mutations introduced into munc 18a to produce munc 18 a/c have had no significant effect on the overall protein folding and shape.

4.3.3 Characterising the syntaxin interactions of munc 18a/c

It had been intended to investigate the binding capabilities of each munc 18-syntaxin interaction using a variety of methods. However, this proved to be problematic (and will be discussed below), and as such only the GST-pull down assay was able to produce positive results.

GST-pull down assay

As described in the Methods section, each munc 18 protein has a his_6-tag and each syntaxin is expressed as a GST-fusion protein. This allowed a GST-pull down assay to be used in order to determine the syntaxin-binding capabilities of the munc 18a/c protein, compared to the wild-type munc 18a and munc 18c.

Two other methods of investigating the binding capabilities of each munc 18-syntaxin interaction were attempted (using Ni^{2+}-NTA agarose beads, and BIACORE techniques). These however proved to be problematic, but will be discussed below.

As can be seen from Figure 4.5, as expected munc 18a is seen to interact with syntaxin1, and munc 18c does not. We have also been able to determine that the mutations introduced to munc 18a cause the loss of its interaction from syntaxin1 (munc 18a/c does not interact with syntaxin1).

The pull-down assay using GST-syntaxin2 confirmed the interaction of both munc 18a and munc 18c with syntaxin2. It was also seen that the munc 18a/c was able to interact with syntaxin2. From this data, the mutations have not altered the syntaxin2 interaction.

The results seen in the pull-down assays with syntaxin3 did not agree with previous findings. It had been previously established that whereas munc 18a binds to syntaxin3, munc 18c does not. However, our results suggested that munc 18c does interact with syntaxin3. As such it is difficult to determine anything from the finding here that munc 18a/c was seen not to interact with syntaxin3.

Crucially the syntaxin4 experiment established that munc 18a/c was able to bind to syntaxin4, like munc 18c is known to. The munc 18a protein was (as expected) unable to interact with syntaxin4, demonstrating that the three mutations introduced to munc18a have altered its syntaxin4 binding capabilities, as was intended.

Therefore, from these GST-pull down assays it can be confirmed that the three mutations introduced into munc 18a have caused loss of binding to syntaxin1, and caused an interaction with syntaxin4 to be established.

BIACORE techniques

Having now established the syntaxin-binding capabilities of each munc 18 protein, it had been hoped to use the BIACORE system in order to investigate the kinetics of each munc 18-syntaxin interaction. However as mentioned before this proved problematic.

In order to investigate the interaction, it was first necessary to amine-couple a GST antibody onto a standard BIACORE chip (Sensor Chip CM5). This was achieved using the EDC/NHS (N-(3-dimethylaminopropyl)-N'-ethylcarbodiimide and N-hydroxysuccinimide) amine-coupling kit. Briefly, the EDC/NHS is passed over the flow cells on the CM5 chip, which activates the functional groups on the surface of the chip. That done, the GST antibody can undergo amine coupling to these activated surfaces, before finally any unreacted surfaces can be deactivated by ethanolamine [The above procedure was carried out following the instructions detailed in the Immobilization Wizard in BIACORE programmes].

Having successfully attached the GST antibody onto the chip, the aim was then to first flow a GST-syntaxin protein over the chip, and then compare the response seen when each munc 18 protein was injected into the system. However, as said before, we encountered problems at this stage. As a control, one of the four flow cells on the chip is 'blanked' (no GST antibody attached) and as such the GST-syntaxin, and hence munc 18, proteins should not interact. This would mean that no response should be produced from this flow cell. However, despite repeating this experiment twice, each

time a response was seen from this blanked flow cell. This response was significant enough to cast doubt over the responses seen from the other activated flow cells.

As a result of this, we were unable to use this system as we had intended, in order to characterise the kinetics of the syntaxin-munc 18 interaction. It had been hoped to study the kinetics by a combination of altering the concentration of one of the substrates (with a constant flow rate), or by altering the flow rate of substrate through the cells (with constant substrate concentrations).

Binding studies using Ni^{2+}-NTA agarose beads

As an alternative to the GST-pull down assay, it should also have been possible to make use of Ni^{2+}-NTA agarose beads (to interact with his_6-tagged munc 18 protein) in order to establish the binding interactions. However, this procedure too proved to be problematic.

Here the his_6-tagged munc 18 protein is first incubated with Ni^{2+}-NTA agarose beads, and then the syntaxin of interest is added. After an incubation period, the beads can be washed and then bound protein eluted by boiling in 1 x SDS buffer. This elutant can then be separated by SDS-PAGE, and the presence of syntaxin established by western blotting, using a GST antibody. As a control, Ni^{2+}-NTA agarose beads were incubated with syntaxin alone, which should not bind as the syntaxin proteins are GST-fused. The results obtained however showed significant levels of GST-syntaxin in the control lanes, and because of this high background this method was shown to be unsuitable.

Therefore, of the three potential mechanisms used in order to charcterise the synatxin-binding capabilities of each munc 18 protein, only the GST-pull down assay proved to have been successful. Using this method, it was possible to determine two key features of the syntaxin-binding behaviour of the munc 18a/c mutant. These are that munc 18a/c is unable to interact with syntaxin1 (like the wild-type munc 18a), but is able to interact with syntaxin4 (like the wild-type munc18c).

4.3.4 Preparation for production of Adenoviral munc 18 proteins

As it had now been confirmed that munc 18a/c is able to bind to syntaxin4, the next aim was to over-express each munc 18 protein using the Adenoviral system.

Initially, primers were designed in order to clone each of the munc 18 sequences into the pShuttle-CMV vector, and place a C-terminal FLAG tag onto the sequence (Figure 4.6A). The PCR reactions were carried out as described in the Methods section, and the product TAQ-treated and cloned into pCR2.1 (see Figure 4.6B). At this point the sequences were confirmed by automated sequencing before continuing with ligation with the pShuttle-CMV (see Figure 4.6B).

4.3.5 Munc 18 ligation with pShuttle-CMV

In order to ligate each munc 18 sequence into the shuttle vector, it was first necessary to digest each munc 18/pCR2.1 and pShuttle-CMV vector DNA with the appropriate restriction enzymes. Figure 4.7 shows a DNA gel of each of these digests. The bands corresponding to the digested munc 18 and pShuttle-CMV DNA were then gel purified in preparation for ligation.

The ligation reaction was carried out as described in Methods section, and once transformed into TOP 10 cells and plated, colonies were selected. DNA from each of the colonies was then digested with the appropriate restriction enzymes in order to establish whether successful ligation has occurred. The results shown in Figure 4.8 confirmed that each ligation had been successful, and the DNA from these ligations was used for future work.

4.3.6 BJ5183 co-transformation

Having successfully ligated each munc 18 gene into the pShuttle-CMV vector, the next step in the process of Adenovirus production was to co-transform the linearised transfer vector (the munc 18/pShuttle-CMV vector digested with *Pme I*) and pAd-Easy vector into electrocompetent BJ5183 cells (see Figure 4.9). This was achieved by electroporation following the procedure in the Methods section. The transformation mix was then plated and the smallest colonies selected as possible recombinants [the larger colonies represent background from the shuttle vector]. DNA from each was then digested with *Pac I* in order to verify whether the co-transformation has been successful. Figure 4.10 is a DNA gel showing the successful recombinants for each of the three munc 18 genes, as well as the pAd-Easy control.

4.3.7 DH5α transformation

The BJ5183 cells, although suitable to allow recombination, are not stable and as such are prone to deletion. As a result, the pAd-Easy/Munc18 plasmid is transformed into more stable DH5α cells, which are suitable for producing large amounts of DNA (which is needed for transfecting cells). The transformation was achieved by electroporation, following the procedure in the Methods section. The transformation mix was then plated and a number of colonies selected. DNA from each was then digested with *Pac I* in order to identify whether the transformation has been successful. The results from Figure 4.11 demonstrate that the transformation has been achieved, and as such larger quantities of DNA, from successful digests, are produced prior to the HEK transfection.

4.3.8 Transfection of HEK cells with pAd-Easy/Munc18 plasmid

At this stage it was then possible to attempt to transfect the PAd-Easy/Munc 18 plasmid into HEK 293 cells. In order to do this, 20μg of each recombinant Adenovirus plasmid is first digested with *Pac I*. The transfection itself was carried out as described in the Methods section. After ~10 days the cells were spun down, and cracked open to give the cell lysate (through a series of freeze-thaw cycles). If successful transfection, and consequent expression of the munc 18 constructs has occurred, then the presence of the protein can be identified by use of an antibody to the FLAG-tag. As can be seen in Figure 4.12, there has been successful transfection and expression for both munc 18a and munc 18a/c, but not for munc 18c. The transfection for munc 18c was repeated another twice, but this too was without success. It had been intended at this stage to continue by amplifying the production of

each recombinant adenovirus, and purifying them. However time constraints plus the problems of achieving expression of the munc 18c adenovirus meant that this could not be done.

4.4 Discussion

GLUT4 has been shown to translocate to the plasma membrane via a SNARE type mechanism (Cheatham *et al.* 1996). The fusion of GSVs with the plasma membrane involves three helices from the t-SNAREs (two from SNAP23 and one from syntaxin4) and one helix from the v-SNARE (VAMP2). This SNARE mechanism (resulting in GLUT4 incorporation onto the plasma membrane) is strikingly similar to the mechanism by which neurotransmitter release occurs in the synapse.

It is known that all intracellular membrane traffic requires a sec1/munc 18 (SM) protein, as when no such protein is expressed there is a block in membrane fusion. These SM proteins are believed to modulate the interaction between vesicle and target membrane SNAREs, and thus regulate intracellular vesicular transport. Perhaps the best characterised isoform is the mammalian neuronal munc 18a, which was identified by virtue of its ability to bind syntaxin1 (Hata *et al.* 1993).

The syntaxin1-munc 18a interaction is now known (Misura *et al* 2000) and this demonstrated that when munc 18a interacts with sytaxin1, it does so in such a way that the H3 domain (used in SNARE complex formation) comes into close proximity with three other N-terminal helices on syntaxin1 (the H_{abc} domain) and as such the

SNARE complex is not able to form. Syntaxin1 is said to be in its "closed" conformation when bound to munc 18a.

Munc 18c is the homolgue found in insulin responsive tissues, although its less well understood than munc 18a. Munc 18c is known to bind strongly to syntaxin4 (Tellam *et al.* 1997), an interaction that dramatically reduces the formation of the SNARE complex. This interaction was deomonstrated to be lost upon insulin stimulation, implying that munc 18c has an inhibitory role in GLUT4 membrane fusion. Thus the actions of munc 18c and munc 18a seem to be quite similar: they both appear to bind to their syntaxin-binding partner, and in doing so prevent SNARE complex formation and membrane fusion until required.

It was thought originally that all SM proteins functioned by binding to closed conformations of syntaxins, and thus when bound to an SM protein the syntaxin was unable to form a SNARE complex. Recent discoveries have shown this not to be the case. For example the crystal structure of the SM protein Sly1 showed considerable conservation, and had the same arch-shape, to that of Munc 18a. However unlike syntaxin1, here the syntaxin homologue (Sed5) does not bind the central cavity of its SM protein, but rather the outside of one of its three domains. As such Sed5 is able to bind its SM protein and form a SNARE complex simultaneously.

In this chapter, we sought to establish whether the neuronal munc 18a could be mutated in such a manner that its syntaxin-binding characteristics would become more like those of munc 18c. Three close points of contact between syntaxin1 and munc 18a provided three possible sites of mutation that theoretically could alter the

syntaxin-binding characteristics without causing any significant alteration to protein structure.

Figures 4.3 and 4.4 (the CD analysis) demonstrate that these three rounds of mutagenesis have not altered the protein structure greatly, since the spectra seen in both cases is very similar between munc18a and the mutated form (munc18a/c).

The binding studies seen in Figure 3.5 demonstrate that (as predicted) the mutated protein is no longer able to interact with syntaxin1, but is now able to interact with syntaxin4 like munc 18c does. It had been hoped to further characterise these interactions using the BIACORE system, but as detailed in Section 4.3.3 this proved to be problematic.

However, having shown the desired alteration in the syntaxin-binding behaviour of the mutated protein we were able to construct a recombinant Adenovirus of the mutated munc 18a (in addition to wild-type munc 18a and munc 18c) in order to drive expression in mammalian cells.

As seen in Figures 4.7-4.11, each munc18 gene was successfully inserted into the pAd-Easy vector that is used to transfect HEK cells. However, upon transfection only the munc18a and munc 18a/c were expressed in HEK cells. Even upon repetition of the transfection step for the pAd-Easy/Munc18c expression could not take place.

At this stage, the study ended. It would have been difficult to progress from here since it had been hoped to ultimately overexpress each munc 18 adenoviral construct in 3T3-L1 adipocytes and establish the effect on glucose transport. In this experiment

the results from an overexpressed munc 18c wild-type would have been an important reference point.

In conclusion then, here we identified three sites on munc18a that theoretically could alter its syntaxin-binding behaviour: in particular cause the mutated protein to interact with the syntaxin involved in GLUT4 vesicle fusion (syntaxin4) and prevent interaction with the neuronal syntaxin (syntaxin1). We determined that this indeed was the case upon expression of munc 18a/c, and was without significant alteration to the protein structure. We also created recombinant Adenovirus constructs of each of the three munc 18 genes, although only two (munc 18a and munc 18a/c) were seen to be expressed in mammalian cells.

Figure 4.1 Alignments of Munc 18a,b, c and unc 18

The 3D structure of the munc 18a- syntaxin1 interaction identified three close interactions (and hence possible points of contact) between the two proteins. The amino acids of munc 18a were noted, and then compared to the corresponding amino acids of munc 18c in a sequence alignment. From these alignments, three possible sites were identified for mutagenesis: T(52)E, an IGEARV to KE mutation starting at position 271, and Q(338)R.

Figure 4.1

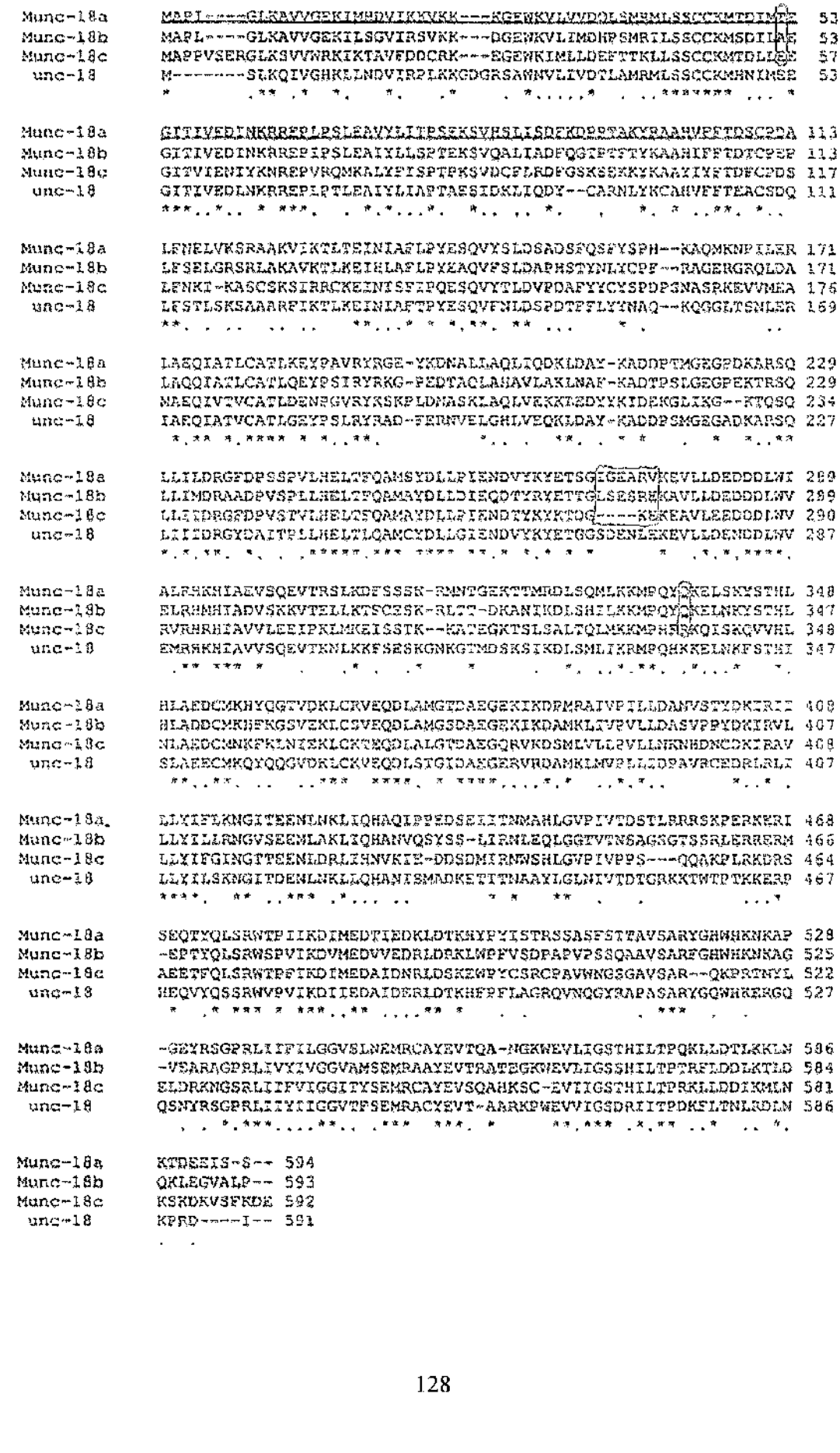

Figure 4.2 Purified his_6-tagged munc 18a/c.

His_6-tagged munc 18a was mutated (as described in Methods), transformed into M15 cells and protein expression induced with IPTG. The cell lysate was then passed through a 3ml Ni^{2+}-NTA agarose column, washed with His_6-tag Purification Buffer (containing 50mM imidazole) and then 12 x 1ml fractions eluted from the column by applying a step gradient of increasing concentrations of imidazole in this buffer (ranging from 95mM-275mM). 20µl of each fraction was then separated by SDS-PAGE. The gel shows a band of ~60 kDa which corresponds to his_6-tagged munc 18a.

Figure 4.2

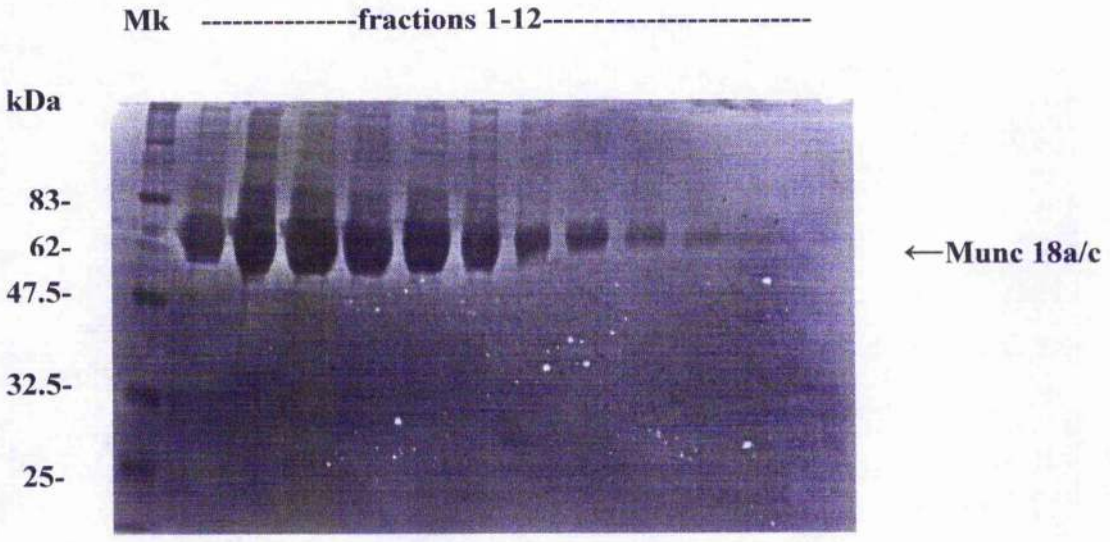

Figure 4.3 Far UV CD Analysis of munc 18a, a/c and c.

0.3mg/ml of each munc 18 protein were needed for Far UV CD Analysis. The figure shows the spectra for each of the three proteins [Munc 18a is pink, 18a/c is red and 18c is blue]. It was first necessary to dialyse the purified proteins to remove imidazole from the samples (This figure is from an experiment done by Dr Sharon Kelly).

Figure 4.3

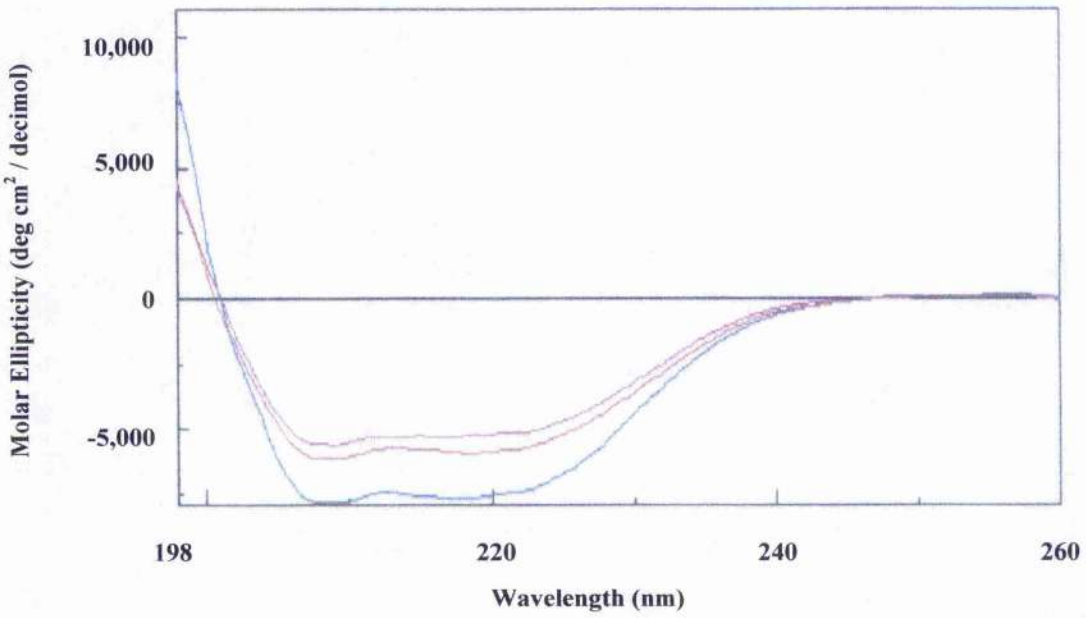
10,000
5,000
0
-5,000
Molar Ellipticity (deg cm^2 / decimol)
198
220
240
260
Wavelength (nm)

Figure 4.4 Near UV CD Analysis of munc 18a, a/c and c.

1.0mg/ml of each munc 18 protein were needed for Near UV CD Analysis. The figure shows the spectra for each of the three proteins [Munc 18a is pink, 18a/c is red and 18c is blue]. Again, it was first necessary to dialyse the purified proteins in order to remove imidazole from the samples (This figure is from an experiment done by Dr Sharon Kelly).

Figure 4.4

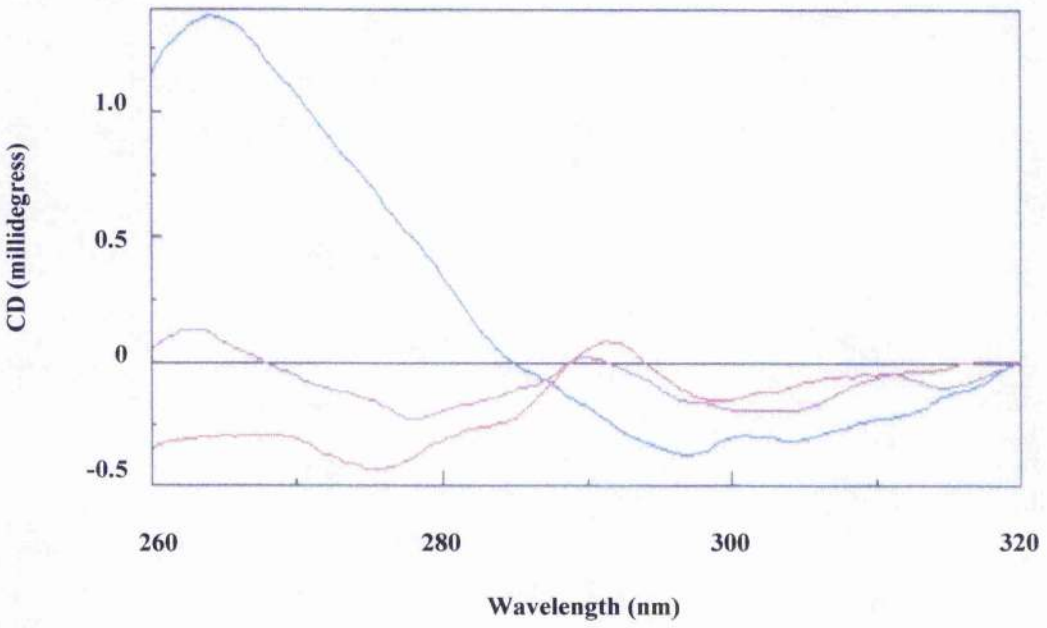

Figure 4.5 His_6-tagged munc 18-syntaxin binding studies

Binding reactions were carried out as described (in Methods) and 20µl of each sample was separated by SDS-PAGE. Briefly 2µM of GST or GST-synatxin protein were added to Glutathione beads, and incubated at 4°C with end-over-end rotation for 1h. An equivalent volume of his_6-tagged munc 18 protein was then added to make a final concentration of 1µM for munc 18, and the mixture was incubated for 2h at 4°C with end-over-end rotation. The beads were then washed twice with Binding Buffer containing 1mg/ml gelatin, and three times with Binding Buffer containing 5% glycerol. Any bound proteins were then eluted by boiling the beads in Sample Buffer. Shown are the immunoblots received for the his_6-tag when interaction with each syntaxin is investigated [The secondary antibody used to recognise the His_6-tag was HRP-conjugated donkey anti-mouse IgG].

The samples in each lane are:

1. his_6-tagged munc 18a + GST-syntaxin
2. his_6-tagged munc 18a + GST
3. his_6-tagged munc 18a/c + GST-syntaxin
4. his_6-tagged munc 18a/c+ GST
5. his_6-tagged munc 18c + GST-syntaxin
6. his_6-tagged munc 18c+ GST
7. his_6-tagged munc 18a alone [0.05µg of purified protein]
8. his_6-tagged munc 18a/c alone [0.05µg of purified protein]
9. his_6-tagged munc 18c alone [0.05µg of purified protein]
10. GST-syntaxin alone [0.05µg of purified protein]

Figure 4.5

syntaxin1:

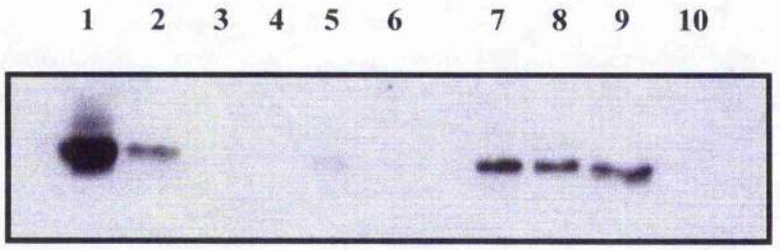

His_6-tag

syntaxin2:

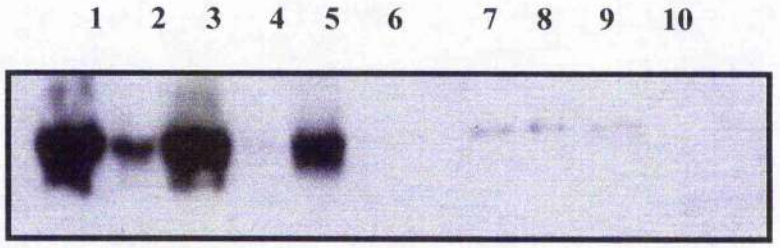

His_6-tag

syntaxin3:

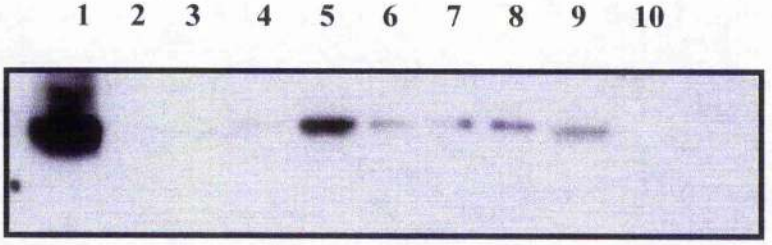

His_6-tag

syntaxin4:

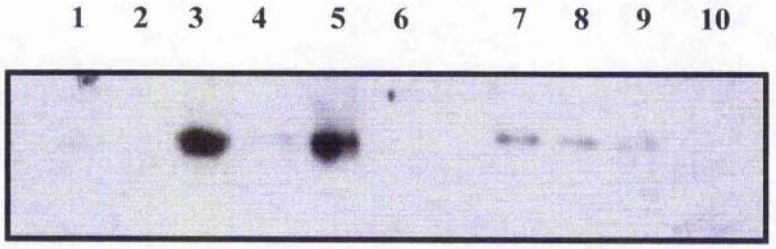

His_6-tag

Figure 4.6A The munc18 genes for production of recombinant Adenovirus

The figures opposite show simplified views of each of the three munc 18 constructs, showing how they have been modified in order to produce recombinant Adenoviral constructs of each. Restriction sites have been added to both the N and the C terminal end of each construct to allow successful ligation into the pShuttle-CMV vector, and a FLAG-tag at the C-terminus means that the expressed protein can be identified.

Figure 4.6A

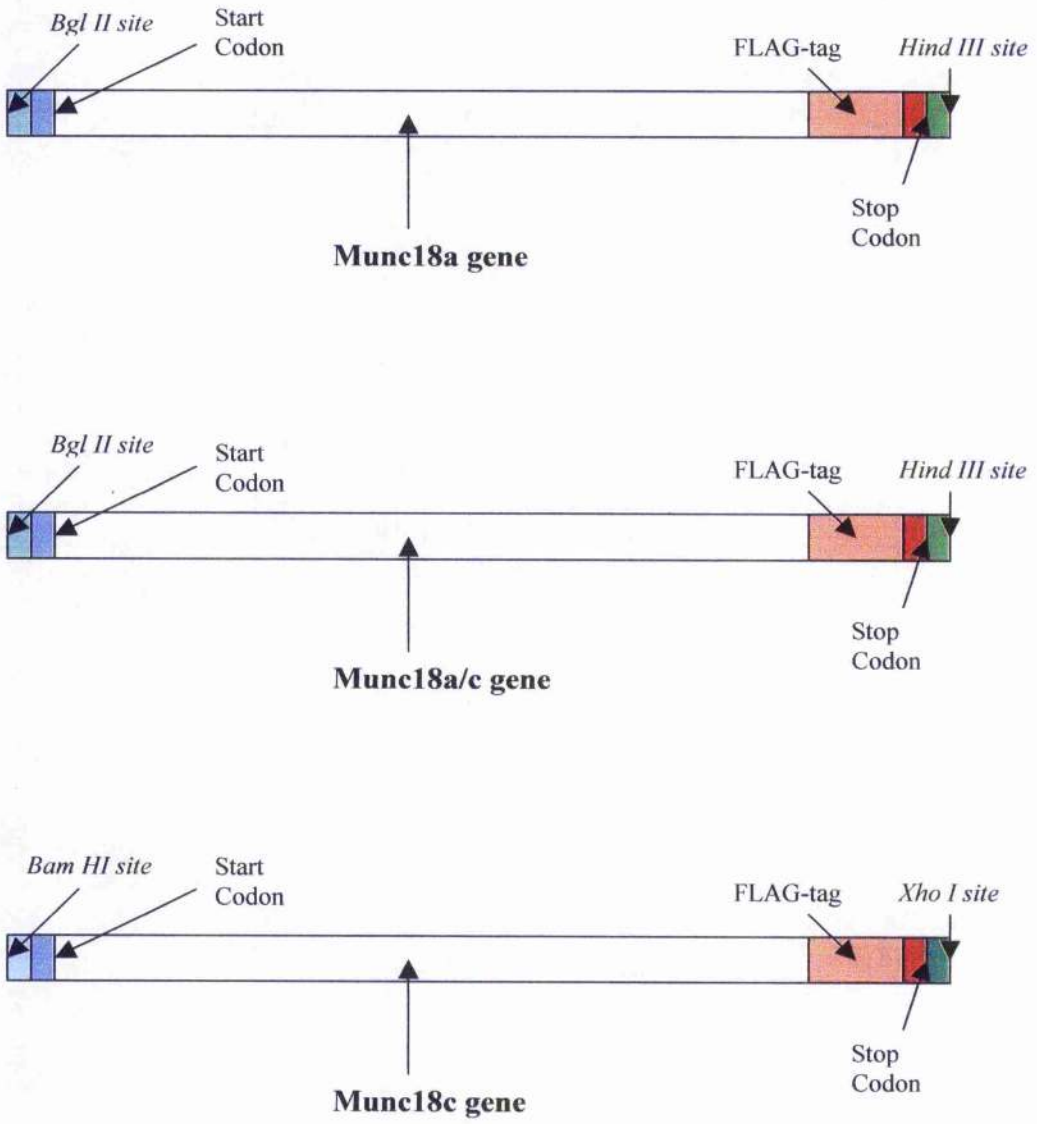
Bgl II site
Start Codon
FLAG-tag
Hind III site
Stop Codon
Munc18a gene
Bgl II site
Start Codon
FLAG-tag
Hind III site
Stop Codon
Munc18a/c gene
Bam HI site
Start Codon
FLAG-tag
Xho I site
Stop Codon
Munc18c gene

Figure 4.6B Plasmid maps of pCR2.1 and pShuttle-CMV

After the completion of the PCR reactions to generate each of the constructs seen in Figure 4.6A, the PCR product is TA cloned into pCR2.1. The plasmid map of pCR2.1 shows the multiple cloning site (MCS) into which the PCR product is cloned. Successful TA cloning will produce a plasmid of ~5.7kb in size.

[Note here the position of a *Bgl II* restriction site outwith the MCS (at position 1282) of pCR2.1, which is significant when the munc18a and munc18a/c/pCR2.1 plasmid is digested (see Figure 4.7)].

The pShuttle-CMV map shows the location of the MCS into which each munc18 construct is ligated. Note here that although the MCS of pShuttle-CMV does not contain a *Bam HI* restriction site (the munc18c construct has been made with a *BamHI* site at its), a *Bgl II* digestion of pShuttle-CMV leaves the same overhang, allowing ligation to occur. Successful ligations will produce a plasmid of ~ 9.2kb in size.

Figure 4.6B

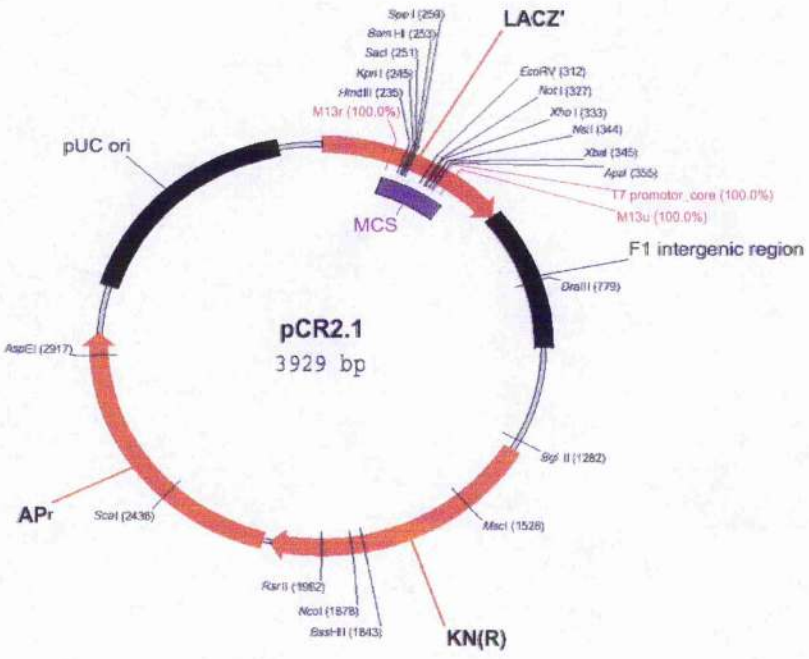

PCR2.1 plasmid map

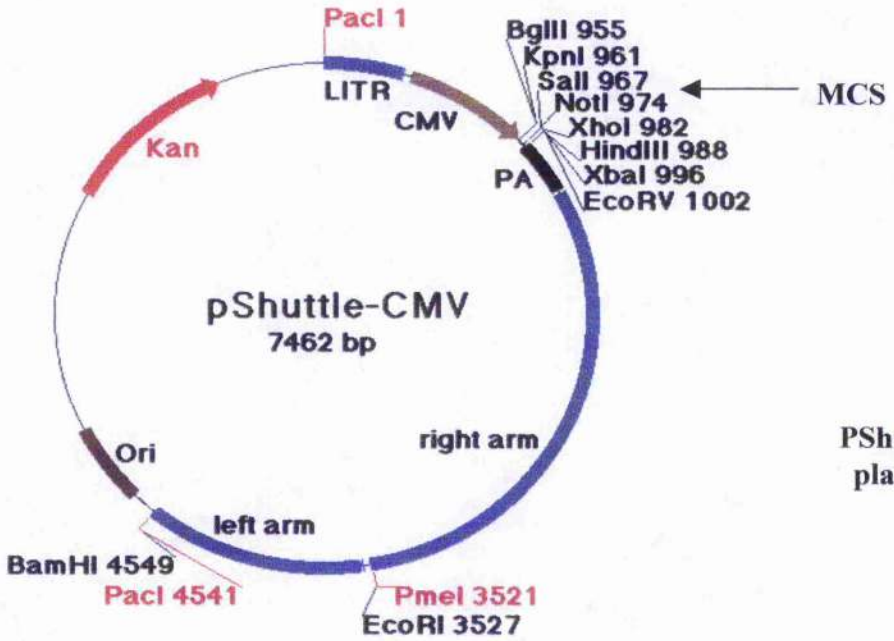

PShuttle-CMV plasmid map

Figure 4.7 Samples for ligation of munc 18 into pShuttle-CMV vector.

Each of the three munc 18/PCR 2.1 constructs was digested with the desired restriction enzymes (as indicated) for ligation to occur (NB. pCR2.1 has an internal *Bgl II* site hence three bands are seen). Likewise the pShuttle vector was digested with the desired restriction enzymes, and a small sample of the digest was resolved by DNA gel electrophoresis. These samples were then gel purified prior to ligation.

1. Munc18a/pCR2.1 digested with *Bgl II & Hind III*
2. Munc18a/c/pCR2.1 digested with *Bgl II & Hind III* [the smallest band here is very feint & its position is highlighted by an arrow on figure 4.7]
3. Munc18c/pCR2.1 digested with *Bam HI & Xho I*
4. pShuttle-CMV digested with *Bgl II & Hind III* (for ligation with munc 18a and a/c)
5. pShuttle-CMV digested with *Bgl II & Xho I* (for ligation with munc 18c)

Figure 4.7

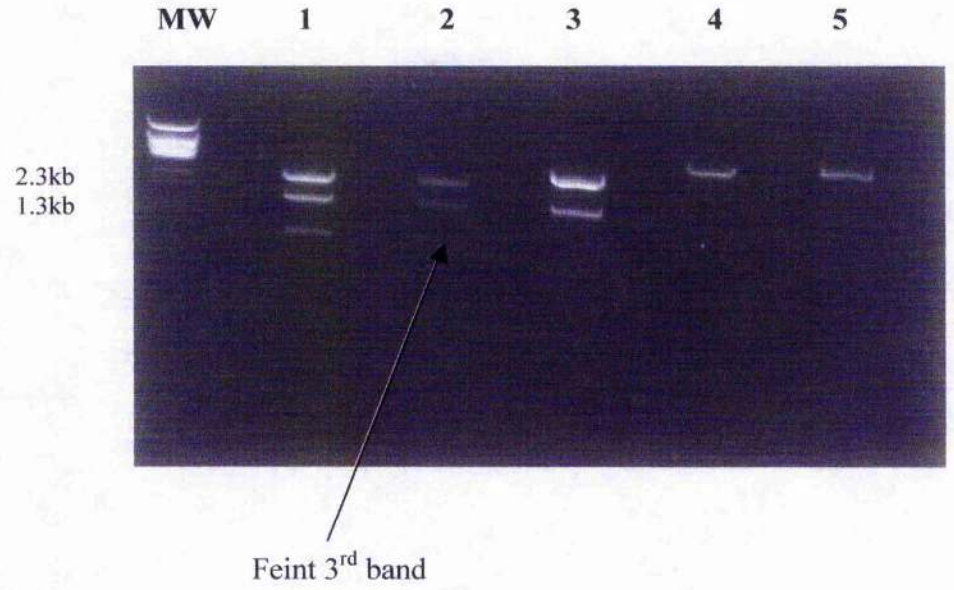

Figure 4.8 Results of ligation between munc18s and pShuttle-CMV

Ligation experiments were carried out as described (in Methods) and various colonies were selected. DNA from each was digested with the restriction enzymes indicated in order to establish whether successful ligation had occurred (NB. since there is no appropriate restriction site at the N-terminal end of the munc 18c sequence, *Nde I* was used to digest the DNA: this has two sites in pShuttle-CMV and one internal site in munc 18c, hence a successful ligation would provide three bands upon digestion). A small sample of each digest was then resolved by DNA gel electrophoresis. The DNA from successful ligations (munc18a lane 7, munc 18a/c lane 9 and munc 18c lane 8) was used in future work.

[The digested munc 18a and munc 18 a/c/pShuttle-CMV vectors give two bands of approximately 7.5 and 1.8 kb. The digested munc 18c/pShuttle-CMV vector gives three bands of approximately 4.6, 3.5 and 1.1 kb].

Figure 4.8

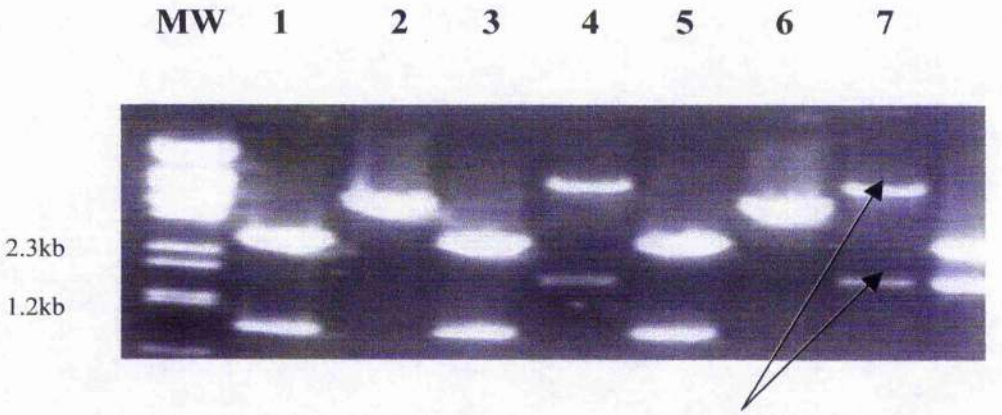

pShuttle-CMV/munc18a ligation digested with *Bgl II* & *Hind III*

pShuttle-CMV/munc18a/c ligation digested with *Bgl II* & *Hind III*

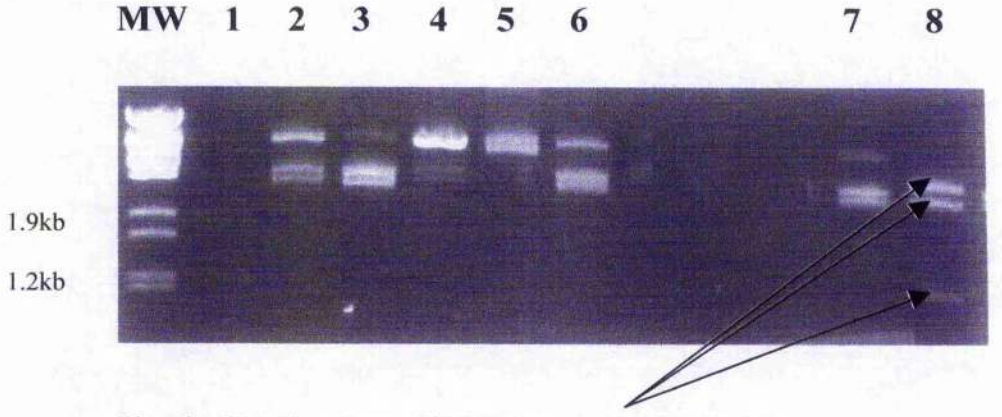

pShuttle-CMV/munc18c ligation digested with *Nde I*

Figure 4.9 Production of a recombinant pAd plasmid

The diagram opposite details how a recombinant Pad plasmid is generated from the linearised transfer vector (pShuttle-CMV/munc18) and the p-Ad Easy vector. When the pShuttle-CMV/munc18 is digested with *Pme I* this produces linearised DNA with the "left arm" and "right arm" regions at either end. These "left arm" and "right arm" sequences represent the regions mediating homologous recombination between the shuttle vector and the adenoviral backbone vector.

In order to achieve the recombination, the transfer vector and pAd Easy vector are co-transformed into BJ5183 cells by electroporation as described in Methods. Successful recombinants will be ~40kb in size, and will show resistance to Kanamycin.

Figure 4.9

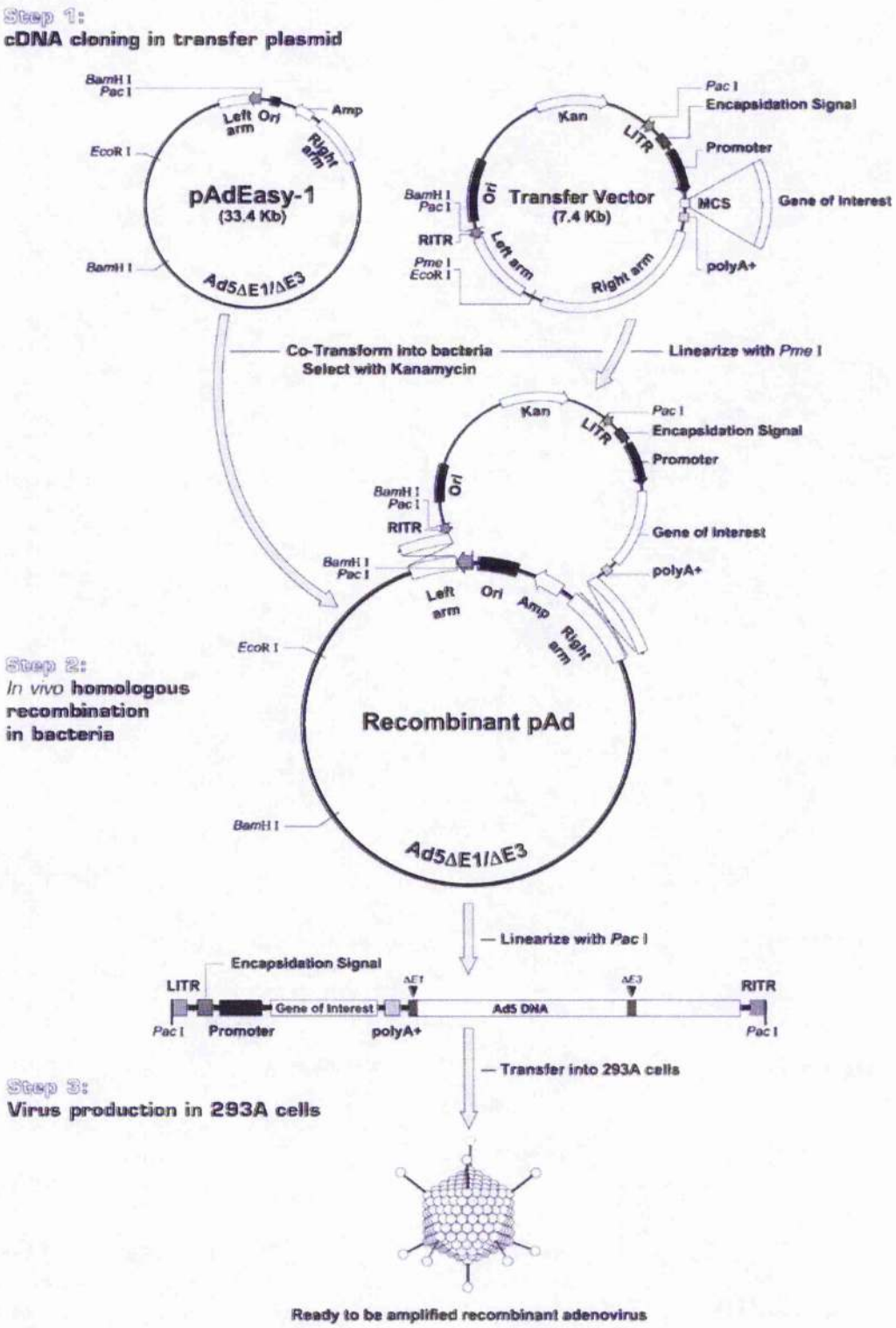
Step 1:
cDNA cloning in transfer plasmid
BamH I
Pac I
Left Ori arm
Amp
Right arm
EcoR I
pAdEasy-1
(33.4 Kb)
BamH I
Ad5ΔE1/ΔE3
Pac I
Encapsidation Signal
Kan
LITR
Promoter
BamH I
Pac I
Ori
Transfer Vector
(7.4 Kb)
MCS
Gene of Interest
RITR
Left arm
Pme I
EcoR I
Right arm
polyA+
Co-Transform into bacteria
Select with Kanamycin
Linearize with Pme I
Kan
Pac I
Encapsidation Signal
LITR
Promoter
Ori
BamH I
Pac I
RITR
Gene of Interest
BamH I
Pac I
polyA+
Left arm
Ori
Amp
Right arm
EcoR I
Step 2:
In vivo homologous recombination in bacteria
Recombinant pAd
BamH I
Ad5ΔE1/ΔE3
Linearize with Pac I
Encapsidation Signal
LITR
ΔE1
ΔE3
RITR
Gene of Interest
Ad5 DNA
Pac I
Promoter
polyA+
Pac I
Transfer into 293A cells
Step 3:
Virus production in 293A cells
Ready to be amplified recombinant adenovirus

Figure 4.10 Results of co-transformation of pAd-Easy and munc 18s into BJ5183 electrocompetent cells

DNA from each successful ligation was first linearised using *Pme I.* This was then mixed with pAd-Easy and added to electrocompetent BJ5183 cells and electroporated (as described in Methods). DNA from colonies obtained was digested with *Pac I* in order to discover if each munc 18 has been incorporated into the pAd-Easy. A small sample of each successful co-transformation was then resolved by DNA gel electrophoresis as shown [successful recombinants are ~40 kb in size].

1. pAd-Easy digested with *Pac I*
2. pAd-Easy/Munc18a digested with *Pac I*
3. pAd-Easy/Munc18a/c digested with *Pac I*
4. pAd-Easy/Munc18c digested with *Pac I*

Figure 4.10

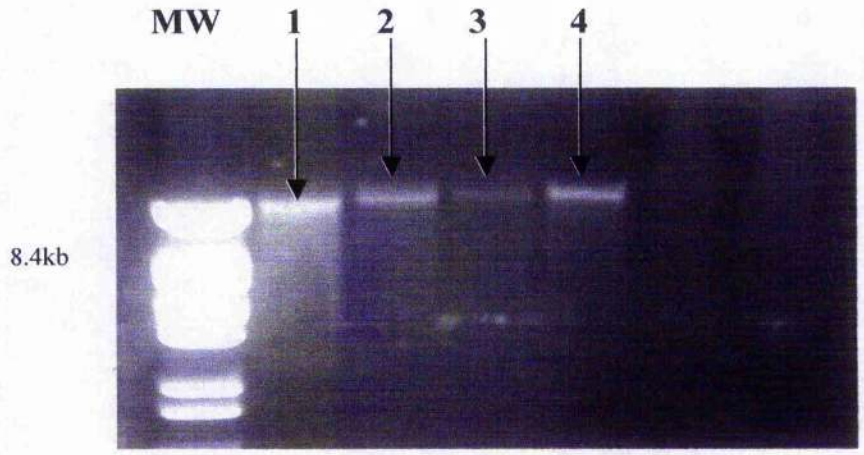

Figure 4.11 Results of transformation of pAd-Easy/munc 18s into DH5α electrocompetent cells

DNA from each successful co-transformation was added to electrocompetent DH5α cells and electroporated (as described in Methods). DNA from colonies obtained was digested with *Pac I* in order to determine whether transformation has been successful. A small sample of each digestion was then resolved by DNA gel electrophoresis. The DNA from successful transformations (control lane 5, munc18a lane 12, munc 18a/c lane 20 and munc 18c lane 24) was used in future work.

[DNA from the successful transformations again is ~40kb in size.]

Figure 4.11

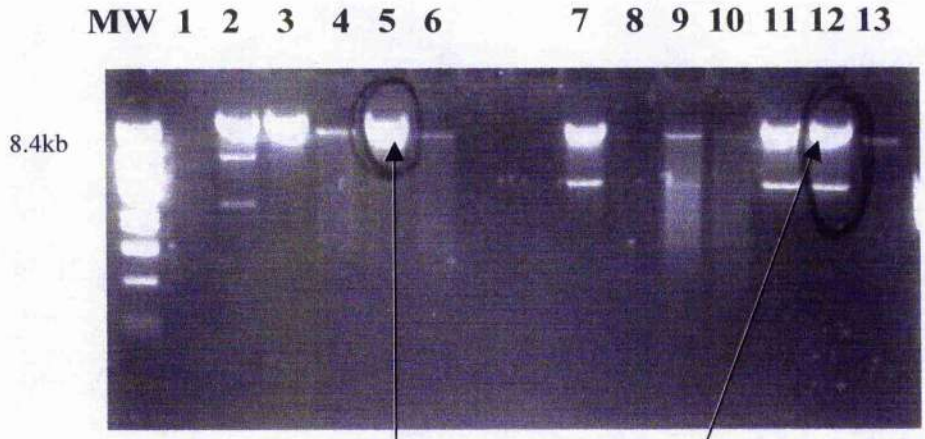

1-6. pAd-Easy control digested with *Pac I*

7-13. pAd-Easy/munc18a digested with *Pac I*

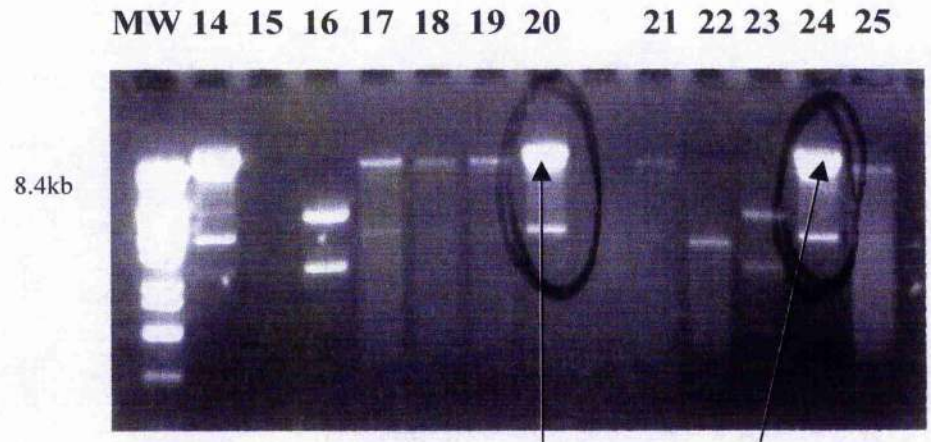

14-20. pAd-Easy/munc18a/c digested with *Pac I*

21-25. pAd-Easy/munc18c digested with *Pac I*

Figure 4.12 Transfection of munc 18s into HEK 293 cells

20μg of each recombinant pAd-Easy/munc 18 plasmid was digested using *Pac I* and transfected into HEK 293 cells (as described in Methods). 10 days after transfection, the cells were spun down (the supernatant gives a media (M) fraction) and resuspended in sterile PBS. This was then subjected to three freeze-thaw cycles, to break cells open, after which samples corresponding to cell membrane pellet (P) and cell lysates (L) were collected. A small aliquot of each was separated by SDS-PAGE. Shown is the immunoblot for the FLAG tag [munc 18 proteins are ~60kDa in size]. [The secondary antibody used to recognise the FLAG-tag was HRP-conjugated donkey anti-mouse IgG].

Figure 4.12

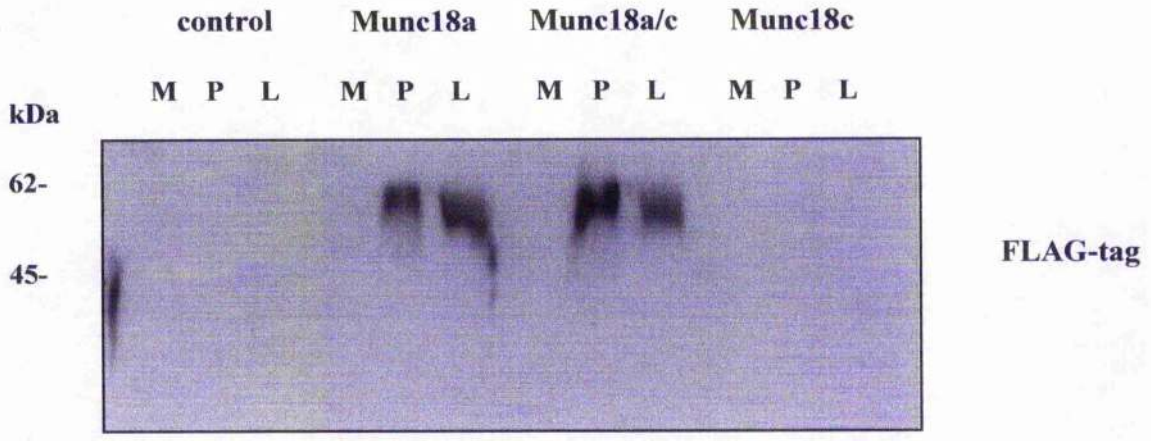
control
Munc18a
Munc18a/c
Munc18c
M P L M P L M P L M P L
kDa
62-
45-
FLAG-tag

CHAPTER 5-OVERVIEW

In reponse to insulin, glucose is taken up by storage tissues such as muscle and fat, via a mechanism known to be mediated by the insulin responsive glucose transporter GLUT4. Under basal conditions, GLUT4 is sequestered intracellularly into two distinct intracellular locations. One of these is known to be endosomal in character, wheras the other represents the highly insulin responsive GLUT4 storage vesicles (GSVs). These GSVs are known to be retained intracellulary in the absence of insulin, but upon insulin stimulation they traffic rapidly to the plasma membrane to allow GLUT4 to fuse to the plasma membrane. It is this rapid translocation of these specialised GSVs that accounts for the large (up to ~20-fold) increase in GLUT4 levels at the plasma membrane in response to insulin, compared to only a slight increase (~2-fold) in levels of recycling proteins such as the transferrin receptor.

It is only when present on the plasma membrane that GLUT4 is able to function and allow glucose transport. The fusion event with the plasma membrane occurs via a SNARE-type mechanism. The v-SNARE VAMP2 (which is present in GSVs) together with the t-SNAREs syntaxin4 and SNAP23 are responsible for the formation of a SNARE complex that is important for membrane fusion. The SM protein munc 18c is known to interact with syntaxin4, which prevents the formation of the SNARE complex. This interaction is seen to be lost upon insulin stimulation. As such, munc 18c could have an inhibitory role in GLUT4 translocation by preventing GLUT4 from fusing to the membrane in the absence of insulin.

A number of methods have been used in order to separate the two intracellular GLUT4 pools. In Chapter 3 we confirmed the validity of a method involving a

sucrose velocity gradient followed by a sucrose equilibrium gradient in 3T3-L1 adipocytes (as described by Guilherme *et al.*). This method demonstrates that the GSVs are indeed far more insulin sensitive than the endosomes. The results in Chapter 3 demonstrate that, in response to insulin stimulation, levels of both GLUT4 and IRAP from fractions containing GSVs were reduced by ~50%. This is in comparison to a more modest 10-20% decrease in levels of the same proteins from fractions corresponding to endosomal GLUT4 vesicles. In this chapter we also looked to see whether other proteins of interest co-localise with GSVs or endosomal GLUT4, and confirmed both that VAMP2 is found in GSVs, and that the transferrin receptor is native to an endosomal compartment.

In this chapter, we also demonstrated the presence of exocyst complex proteins (Sec6 and Sec8) in GLUT4 containing fractions. Recently the exocyst complex has been identified as having a role in GLUT4 trafficking and fusion to the plasma membrane (Inoue *et al.* 2003). Therefore the fact that we found these proteins in the same fractions as some of the GLUT4 vesicles suggests that there is some co-localisation between the exocyst complex and GLUT4, although it does not provide direct evidence of the exocyst complex being involved in GLUT4 translocation.

Results in Chapter 3 also suggest that there may be some co-localisation between ACRP30 and GLUT4. This finding is in conflict with previous results (Bogan & Lodish 1999). As such further analysis of this potential co-localisation would have to be carried out before any relevance can be placed on this result.

Using Stains-all dye a putative Ca^{2+} dependent kinase has been identified, although further investigation into this has not been able to be carried out. This finding could have been significant since Ca^{2+} has been shown to be involved in the insulin-

stimulated transport of glucose in 3T3-L1 adipocytes (Whitehead *et al.* 2001) and as such any calcium-binding proteins found in GLUT4 containing vesicles would be of potential interest. Unfortunately as we were unable to obtain any cDNA or an antibody, this finding could not be explored further.

All membrane fusion events are known to involve SNARE proteins and an SM protein. The SM protein munc 18c is known to interact with syntaxin4 and hence interfere with the formation of a SNARE complex. By doing so the fusion of GSVs with the plasma membrane is prevented, and as such munc 18c is believed to have an inhibitory role in GLUT4 translocation. This mechanism is very similar to the method of neurotransmitter release, where munc 18a holds syntaxin1 in a "closed" conformation preventing membrane fusion until the desired time. In Chapter 4 we attempted to create a mutated version of this munc 18a (called munc 18a/c) with the aim of identifying if it was possible to alter the syntaxin-binding characteristics of the protein. Namely, we aimed to prevent this munc 18a/c from interacting with syntaxin1 (like wild-type munc 18a does) while at the same time allowing interaction with syntaxin4 to occur (like wild-type munc 18c). We demonstrated that the mutations introduced into munc 18a had no significant effect on the protein structure (by Circular Dichroism), and upon carrying out binding studies the predicted alterations in syntaxin binding were confirmed. Unfortunately we were unable to make use of BIACORE techniques in order to study the kinetics of these munc 18- syntaxin interactions in detail.

We also made Adenoviral constructs of munc 18a/c (in addition to wild-type munc 18a and munc 18c) with the intention of driving the expression of these constructs in mammalian cells. A future aim would be to overexpress these in insulin responsive cells in order to identify the effect on glucose transport of the munc 18a/c protein in comparison to the wild-type munc 18c.

In conclusion, we have made use of the sucrose gradient technique in order to examine the intracellular distribution of GLUT4, and to identify proteins that may (based on there presence in the same fractions) co-localise with either GSVs or recycling endosomes. Further analysis would have to be carried out in order to confirm or rule out any co-localisation.

We have also been able to alter the syntaxin-binding characteristics of a munc 18 protein, as we aimed to do. However we were unable to drive expression of all the Adenoviral constructs and as such we were unable to investigate any effects that the mutated munc 18a/c protein may have on GLUT4 translocation at this time.

REFERENCES

Advani, R. J., Bae, H-R, Bock., J. B., Chao, D .S., Doung, Y-C., Prekeris, R., Yoo, J-S., and Scheller, R. H. (1998) Seven novel mammalian SNARE proteins localize to distinct membrane compartments. *The Journal of Biological Chemistry* **273,** 10317-10324

Albiston, A. L., McDowall, S. G., Matsacos, D., Sim, P., Clune, E., Mustafa, T., Lee, J., Mendelsohn, F. A., Simpson, R. J., Connolly, L. M., and Chai, S. Y. (2001) Evidence that the angiotensin IV (AT(4)) receptor is the enzyme insulin-regulated aminopeptidase. *The Journal of Biological Chemistry* **276,** 48623-48626

Aledo, J. C., Lavoie, L., Volchuk, A., Keller, S. R., Klip, A., and Hundal, H. S. (1997) Identification and characterization of two distinct intracellular GLUT4 pools in rat skeletal muscle: evidence for an endosomal and an insulin-sensitive GLUT4 compartment. *Biochemical Journal* **325,** 727-732

Araki, S., Tamori, Y., Kawanishi, M., Shinoda, H., Masugi, J., Mori, H., Niki, T., Okazawa, H., Kubota, T., and Kasuga, M. (1997) Inhibition of the binding of SNAP-23 to syntaxin 4 by Munc18c. *Biochemical and Biophysical Research Communications* **234,** 257-262

Barnard, R. J., Morgan, A., and Burgoyne, R. D. (1997) Stimulation of NSF ATPase activity by alpha-SNAP is required for SNARE complex disassembly and exocytosis. *The Journal of Cell Biology* **139,** 875-883

Barrett, M. P., Walmsley, A. R., and Gould, G. W. (1999) Structure and function of facilitative sugar transporters. *Current Opinion in Cell Biology* **11,** 496-502

Baumann, C. A., Ribon, V., Kanzaki, M., Thurmond, D. C., Mora, S., Shigematsu, S., Bickel, P. E., Pessin, J. E., and Saltiel, A. R. (2000) CAP defines a second signalling pathway required for insulin-stimulated glucose transport. *Nature* **407,** 202-207

Bell, G. I., Burant, C. F., Takeda. J., and Gould, G. W. (1993) Structure and function of mammalian facilitative sugar transporters. *The Journal of Biological Chemistry* **268,** 19161-19164

Bennett, M. K., Calakos, N., and Scheller, R. H. (1992) Syntaxin: a synaptic protein implicated in docking of synaptic vesicles at presynaptic active zones. *Science* **257,** 255-259

Betz, A., Okamoto, M., Benseler, F., and Brose, N. (1997) Direct interaction of the rat unc-13 homologue Munc13-1 with the N terminus of syntaxin. *The Journal of Biological Chemistry* **272,** 2520-2526

Betz, A., Thakur, P., Junge, H. J., Ashery, U., Rhee, J. S., Scheuss, V., Rosenmund, C., Rettig, J., and Brose, N. (2001) Functional interaction of the active zone proteins Munc13-1 and RIM1 in synaptic vesicle priming. *Neuron* **30,** 183-196

Bjornholm, M., Kawano, Y., Lehtihet, M., and Zierath, J. R. (1997) Insulin receptor substrate-1 phosphorylation and phosphatidylinositol 3-kinase activity in skeletal muscle from NIDDM subjects after in vivo insulin stimulation. *Diabetes* **46,** 524-527

Block, M. R., Glick, B. S., Wilcox, C. A., Wieland, F. T., and Rothman, J. E. (1988) Purification of an N-ethylmaleimide-sensitive protein catalyzing vesicular transport. *Proceedings of the National Academy of Sciences USA* **85,** 7852-7856

Bock, J. B., Lin, R. C., and Scheller, R. H. (1996) A New Syntaxin Family Member Implicated in Targeting of Intracellular Transport Vesicles. *The Journal of Biological Chemistry* **271,** 17961-17965

Bonadonna, R.C., Del Prato, S., Saccomani, M. P., Bonora, E., Gulli, G., Ferrannin, E., Bier, D., Cobelli, C., and DeFronzo, R. A. (1993) Transmembrane glucose transport in skeletal muscle of patients with non-insulin-dependent diabetes. *The Journal of Clinical Investigation* **92,** 486-494

Bonadonna, R. C., Del Prato, S., Bonora, E., Saccomani, M. P., Gulli, G., Natali, A., Frascerra, S., Pecori, N., Ferrannini, E., Bier, D., Cobelli, C., and DeFronzo, R. A. (1996) Roles of glucose transport and glucose phosphorylation in muscle insulin resistance of NIDDM. *Diabetes* **45,** 915-925

Bracher, A., and Weissenhorn, W. (2002) Structural basis for the Golgi membrane recruitment of Sly1p by Sed5p. *EMBO Journal* **21,** 6114-6124.

Brenner, S. (1974) The genetics of Caenorhabditis elegans. *Genetics* **77,** 71-94

Brooks, C. C., Scherer, P. E, Cleveland, K., Whittemore, J. L., Lodish, H. F, and Cheatham, B. (2000) Pantophysin is a phosphoprotein component of adipocyte transport vesicles and associates with GLUT4-containing vesicles. *The Journal of Biological Chemistry* **275,** 2029-2036

Bryant, N. J., Govers, R., James, D. E. (2002) Regulated transport of the glucose transporter GLUT4. *Nature Reviews Molecular Cell Biology* **3,** 267-277

Cain, C. C., Trimble W. S., and Lienhard G. E. (1992) Members of the VAMP family of synaptic vesicle proteins are components of glucose transporter-containing vesicles from rat adipocytes. *The Journal of Biological Chemistry* **267,** 11681-11684

Calakos, N., Bennett, M. K., Peterson, K. E., and Scheller R. H. (1994) Protein-protein interactions contributing to the specificity of intracellular vesicular trafficking. *Science* **263,** 1146-1149

Calderhead, D. M., Kitagawa, K., Tanner, L. I., Holman, G. D., and Lienhard, G. E. (1990) Insulin regulation of the two glucose transporters in 3T3-L1 adipocytes. *The Journal of Biological Chemistry* **265,** 13800-13808

Carr, C. M., Grote, E., Munson, M., Hughson, F. M., and Novick, P. J. (1999) Sec1p binds to SNARE complexes and concentrates at sites of secretion. *Journal of Cell Biology* **146,** 333-344

Chapman, E. R., An, S., Barton, N., and Jahn, R. (1994) SNAP-25, a t-SNARE which binds to both syntaxin and synaptobrevin via domains that may form coiled coils. *The Journal of Biological Chemistry* **269,** 27427-27432

Cheatham, B., Vlahos, C. J., Cheatham, L., Wang, L., Blenis, J., and Kahn, C. R. (1994) Phosphatidylinositol 3-kinase activation is required for insulin stimulation of pp70 S6 kinase, DNA synthesis, and glucose transporter translocation. *Molecular and Cellular Biology* **14,** 4902-4911

Cheatham, B., Volchuk, A., Kahn, C. R., Wang, L., Rhodes, C. J., and Klip, A. (1996) Insulin-stimulated translocation of GLUT4 glucose transporters requires SNARE-complex proteins. *Proceedings of the National Academy of Sciences USA* **93,** 15169-15173

Chamberlain, L. H., Graham, M. E., Kane, S., Jackson, J. L., Maier, V. H., Burgoyne, R. D., and Gould GW. (2001) The synaptic vesicle protein, cysteine-string protein, is associated with the plasma membrane in 3T3-L1 adipocytes and interacts with syntaxin 4. *The Journal of Cell Science* **114,** 445-455

Clarke, J. F., Young, P. W., Yonezawa, K., Kasuga, M., and Holman, G. D. (1994) Inhibition of the translocation of GLUT1 and GLUT4 in 3T3-L1 cells by the phosphatidylinositol 3-kinase inhibitor, wortmannin. *Biochemical Journal* **300,** 631-635

Cushman, S. W., and Wardzala, L. J. (1980) Potential mechanism of insulin action on glucose transport in the isolated rat adipose cell. Apparent translocation of intracellular transport systems to the plasma membrane. *The Journal of Biological Chemistry* **255,** 4758-4762

DeBello, W. M., O'Connor, V., Dresbach, T., Whiteheart, S. W., Wang, S. S., Schweizer, F. E., Betz, H., Rothman, J. E., and Augustine, G. J. (1995) SNAP-mediated protein-protein interactions essential for neurotransmitter release. *Nature* **373,** 626-630

Dulubova, I., Yamaguchi, T., Gao, Y., Min, S. W., Huryeva, I., Südhof, T. C., Rizo, J. (2002) How Tlg2p/syntaxin 16 'snares' Vps45. *EMBO Journal* **21,** 3620-3631

Elmendorf, J. S., and Pessin, J. E. (1999) Insulin signaling regulating the trafficking and plasma membrane fusion of GLUT4-containing intracellular vesicles. *Experimental Cell Research* **253,** 55-62

Foster, L. J., and Klip, A. (2000) Mechanism and regulation of GLUT-4 vesicle fusion in muscle and fat cells. *The American Journal of Physiology - Cell Physiology* **279,** C877-C890

Foster, L. J., Weir, M. L., Lim, D. Y., Liu, Z., Trimble, W. S., and Klip, A. (2000) A functional role for VAP-33 in insulin-stimulated GLUT4 traffic. *Traffic* **1,** 512-521

Freidenberg, G. R., Reichart, D., Olefsky, J. M., and Henry, R. R. (1988) Reversibility of defective adipocyte insulin receptor kinase activity in non-insulin-dependent diabetes mellitus. Effect of weight loss. *The Journal of Clinical Investigation* **82,** 1398-1406

Fruman, D. A., Meyers, R. E., and Cantley, L. C. (1998) Phosphoinositide kinases. *Annual Review of Biochemistry* **67,** 481-507

Fujita, Y., Sasaki, T., Fukui, K., Kotani, H., Kimura, T., Hata, Y., Südhof, T. C., Scheller, R. H., and Takai, Y. (1996) Phosphorylation of Munc-18/n-Sec1/rbSec1 by protein kinase C: its implication in regulating the interaction of Munc-18/n-Sec1/rbSec1 with syntaxin. *The Journal of Biological Chemistry* **271,** 7265-7268

Garvey, W. T., Huecksteadt, T. P., Matthaei, S., and Olefsky, J. M. (1988) Role of glucose transporters in the cellular insulin resistance of type II non-insulin-dependent diabetes mellitus. *The Journal of Clinical Investigation* **81,** 1528-1536

Garvey, W. T., Maianu, L., Huecksteadt, T. P., Birnbaum, M. J., Molina, J. M., and Ciaraldi, T. P. (1991) Pretranslational suppression of a glucose transporter protein

causes insulin resistance in adipocytes from patients with non-insulin-dependent diabetes mellitus and obesity. *The Journal of Clinical Investigation* **87,** 1072-1081

Garvey, W. T., Maianu, L., Hancock, J. A., Golichowski, A. M., and Baron. A. (1992) Gene expression of GLUT4 in skeletal muscle from insulin-resistant patients with obesity, IGT, GDM, and NIDDM. *Diabetes* **41,** 465-475

Garvey. W. T., Maianu, L., Zhu, J. H., Brechtel-Hook, G., Wallace, P., and Baron, A. D. (1998) Evidence for defects in the trafficking and translocation of GLUT4 glucose transporters in skeletal muscle as a cause of human insulin resistance. *The Journal of Clinical Investigation* **101,** 2377-2386

Garza, L. A., and Birnbaum, M. J. (2000) Insulin-responsive Aminopeptidase Trafficking in 3T3-L1 Adipocytes. *The Journal of Biological Chemistry* **275,** 2560-2567

George, S., Rochford, J. J., Wolfrum, C., Gray, S. L., Schinner, S., Wilson, J. C., Soos, M. A., Murgatroyd, P. R., Williams, R. M., Acerini, C. L., Dunger, D. B., Barford, D., Umpleby, A. M., Wareham, N. J., Davies, H. A., Schafer, A. J., Stoffel, M., O'Rahilly, S., and Barroso I. (2004) A family with severe insulin resistance and diabetes due to a mutation in AKT2. *Science* **304,** 1325-1328

Gould, G. W., and Holman, G. D. (1993) The glucose transporter family: structure, function and tissue-specific expression. *Biochemical Journal* **295,** 329-341

Gould, G. W., and Scatter, M. J. (1997) Introduction to the facilitative glucose transporter family, in *Facilitative Glucose Transporters* (Gould G. W., ed.), pp. 1–37. R. G. Landes Company, Austin.

Guilherme, A., Emoto, M., Buxton, J. M., Bose, S., Sabini, R., Theurkauf, W. E., Leszyk, J., and Czech, M. P. (2000) Perinuclear localization and insulin responsiveness of GLUT4 requires cytoskeletal integrity in 3T3-L1 adipocytes. *The Journal of Biological Chemistry* **275,** 38151-38159

Hanson, P. I., Roth, R., Morisaki, H., Jahn, and R., Heuser, J. E. (1997) Structure and conformational changes in NSF and its membrane receptor complexes visualized by quick-freeze/deep-etch electron microscopy. *Cell* **90,** 523-535

Hanson, P. I., Otto, H., Barton, N., and Jahn, R. (1995) The N-ethylmaleimide-sensitive fusion protein and alpha-SNAP induce a conformational change in syntaxin. *The Journal of Biological Chemistry* **270,** 16955-16961

Harris, M. I., Flegal, K. M., Cowie, C. C, Eberhardt, M. S., Goldstein, D. E., Little, R. R., Wiedmeyer, H. M., and Byrd-Holt, D. D. (1998) Prevalence of diabetes, impaired fasting glucose, and impaired glucose tolerance in U.S. adults. The Third National Health and Nutrition Examination Survey, 1988-1994. *Diabetes Care* **21,** 518-524

Hashiramoto, M., and James, D. E. (2000) Characterization of insulin-responsive GLUT4 storage vesicles isolated from 3T3-L1 adipocytes. *Molecular and Cellular Biology* **20,** 416-427

Hata, Y., Slaughter, C. A., and Südhof, T. C. (1993) Synaptic vesicle fusion complex contains unc-18 homologue bound to syntaxin. *Nature* **366,** 347-351

Hayashi, T., McMahon, H., Yamasaki, S., Binz, T., Hata, Y., Südhof, T. C., and Niemann, H. (1994) Synaptic vesicle membrane fusion complex: action of clostridial neurotoxins on assembly. *The EMBO Journal* **13,** 5051-5061

Hayashi, T., Yamasaki, S., Nauenburg, S., Binz, T., and Niemann. H. (1995) Disassembly of the reconstituted synaptic vesicle membrane fusion complex in vitro. *The EMBO Journal* **14,** 2317-2325

Herbst, J. J., Ross, S. A., Scott, H. M., Bobin, S. A., Morris, N. J., Lienhard, G. E., and Keller, S. R. (1997) Insulin stimulates cell surface aminopeptidase activity toward vasopressin in adipocytes. *The American Journal of Physiology - Endocrinology and Metabolism* **272,** E600-E606

Holman, G. D., and Kasuga, M. (1997) From receptor to transporter: insulin signalling to glucose transport. *Diabetologia* **40,** 991-1003

Holman, G. D., Lo Leggio, L., and Cushman, S. W. (1994) Insulin-stimulated GLUT4 glucose transporter recycling. A problem in membrane protein subcellular trafficking through multiple pools. *The Journal of Biological Chemistry* **269,** 17516-17524

Hunt, J. M., Bommert, K., Charlton, M. P., Kistner, A., Habermann, E., Augustine, G. J., and Betz H. (1994) A post-docking role for synaptobrevin in synaptic vesicle fusion. *Neuron* **12,** 1269-1279

Hunter, S. J., and Garvey, W. T. (1998) Insulin action and insulin resistance: diseases involving defects in insulin receptors, signal transduction, and the glucose transport effector system. *The American Journal of Medicine* **105,** 331-345

Inoue, M., Chang, L., Hwang, J., Chiang, S. H., and Saltiel, A. R. (2003) The exocyst complex is required for targeting of Glut4 to the plasma membrane by insulin. *Nature* **422,** 629-633

Jahn, R., and Südhof, T. C. (1999) Membrane fusion and exocytosis. *Annual Review of Biochemistry* **68,** 863-911

Johnson, A. O., Subtil, A., Petrush, R., Kobylarz, K., Keller, S. R., and McGraw, T. E. (1998) Identification of an insulin-responsive, slow endocytic recycling mechanism in Chinese hamster ovary cells. *The Journal of Biological Chemistry* **273,** 17968-17977

Joost, H. G., and Thorens, B. (2001) The extended GLUT-family of sugar/polyol transport facilitators: nomenclature, sequence characteristics, and potential function of its novel members (review). *Molecular Membrane Biology* **18,** 247-256

Kahn, C. R. (1994) Insulin action, diabetogenes, and the cause of type II diabetes. *Diabetes* **43,** 1066-1084

Kandror, K. V., Coderre, L., Pushkin, A. V., and Pilch, P. F. (1995) Comparison of glucose-transporter-containing vesicles from rat fat and muscle tissues: evidence for a unique endosomal compartment. *Biochemical Journal* **307,** 383-390

Kandror, K. V., and Pilch, P. F. (1996) The insulin-like growth factor II/mannose 6-phosphate receptor utilizes the same membrane compartments as GLUT4 for insulin-dependent trafficking to and from the rat adipocyte cell surface. *The Journal of Biological Chemistry* **271,** 21703-21708

Kandror, K. V., and Pilch, P. F. (1998) Multiple endosomal recycling pathways in rat adipose cells. *Biochemical Journal* **331,** 829-835

Kanzaki, M., and Pessin, J. E. (2003) Insulin Signaling: GLUT4 Vesicles Exit via the Exocyst. *Current Biology* **13,** R574-R576

Katz, E. B., Stenbit, A. E., Hatton, K., DePinho, R., and Charron, M. J. (1995) Cardiac and adipose tissue abnormalities but not diabetes in mice deficient in GLUT4. *Nature* **377,** 151-155

Kee, Y., Lin, R. C., Hsu, S. C., and Scheller, R. H. (1995) Distinct domains of syntaxin are required for synaptic vesicle fusion complex formation and dissociation. *Neuron* **14,** 991-998

Keller, S. R., Scott, H. M., Mastick, C. C., Aebersold, R., and Lienhard, G. E. (1995) Cloning and characterization of a novel insulin-regulated membrane aminopeptidase from Glut4 vesicles. *The Journal of Biological Chemistry* **270,** 23612-23618

Keller, S. R. (2004) Role of the Insulin-Regulated Aminopeptidase IRAP in Insulin Action and Diabetes. *Biological & Pharmaceutical Bulletin* **27,** 761-764

Kelley, D. E., Mintun, M. A., Watkins, S. C., Simoneau, J. A., Jadali, F., Fredrickson, A., Beattie, J., and Theriault, R. (1996) The effect of non-insulin-dependent diabetes mellitus and obesity on glucose transport and phosphorylation in skeletal muscle. *The Journal of Clinical Investigation* **97,** 2705-2713

Kristiansen, S., Hargreaves, M., and Richter, E. A. (1996) Exercise-induced increase in glucose transport, GLUT-4, and VAMP-2 in plasma membrane from human muscle. *The American Journal of Physiology* **270,** E197-E201

Larance, M., Ramm, G., Stockli, J., van Dam, E. M., Winata, S., Wasinger, V., Simpson, F., Graham, M., Junutula, J. R., Guilhaus, M., and James, D. E. (2005) Characterization of the role of the Rab GTPase-activating protein AS160 in insulin-regulated GLUT4 trafficking. *The Journal of Biological Chemistry* **280,** 37803-37813

Lee, W., Ryu, J., Souto, R. P., Pilch, P. F., and Jung, C. Y. (1999) Separation and partial characterization of three distinct intracellular GLUT4 compartments in rat adipocytes. Subcellular fractionation without homogenization. *The Journal of Biological Chemistry* **274,** 37755-37762

Lin, R. C., and Scheller, R. H. (2000) Mechanisms of synaptic vesicle exocytosis. *Annual Review of Cell and Developmental Biology* **16,** 19-49

Lipschutz, J. H., and Mostov, K. E. (2002) Exocytosis: the many masters of the exocyst. *Current Biology* **12,** R212-R214

Livingstone, C., James, D. E., Rice, J. E., Hanpeter, D., and Gould, G. W. (1996) Compartment ablation analysis of the insulin-responsive glucose transporter (GLUT4) in 3T3-L1 adipocytes. *Biochemical Journal* **315,** 487-495

Macaulay, S. L., Hewish, D. R., Gough, K. H., Stoichevska, V., Macpherson, S. F., Jagadish, M., and Ward, C. W. (1997) Functional studies in 3T3-L1 cells support a vital role for SNARE proteins in insulin stimulation of GLUT4 translocation. *Biochemical Journal* **324,** 217-224

Macaulay, S. L., Grusovin, J., Stoichevska, V., Ryan, J. M., Castelli, L. A., and Ward, C. W. (2002) Cellular munc18c levels can modulate glucose transport rate and GLUT4 translocation in 3T3L1 cells. *FEBS Letters* **528,** 154-160

Malide, D., Dwyer, N. K., Blanchette-Mackie, E. J., and Cushman, S. W. (1997a) Immunocytochemical evidence that GLUT4 resides in a specialized translocation post-endosomal VAMP2-positive compartment in rat adipose cells in the absence of insulin. *Journal of Histochemistry and Cytochemistry* **45,** 1083-1096

Malide, D., St-Denis, J. F., Keller. S. R., Cushman, S. W. (1997c) Vp165 and GLUT4 share similar vesicle pools along their trafficking pathways in rat adipose cells. *FEBS Letters* **409,** 461-468

Martin, L. B., Shewan. A., Millar, C. A., Gould, G. W., and James, D. E. (1998) Vesicle-associated membrane protein 2 plays a specific role in the insulin-dependent trafficking of the facilitative glucose transporter GLUT4 in 3T3-L1 adipocytes. *The Journal of Biological Chemistry* **273,** 1444-1452

Martin, S., Reaves, B., Banting, G., and Gould G. W. (1994) Analysis of the co-localization of the insulin-responsive glucose transporter (GLUT4) and the trans Golgi network marker TGN38 within 3T3-L1 adipocytes. *Biochemical Journal* **300,** 743-749

Martin, S., Livingstone, C., Slot, J. W. Gould, G. W., and James, D. E. (1996) The glucose transporter (GLUT-4) and vesicle-associated membrane protein-2 (VAMP-2) are segregated from recycling endosomes in insulin-sensitive cells. *The Journal of Cell Biology* **134,** 625-635

Martin, S., Rice, J. E., Gould, G. W., Keller, S. R., Slot, J. W., and James, D. E. (1997) The glucose transporter GLUT4 and the aminopeptidase vp165 colocalise in tubulo-vesicular elements in adipocytes and cardiomyocytes. *The Journal of Cell Science* **110,** 2281-2291

Martin, S., Ramm, G., Lyttle, C. T., Meerloo, T., Stoorvogel, W., and James, D. E. (2000) Biogenesis of Insulin-Responsive GLUT4 Vesicles is Independent of Brefeldin A-Sensitive Trafficking. *Traffic* 1, 652-660

Mastick, C. C. and Falick, A. L. (1997) Association of N-ethylmaleimide sensitive fusion (NSF) protein and soluble NSF attachment proteins-alpha and -gamma with glucose transporter-4-containing vesicles in primary rat adipocytes. *Endocrinology* **138,** 2391-2397

Mayer, A., Wickner, W., and Haas, A. (1996) Sec18p (NSF)-driven release of Sec17p (alpha-SNAP) can precede docking and fusion of yeast vacuoles. *Cell* **85,** 83-94

McBride, H. M., Rybin, V., Murphy, C., Giner, A., Teasdale, R., and Zerial, M. (1999) Oligomeric complexes link Rab5 effectors with NSF and drive membrane fusion via interactions between EEA1 and syntaxin 13. *Cell* **98,** 377-386

McMahon, H. T., and Südhof, T. C. (1995) Synaptic core complex of synaptobrevin, syntaxin, and SNAP25 forms high affinity alpha-SNAP binding site. *The Journal of Biological Chemistry* **270,** 2213-2217

Millar, C. A., Shewan, A., Hickson G. R., James D. E., and Gould G. W. (1999) Differential regulation of secretory compartments containing the insulin-responsive glucose transporter 4 in 3T3-L1 adipocytes. *Molecular Biology of the Cell* **10,** 3675-3688

Min, J., Okada, S., Kanzaki, M., Elmendorf, J. S., Coker, K. J., Ceresa, B. P., Syu, L. J., Noda, Y., Saltiel, A. R., and Pessin J. E. (1999) Synip: a novel insulin-regulated syntaxin 4-binding protein mediating GLUT4 translocation in adipocytes. *Molecular Cell* **3,** 751-760

Misura, K. M., Scheller, R. H., and Weis, W. I. (2000) Three-dimensional structure of the neuronal-Sec1-syntaxin 1a complex. *Nature* **404,** 355-362

Mitra P., Zheng X., and Czech M. P. (2004) RNAi-based Analysis of CAP, Cbl, and CrkII Function in the Regulation of GLUT4 by Insulin. *The Journal of Biological Chemistry* **279,** 37431-37435

Morris, N. J., Ross, S. A., Lane, W. S., Moestrup, S. K., Petersen, C. M., Keller, S. R., and Lienhard, G. E. (1998) Sortilin is the major 110-kDa protein in GLUT4 vesicles from adipocytes. *The Journal of Biological Chemistry* **273,** 3582-3587

Mueckler, M. M. and Holman, G. D. (1995) Homeostasis without a GLUT. *Nature* **377,** 100-101

Nagiec, E. E., Bernstein, A., and Whiteheart, S. W. (1995) Each domain of the N-ethylmaleimide-sensitive fusion protein contributes to its transport activity. *The Journal of Biological Chemistry* **270,** 29182-29188

Nichols, B. J., Ungermann, C., Pelham, H. R., Wickner, W. T., and Haas, A. (1997) Homotypic vacuolar fusion mediated by t- and v-SNAREs. *Nature* **387.** 199-202

Novick, P., Field, C., and Schekman, R. (1980) Identification of 23 complementation groups required for post-translational events in the yeast secretory pathway. *Cell* **21,** 205-215

Okada, T., Kawano, Y., Sakakibara, T., Hazeki, O., and Ui, M. (1994) Essential role of phosphatidylinositol 3-kinase in insulin-induced glucose transport and antilipolysis in rat adipocytes. Studies with a selective inhibitor wortmannin. *The Journal of Biological Chemistry* **269,** 3568-3573

Olson, A. L., Knight, J. B., and Pessin, J. E. (1997) Syntaxin 4, VAMP2, and/or VAMP3/cellubrevin are functional target membrane and vesicle SNAP receptors for insulin-stimulated GLUT4 translocation in adipocytes. *Molecular and Cellular Biology* **17,** 2425-2435

Pevsner, J., Hsu, S. C., Braun, J. E., Calakos, N., Ting, A. E., Bennett, M. K., and Scheller, R. H. (1994) Specificity and regulation of a synaptic vesicle docking complex. *Neuron* **13,** 353-361

Piper, R. C., Hess, L. J., and James, D. E. (1991) Differential sorting of two glucose transporters expressed in insulin-sensitive cells. *The American Journal of Physiology* **260,** C570-C580

Ploug, T., van Deurs, B., Ai, H., Cushman, S. W., and Ralston, E. (1998) Analysis of GLUT4 distribution in whole skeletal muscle fibers: identification of distinct storage compartments that are recruited by insulin and muscle contractions. *The Journal of Cell Biology* **142,** 1429-1446

Prekeris, R., Klumperman, J., Chen, Y. A., and Scheller, R. H. (1998) Syntaxin 13 Mediates Cycling of Plasma Membrane Proteins via Tubulovesicular Recycling Endosomes. *The Journal of Cell Biology* **143,** 957-971

Rameh, L. E., and Cantley, L. C. (1999) The role of phosphoinositide 3-kinase lipid products in cell function. *The Journal of Biological Chemistry* **274,** 8347-8350

Ramm, G., Slot, J. W., James, D. E., and Stoorvogel, W. (2000) Insulin Recruits GLUT4 from Specialized VAMP2-carrying Vesicles as well as from the Dynamic Endosomal/Trans-Golgi Network in Rat Adipocytes. *Molecular Biology of the Cell* **11,** 4079-4091

Ravichandran, V., Chawla, A., and Roche, P. A. (1996) Identification of a novel syntaxin- and synaptobrevin/VAMP-binding protein, SNAP-23, expressed in non-neuronal tissues. *The Journal of Biological Chemistry* **271,** 13300-13303

Rea, S., and James, D. E. (1997) Moving GLUT4: the biogenesis and trafficking of GLUT4 storage vesicles. *Diabetes* **46,** 1667-1677

Rea, S., Martin, L. B., McIntosh, S., Macaulay, S. L., Ramsdale, T., Baldini, G., and James, D. E. (1998) Syndet, an adipocyte target SNARE involved in the insulin-induced translocation of GLUT4 to the cell surface. *The Journal of Biological Chemistry* **273,** 18784-18792

Ribon, V., and Saltiel, A. R. (1997) Insulin stimulates tyrosine phosphorylation of the proto-oncogene product of c-Cbl in 3T3-L1 adipocytes. *Biochemical Journal* **324,**839-846

Ribon, V., Printen, J. A., Hoffman, N. G., Kay, B. K., and Saltiel, A. R. (1998) A novel, multifuntional c-Cbl binding protein in insulin receptor signaling in 3T3-L1 adipocytes. *Molecular and Cellular Biology* **18,** 872-879

Rice, L. M., Brunger, A. T. (1999) Crystal structure of the vesicular transport protein Sec17: implications for SNAP function in SNARE complex disassembly. *Molecular Cell* **4,** 85-95

Robinson, L. J., and James, D. E. (1992) Insulin-regulated sorting of glucose transporters in 3T3-L1 adipocytes. *The American Journal of Physiology* **363,** E383-E393

Robinson, L. J., Pang, S., Harris, D. S., Heuser, J., and James, D. E. (1992) Translocation of the glucose transporter (GLUT4) to the cell surface in permeabilized 3T3-L1 adipocytes: effects of ATP insulin, and GTP gamma S and localization of GLUT4 to clathrin lattices. *The Journal of Cell Biology* **117,** 1181-1196

Robinson, M. S., Watts, C., and Zerial, M. (1996) Membrane dynamics in endocytosis. *Cell* **84,** 13-21

Ross, S. A., Scott, H. M., Morris, N. J., Leung, W. Y., Mao, F., Lienhard, G. E., and Keller, S. R. (1996) Characterization of the insulin-regulated membrane aminopeptidase in 3T3-L1 adipocytes. *The Journal of Biological Chemistry* **271,** 3328-3332

Ross, S. A., Herbst, J. J., Keller, S. R., and Lienhard, G. E. (1997) Trafficking kinetics of the insulin-regulated membrane aminopeptidase in 3T3-L1 adipocytes. *Biochemical and Biophysical Research Communications* **239,** 247-251

Saltiel, A. R. (2001) New perspectives into the molecular pathogenesis and treatment of type 2 diabetes. *Cell* **104,** 517-529

Sassa, T., Harada, S., Ogawa, H., Rand, J. B., Maruyama, I. N., and Hosono, R. (1999) Regulation of the UNC-18-Caenorhabditis elegans syntaxin complex by UNC-13. *The Journal of Neuroscience* **19,** 4772-4777

Scales, S. J., Yoo, B. Y., and Scheller, R. H. (2001) The ionic layer is required for efficient dissociation of the SNARE complex by alpha-SNAP and NSF. *Proceedings of the National Academy of Sciences USA* **98,** 14262-14267

Schaar, D. G., Varia, M. R., Elkabes, S., Ramakrishnan, L., Dreyfus, C. F., and Black, I. B. (1996) The identification of a novel cDNA preferentially expressed in the olfactory-limbic system of the adult rat. *Brain Research* **721,** 217-228

Shepherd, P. R., Withers, D. J., and Siddle, K. (1998) Phosphoinositide 3-kinase: the key switch mechanism in insulin signalling. *Biochemical Journal* **333,** 471-490

Shepherd, P. R., and Kahn, B. B. (1999) Glucose transporters and insulin action--implications for insulin resistance and diabetes mellitus. *The New England Journal of Medicine* **341,** 248-257

Slot, J. W., Geuze, H. J., Gigengack, S., Lienhard, G. E., and James, D. E. (1991a) Immuno-localization of the insulin regulatable glucose transporter in brown adipose tissue of the rat. *The Journal of Cell Biology* **113,** 123-135

Slot, J. W., Geuze, H. J., Gigengack, S., James, D. E., and Lienhard, G. E. (1991b) Translocation of the glucose transporter GLUT4 in cardiac myocytes of the rat. *Proceedings of the National Academy of Sciences USA* **88,** 7815-7819

Slot, J. W., Garruti, G., Martin, S., Oorschot, V., Posthuma, G., Kraegen, E. W., Laybutt, R., Thibault, G., and James, D. E. (1997) Glucose transporter (GLUT-4) is targeted to secretory granules in rat atrial cardiomyocytes. *The Journal of Cell Biology* **137,** 1243-1254

Søgaard, M., Tani, K., Ye, R. R., Geromanos, S., Tempst, P., Kirchhausen, T., Rothman, J. E., and Söllner, T. (1994) A rab protein is required for the assembly of SNARE complexes in the docking of transport vesicles. *Cell* **78,** 937-948

Söllner, T., Whiteheart, S. W., Brunner, M., Erdjument-Bromage, H., Geromanos, S., Tempst, P., and Rothman, J.E. (1993a) SNAP receptors implicated in vesicle targeting and fusion. *Nature* **362,** 318-323

Söllner, T., Bennett, M. K., Whiteheart, S. W., Scheller, R. H., and Rothman, J. E. (1993b) A protein assembly-disassembly pathway in vitro that may correspond to sequential steps of synaptic vesicle docking, activation, and fusion. *Cell* **75,** 409-418

St-Denis, J. F., Cabaniols, J. P., Cushman, S. W., and Roche, P. A. (1999) SNAP-23 participates in SNARE complex assembly in rat adipose cells. *Biochemical Journal* **338,** 709-715

Stenbit, A. E., Tsao, T. S., Li, J., Burcelin, R., Geenen, D. L., Factor, S. M., Houseknecht, K., Katz, E. B., and Charron, M. J. (1997) GLUT4 heterozygous knockout mice develop muscle insulin resistance and diabetes. *Nature Medicine* **3,** 1096-1101

Subtil, A., Lampson, M. A., Keller, S. R., and McGraw, T.E. (2000) Characterization of the insulin-regulated endocytic recycling mechanism in 3T3-L1 adipocytes using a novel reporter molecule. *The Journal of Biological Chemistry* **275,** 4787-4795

Südhof, T. C. (1995) The synaptic vesicle cycle: a cascade of protein-protein interactions. *Nature* **375,** 645-653

Sutton, R. B., Fasshauer, D., Jahn, R., and Brunger, A. T. (1998) Crystal structure of a SNARE complex involved in synaptic exocytosis at 2.4 Å resolution. *Nature* **395,** 347-353

Suzuki, K., and Kono, T. (1980) Evidence that insulin causes translocation of glucose transport activity to the plasma membrane from an intracellular storage site. *Proccedings of the National Academy of Sciences USA* **77,** 2542-2545

Tamori, Y., Hashiramoto, M., Araki, S., Kamata, Y., Takahashi, M., Kozaki, S., and Kasuga, M. (1996) Cleavage of vesicle-associated membrane protein (VAMP)-2 and cellubrevin on GLUT4-containing vesicles inhibits the translocation of GLUT4 in 3T3-L1 adipocytes. *Biochemical and Biophysical Research Communications* **220,** 740-745

Tamori, Y., Kawasnishi, M., Niki, T., Shinoda, H., Araki, S., Okazawa, H., and Kasuga, M. (1998) Inhibition of insulin-induced GLUT4 translocation by Munc18c through interaction with syntaxin4 in 3T3-L1 adipocytes. *The Journal of Biological Chemistry* **273,** 19740-19746

Tang, B. L., Tan, A. E., Lim, L. K., Lee, S. S., Low, D. Y., and Hong, W. (1998) Syntaxin 12, a member of the syntaxin family localized to the endosome. *The Journal of Biological Chemistry* **273,** 6944-6950

Tanner, L. I., and Lienhard, G. E. (1987) Insulin elicits a redistribution of transferrin receptors in 3T3-L1 adipocytes through an increase in the rate constant for receptor externalization. *The Journal of Biological Chemistry* **262,** 8975-8980

Tanner, L. I., and Lienhard, G. E. (1989) Localization of transferrin receptors and insulin-like growth factor II receptors in vesicles from 3T3-L1 adipocytes that contain intracellular glucose transporters. *The Journal of Cell Biology* **108,** 1537-1545

Tellam, J. T., McIntosh, S., and James, D. E. (1995) Molecular identification of two novel Munc-18 isoforms expressed in non-neuronal tissues. *The Journal of Biological Chemistry* **270,** 5857-5863

Tellam, J. T., Macaulay, S. L., McIntosh, S., Hewish, D. R., Ward, C. W., and James, D. E. (1997) Characterization of Munc-18c and syntaxin-4 in 3T3-L1 adipocytes.

Putative role in insulin-dependent movement of GLUT-4. *The Journal of Biological Chemistry* **272,** 6179- 6186

Terrian, D. M., and White, M. K. (1997) Phylogenetic analysis of membrane trafficking proteins: a family reunion and secondary structure predictions. *European Journal of Cell Biology* **73,** 198-204

Thurmond, D. C., Ceresa, B. P., Okada, S., Elmendorf, J. S., Coker, K., and Pessin, J. E. (1998) Regulation of insulin-stimulated GLUT4 translocation by Munc18c in 3T3L1 adipocytes. *The Journal of Biological Chemistry* **273,** 33876-33883

Thurmond, D. C., Kanzaki, M., Khan, A. H., and Pessin, J. E. (2000) Munc18c function is required for insulin-stimulated plasma membrane fusion of GLUT4 and insulin-responsive amino peptidase storage vesicles. *Molecular and Cellular Biology* **20,** 379-388

Timmers, K. I., Clark, A. E., Omatsu-Kanbe, M., Whiteheart, S. W., Bennett, M. K., Holman, G. D, and Cushman, S. W. (1996) Identification of SNAP receptors in rat adipose cell membrane fractions and in SNARE complexes co-immunoprecipitated with epitope-tagged N-ethylmaleimide-sensitive fusion protein. *Biochemical Journal* **320,** 429-436

Trimble, W. S., Cowan, D. M., and Scheller, R. H. (1988) VAMP-1: A synaptic vesicle associated integral membrane protein. *Proccedings of the National Academy of Sciences USA* **85,** 4538-4542

Virkamäki, A., Ueki, K., and Kahn, C. R. (1999) Protein-protein interaction in insulin signaling and the molecular mechanisms of insulin resistance. *The Journal of Clinical Investigation* **103,** 931-943

Volchuk, A., Mitsumoto, Y., He, L., Liu, Z., Habermann, E., Trimble, W. S., and Klip, A. (1994) Expression of vesicle-associated membrane protein 2 (VAMP-2)/synaptobrevin II and cellubrevin in rat skeletal muscle and in a muscle cell line. *Biochemical Journal* **304,** 139-145

Volchuk, A., Sargeant, R., Sumitani, S., Liu Z., He, L., and Klip, A. (1995) Cellubrevin is a resident protein of insulin-sensitive GLUT4 glucose transporter vesicles in 3T3-L1 adipocytes. *The Journal of Biological Chemistry* **270,** 8233-8240

Volchuk, A., Wang, Q., Ewart, H. S., Liu, Z., He, L., Bennett, M. K., and Klip, A. (1996) Syntaxin 4 in 3T3-L1 adipocytes: regulation by insulin and participation in insulin-dependent glucose transport. *Molecular Biology of the Cell* **7,** 1075-1082

Waters, S. B., D'Auria, M., Martin, S. S., Nguyen, C., Kozma, L. M., and Luskey, K. L. (1997) The amino terminus of insulin-responsive aminopeptidase causes Glut4 translocation in 3T3-L1 adipocytes. *The Journal of Biological Chemistry* **272,** 23323-23327

Watson, R. T., Shigematsu, S., Chiang, S. H., Mora, S., Kanzaki, M., Macara, I. G., Saltiel, A. R., and Pessin, J. E. (2001) Lipid raft microdomain compartmentalization of TC10 is required for insulin signaling and GLUT4 translocation. *The Journal of Cell Biology* **154,** 829-840

Weber, T., Zemelman, B. V., McNew, J. A., Westermann, B., Gmachl, M., Parlati, F., Söllner, T. H., and J E Rothman, J. E. (1998) SNAREpins: minimal machinery for membrane fusion. *Cell* **92,** 759-772

Weimbs, T., Low, S. H., Chapin, S. J., Mostov, K. E., Bucher, P., and Hofmann, K. (1997) A conserved domain is present in different families of vesicular fusion proteins: a new superfamily. *Proccedings of the National Academy of Sciences USA* **94,** 3046-3051

Weimbs, T., Mostov, K., Low, S. H., and Hofmann, K. (1998) A model for structural similarity between different SNARE complexes based on sequence relationships. *Trends in Cell Biology* **8,** 260-262

Whiteheart, S. W., Rossnagel, K., Buhrow, S. A., Brunner, M., Jaenicke, R., and Rothman, J. E. (1994) N-ethylmaleimide-sensitive fusion protein: a trimeric ATPase

whose hydrolysis of ATP is required for membrane fusion. *The Journal of Cell Biology* **126,** 945-954

Whitehead, J. P., Molero, J. C., Clark, S., Martin, S., Meneilly, G., and James, D. E. (2001) The role of Ca2+ in insulin-stimulated glucose transport in 3T3-L1 cells. *The Journal of Biological Chemistry* **276,** 27816-27824

Wilson, D. W., Whiteheart, S. W., Wiedmann, M., Brunner, M., and Rothman, J. E. (1992) A multisubunit particle implicated in membrane fusion. *The Journal of Cell Biology* **117,** 531-538

Wong, P. P., Daneman, N, Volchuk, A., Lassam, N., Wilson, M., C., Klip, A., and Trimble, W. S. (1997) Tissue distribution of SNAP-23 and its subcellular localization in 3T3-L1 cells. *Biochemical and Biophysical Research Communications* **230,** 64-68

Wu, M. N., Fergestad, T., Lloyd, T. E., He, Y., Broadie, K., and Bellen, H. J. (1999) Syntaxin 1A interacts with multiple exocytic proteins to regulate neurotransmitter release in vivo. *Neuron* **23,** 593-605

Yamaguchi, T., Dulubova, I., Min, S. W., Chen, X., Rizo, J., and Südhof, T. C. (2002) Sly1 binds to Golgi and ER syntaxins via a conserved N-terminal peptide motif. *Developmental Cell* **2,** 295-305

Yang, J., and Holman, G. D. (1993) Comparison of GLUT4 and GLUT1 subcellular trafficking in basal and insulin-stimulated 3T3-L1 cells. *The Journal of Biological Chemistry* **268,** 4600-4603

Zhou, L., Chen, H., Lin, C. H., Cong, L. N., McGibbon, M. A., Sciacchitano, S., Lesniak, M. A., Quon, M. J., and Taylor, S. I. (1997) Insulin receptor substrate-2 (IRS-2) can mediate the action of insulin to stimulate translocation of GLUT4 to the cell surface in rat adipose cells. *The Journal of Biological Chemistry* **272,** 29829-29833